FEDERAL UNIVERSITY OF JUIZ DE FORA
EXACT SCIENCES INSTITUTE
GRADUATE PROGRAM IN PHYSICS

Thales B. S. F. Rodrigues

A Semidefinite Programming Analysis of Quantum Bayesian Solutions to the Coarse-Graining Problem

Juiz de Fora

2026

Thales B. S. F. Rodrigues

A Semidefinite Programming Analysis of Quantum Bayesian Solutions to the Coarse-Graining Problem

Dissertation presented to the Graduate Program in Physics of the Federal University of Juiz de Fora as a partial requirement for obtaining the title of Master in Physics.

Advisor: Prof. Dr. Bruno Ferreira Rizzuti

Coadvisor: Prof. Dr. Cristhiano Duarte

Juiz de Fora

2026

Catologing record prepared using the UFJF CDC Latex Model with data provided by the author

Rodrigues, Thales Brito de Souza Fonseca.
A Semidefinite Programming Analysis of Quantum Bayesian Solutions to the Coarse-Graining Problem / Thales B. S. F. Rodrigues. – 2026.
79 f. : il.

Advisor: Bruno Ferreira Rizzuti
Coadvisor: Cristhiano Duarte
Dissertation (Master) – Federal University of Juiz de Fora, Exact Sciences Institute. Graduate Program in Physics, 2026.

1. Semidefinite programming. 2. Coarse-grained descriptions. 3. Emergent quantum dynamics. 4. Quantum Bayesian inference. I. Rizzuti, Bruno F., orient. II. Duarte, Cristhiano. III. Title.

Thales Brito de Souza Fonseca Rodrigues

A Semidefinite Programming Analysis of Quantum Bayesian Solutions to the Coarse-Graining Problem

Dissertação apresentada ao Programa de Pós-Graduação em Física da Universidade Federal de Juiz de Fora como requisito parcial à obtenção do título de Mestre em Física. Área de concentração: Física.

Aprovada em 13 de fevereiro de 2026.

BANCA EXAMINADORA

Prof. Dr. Bruno Ferreira Rizzuti - Orientador
Universidade Federal de Juiz de Fora (UFJF)

Dr. Cristhiano Andre Gamarano Duarte Carneiro Silva - Coorientador
Chapman University (CHAPMAN)

Prof. Dr. Fernando da Rocha Vaz Bandeira de Melo
Centro Brasileiro de Pesquisas Físicas (CBPF)

Prof. Dr. Rodrigo Alves Dias
Universidade Federal de Juiz de Fora (UFJF)

Juiz de Fora, 13/02/2026.

Documento assinado eletronicamente por **Bruno Ferreira Rizzuti**, **Membro**, em 13/02/2026, às 17:18, conforme horário oficial de Brasília, com fundamento no § 3º do art. 4º do Decreto nº 10.543, de 13 de novembro de 2020.

Documento assinado eletronicamente por **Fernando da Rocha Vaz Bandeira de Melo**, **Usuário Externo**, em 13/02/2026, às 18:34, conforme horário oficial de Brasília, com fundamento no § 3º do art. 4º do Decreto nº 10.543, de 13 de novembro de 2020.

Documento assinado eletronicamente por **Cristhiano Andre Gamarano Duarte Carneiro Silva**, **Usuário Externo**, em 13/02/2026, às 19:29, conforme horário oficial de Brasília, com fundamento no § 3º do art. 4º do Decreto nº 10.543, de 13 de novembro de 2020.

Documento assinado eletronicamente por **Rodrigo Alves Dias**, **Servidor(a)**, em 13/02/2026, às 19:53, conforme horário oficial de Brasília, com fundamento no § 3º do art. 4º do Decreto nº 10.543, de 13 de novembro de 2020.

A autenticidade deste documento pode ser conferida no Portal do SEI-Ufjf (www2.ufjf.br/SEI) através do ícone Conferência de Documentos, informando o código verificador **2877122** e o código CRC **CE3A11CE**.

I dedicate this work to my parents, Eliana Brito and João Fonseca.

ACKNOWLEDGMENTS

During my master's studies, I have the opportunity to dedicate myself and felt excited in every moment of the work and the results that gave birth to this manuscript. Nevertheless, none of theses results, nor even such a motivation to pursue this line of research, would have been possible without the collective effort of many people around me to make this happen.

First, I would like to thank my advisor, Prof. Bruno Rizzuti, and my co-advisor Prof. Cristhiano Duarte, for their meaningful supervision and support throughout every conversation and meeting we had. In particular, I would like to thank them for our friendly working relationship; for allowing me to make mistakes and conscientiously guiding me toward the right path; for the trust and opportunity to follow and pursue my own investigations, without preventing me from proposing and delving into fresh, exciting ideas; and for their enlightening advice during moments when I felt lost—not only in my research but also in my academic career itself.

I am also grateful for all my colleagues and friends of the PPGF-UFJF and the Quantum Information Group, who have made my time as master's student fulfilling through excellent human interactions. Specially, I am very thankful to my friend and collaborator, Lucas Brugger, for trusting my work enough to extent the results achieved in his own master's thesis, and for the fruitful discussions throughout all the topics and results addressed in this thesis. I also thank Vinicius Valle for his collaboration and for his precise comments and discussions on the topics covered in this work.

I thank the PPGF-UFJF for the infrastructure and financial support that made it possible for me to go abroad and present this work at an international event, as well as CAPES for my master's scholarship.

Finally and foremost, I must express my deepest gratitude to my dad, João, and my mom, Eliana, for the immensurable support throughout these years; for holding my hand at the moment when I was almost giving up; and for trusting me and in my dreams, even at times when I did not. I would also like to thank my sister, Erika, for staying by my side during the worst moments and for being the best shoulder to lean on that I could have, and my partner, Gabriela, for her constant motivation and encouragement that cheered me up during the difficult moments I went through.

This study was financed in part by the Coordenação de Aperfeiçoamento de Pessoal de Nível Superior – Brasil (CAPES) – Finance Code 001.

Every man takes the limits of his own field of vision for the limits of the world. This is an error of the intellect as inevitable as that error of the eye which lets us fancy that on the horizon heaven and earth meet.
(Arthur Schopenhauer, 1890)

RESUMO

Descrições *coarse-grained* de sistemas quânticos podem ser utilizadas para abordar processos nos quais há perda de informação sobre o sistema ou quando não é possível acessar todos os seus graus de liberdade. Existem alguns esforços na literatura para conectar essas descrições ao formalismo de estados condicionais para a teoria quântica, abordando as condições necessárias e suficientes para a existência de uma dinâmica emergente sob uma perspectiva bayesiana, como a dinâmica emergente proposta por Brugger et al. No entanto, essa dinâmica mostrou-se analiticamente limitada: ela é proporcional ao mapa de recuperação de Petz, depende de um estado inicial e resolve o problema apenas de forma estado a estado. Tendo essa limitação analítica em mente, neste trabalho propomos um benchmarking numérico dessa solução em diferentes cenários do problema de *coarse-graining*. Além disso, por meio de técnicas de programação semidefinida, investigamos a existência de uma dinâmica efetiva para o problema de *coarse-graining* no âmbito do formalismo de estados condicionais que contorne a limitação de dependência do estado da abordagem anterior. Também conduzimos investigações adicionais do problema de *coarse-graining* dentro do formalismo de estados condicionais, de forma independente dessa solução prévia, tais como a proposição de uma nova medida de robustez para quantificar quanto ruído pode ser adicionado a uma dinâmica microscópica compatível com uma dada descrição *coarse-grained*, bem como a formulação de um programa semidefinido que busca dinâmicas unitárias compatíveis em cenários de *coarse-graining* não compatíveis. Nossos resultados indicam que, em geral, a solução proposta por Brugger et al. apresenta melhor desempenho quando gerada a partir do estado maximamente misto, e que, por meio dos programas semidefinidos propostos, é possível identificar os cenários nos quais existe uma dinâmica efetiva capaz de resolver o problema para estados iniciais arbitrários.

Palavras-chave: programação semidefinida; descrições coarse-grained; dinâmicas quânticas emergentes; inferencia Bayesiana quântica.

ABSTRACT

Coarse-grained descriptions of quantum systems can be used to address processes where information about the system is lost or when it is not possible to access all its degrees of freedom. There are some efforts in the literature to connect these descriptions with the conditional states formalism for quantum theory, approaching the necessary and sufficient conditions for the existence of an emergent dynamics through a Bayesian perspective, such as the emergent dynamics proposed by Brugger et al. However, this dynamics has been shown to be analytically limited: it is proportional to the Petz recovery map, depends on a initial state, and solves the problem only on a state-by-state case. With this analytical limitation in mind, in this work we propose a numerical benchmark of this solution across different coarse-graining scenarios. Moreover, by means of semidefinite programming techniques, we investigate the existence of an effective dynamics to the coarse-graining problem within the conditional state formalism that circumvent the state-dependence limitation of the previous approach. We also pursue additional investigations of the coarse-graining problem within the conditional state formalism, independently of this previous solution, such as proposing a new robustness measure to quantify how much noise can be added to a microscopic dynamics compatible with a given coarse-grained description, as well as formulating a semidefinite program that searches for compatible unitary dynamics in non-compatible coarse-graining scenarios. Our findings indicate that, in general, the solution proposed by Brugger et al. performs better when generated by the maximally mixed state, and that, through the proposed semidefinite programs, we identify the scenarios in which it is possible to find an effective dynamics that solves the problem for arbitrary initial states.

Keywords: semidefinite programming; coarse-grained descriptions; emergent quantum dynamics; quantum Bayesian inference.

LIST OF FIGURES

LIST OF TABLES

LIST OF SYMBOLS

$\mathbb{N}$	Set of natural numbers
$\mathbb{R}$	Set of real numbers
$\mathbb{C}$	Set of complex numbers
$\otimes$	Tensor product
$\mathcal{H}$	Hilbert space
A^T	Transpose of the matrix of A
$B^\dagger$	Adjoint of the operator B
$\mathrm{Tr}(A)$	Trace of the matrix or operator A
$\mathrm{Out}(X)$	The set of possible values x that the random variable X can assume

SUMMARY

1 INTRODUCTION

1.1 OVERVIEW

Optimization strategies have been among the cornerstones of modern technologies' development. From machine learning and data-driven decision making (1, 2) to the design of optimal oncological treatments and pharmaceutical formulations (3, 4), optimization techniques—together with the computational power raised by modern computers—have played a major role in solving complex problems in a variety of areas.

In particular, concerning quantum information science, convex optimization approaches such as semidefinite programming (SDP) and conic programming have been widely applied to study several topics in the field (47, 8, 57). The usefulness of deploying SDP to approach tasks within this paradigm lies mainly in the fact that quantum states are mathematically represented by positive semidefinite operators, $\rho \succeq 0$, which are normalized, $\mathrm{Tr}(\rho) = 1$. Since the first condition is a linear operator inequality and the latter an equality, these can be directly incorporated as constraints inside semidefinite programs. As a result, many problems involving optimization procedures of quantum states can be cast efficiently as these kinds of optimization programs. Moreover, the applicability of convex optimization extends beyond the study of quantum states. Another crucial component within quantum information protocols—namely, quantum channels, completely positive and trace-preserving (CPTP) linear maps of operators—has also found its place within this convex optimization picture in the literature (47, 11). Due to the fact that the Choi-Jamiołkowski isomorphism (12, 13) establishes a correspondence between completely positive and trace-preserving maps and quantum states, it turns out to be possible also to approach such maps in semidefinite programs by anchoring in the aforementioned constraints as well.

In line with that exposition, there exists a strand of studies that seek to employ the mathematical rigor of the quantum channels frameworks in order to obtain effective descriptions of many-body quantum systems. Since a description of these systems accounting for all their degrees of freedom is computationally intractable (21), the *coarse-graining problem* that we study here has emerged within the quantum information literature in (24), but also further studied in (27, 28, 25, 30), as a mathematical framework for investigating the existence of an effective dynamics Γ_t, arising from a lack of information or inability to access a high-resolution description of an underlying closed microscopic system evolving through a unitary dynamics $\mathcal{U}_t$. Such an imperfect description is modeled mathematically by a dimension-reducing, completely positive, trace-preserving coarse-graining map, Λ_{CG}, which presumably represents any physical process related to loss of or restricted access to information. The effectiveness character of Γ_t in describing the coarse-grained situation

comes from an additional commutativity constraint imposed on the whole scenario, namely:

$$\Gamma_t \circ \Lambda_{\mathrm{CG}} = \Lambda_{\mathrm{CG}} \circ \mathcal{U}_t, \tag{1.1}$$

which express a certain compatibility between the coarse-grained description and the unitary dynamics involved in a coarse-graining scenario (30, 27). This expression lies at the heart of the coarse-graining problem, as it connects to one of the central questions in physics addressed by thermodynamics (26): how a less complex, macroscopic description of a system emerges from a microscopic, quantum-mechanical evolution of all its atomic-scale constituents.

Strolling in another direction, while still concerned with descriptions of quantum systems involving quantum channels, there exists a Bayesian approach to quantum theory that seeks to bring the flavor of independence from causal structure, which occurs in conventional classical probability theory of Bayesian inference, into the quantum formalism. Particularly, in 2013, M.S. Leifer and Robert W. Spekkens propose a formalism for quantum theory (5), named the *conditional states formalism*, that aims to circumvent the shortcoming of the conventional formalism that appears when one looks at quantum theory as a generalization of classical probability theory.

In the conventional formalism, the mathematical description employed to describe an experiment involving two quantum systems spacelike separated at different times are different from the description used to describe the same quantum system at two different times. The former is usually described by a joint state on the tensor product of two Hilbert spaces, and the latter by a quantum channel, the input state and output state of that channel potentially being the same Hilbert space. This intrinsically differs from how classical probability deals with causal structures. In the classical case, it is indeed possible to use the same mathematical structure and define a joint probability distribution involving two random variables independent of the causal structure between them. It is as if classical probability is blind to causal relations.

Therefore, to circumvent those structural limitations, the conditional states formalism, in its very formulation, attempts to provide a unified description of these two sorts of experiments by instances of the acausal conditional states and the causal conditional states. Also, concepts that have a different description in the conventional formalism become unified as instances of conditional states and belief propagation rules—the latter being an analogue expression to the classical law of total probability (5).

Despite some inherent limitations and situations where the conditional states formalism fails to establish analogies with classical probability theory, the Bayesian inference character and the framework provided to characterize quantum channels through conditional quantum states have motivated some efforts in the literature to study the earlier mentioned coarse-graining problem in light of this formalism (27, 29). In particular, in (27), by seeing quantum theory as a framework for Bayesian inference and making extensive use

of the conditional state formalism, the author has connected the quantum state pooling to the conventional coarse-graining scenario in order to obtain more approachable necessary and sufficient conditions for the existence of a well-defined coarse-grained state. Moreover, in Brugger et al. (29), the authors relied solely on the conditional state formalism to reframe the original coarse-graining problem and propose an emergent dynamics that depends directly on the Petz recovery map (6) associated with the initial coarse-graining map and the microscopic state. Unfortunately, the emergent dynamics proposed by those authors have shown some limitations in its own formulation: it depends of a initial microscopic state, and only solves the coarse-graining problem analytically in a state-by-state case, not having the capacity to satisfy the commutativity relation for any microscopic state, given a unitary dynamics and coarse-grained description. It is upon such analytical limitation, together with this Bayesian picture of the coarse-graining problem, that our contribution of this present work dwells.

1.2 RESEARCH OBJECTIVES

More precisely, in this research we aim to establish a numerical and semidefinite programming-based analysis of the previously proposed state-dependent solution to the coarse-graining problem by Brugger et al. (29) (hereafter referred to as the Brugger et al. solution), within the framework of the conditional states formalism. We first conduct a numerical investigation of this solution in order to benchmark its performance across four coarse-graining scenarios in the two-qubit case. Additionally, this work seeks to address the state-by-state limitation by proposing optimization procedures based on semidefinite programs. By grounding the analysis in the conditional states associated with each quantum channel of the coarse-graining scenario, the proposed optimization programs not only search for a definitive solution that satisfies the commutativity relation for all microscopic initial states and solve the problem regardless of particular choices thereof, but also propose novel investigations to the coarse-graining problem within the framework of the conditional states formalism.

Particularly, in line with the discussion around the compatibility of quantum channels in a coarse-graining scenario conducted in (27) and likewise addressed in (30), we introduce a new robustness measure to quantify, within the conditional states formalism, how much noise can be added to a given unitary dynamics of a compatible coarse-graining scenario in such a way that it remains compatible. This quantifier further serves as inspiration for proposing a convex optimization routine that, for a given convex combination parameter, circumvent the non-compatibility between quantum channels in a non-compatible coarse-graining scenario within this quantum Bayesian picture.

Throughout the following chapters, we seek to strike a balance between presenting our main contributions and offering an explanatory treatment of some advanced concepts

that were used to obtain our main results, thereby ensuring not only internal consistency for the text itself but also a comprehensive narrative for readers who are not familiar with some of the concepts discussed herein.

1.3 STRUCTURE

This work is structured as follows. In Chapter 2, the mathematical notation and the basic mathematical framework adopted throughout this work are elucidated. The coarse-graining problem is reviewed and presented in more detail in Chapter 3, and the same was done with the conditional state formalism in Chapter 4. In particular, in Section 4.2 we have shown the Bayesian perspective of the coarse-graining problem, as well as the previous solution that we further analyze numerically. Moving on, Chapter 5 presents convex optimization programs designed to face and numerically circumvent the limitations of the previous solution proposed in (29), as well as to evaluate additional aspects of the coarse-graining problem within this quantum Bayesian picture. Chapter 6 concentrates all the results of the computational analyzes conducted here regarding the previous solution along four benchmark coarse-graining scenarios, in addition to the results of the numerical implementations of the proposed semidefinite programs. Finally, Chapter 7 summarizes the findings and contains the key takeaways from the proposed analysis and its results, as well as guidance for possible further work.

2 MATHEMATICAL PRELIMINARIES

In this chapter, we establish the notation and present the mathematical building blocks on which this work and our main contributions rest.

2.1 NOTATIONS

We start labeling quantum systems[1] by capital Latin letters, namely, A, B, C, for example. Also, (finite-dimensional) Hilbert spaces are denoted by $\mathcal{H}$ and, when employed to describe a specific quantum system, a respective subscript will be attached to it, such as $\mathcal{H}_A, \mathcal{H}_B$, and $\mathcal{H}_C$. In certain specific contexts, we will label the Hilbert space according to its dimension, and this will be evident throughout the text. For any system A, we denote by $\mathcal{L}(\mathcal{H}_A)$ the set of linear operators on $\mathcal{H}_A$, and we will sometimes use the same label to indicate operators, such as $X_A \in \mathcal{L}(\mathcal{H}_A)$. The same applies for tensor product spaces $\mathcal{H}_A \otimes \mathcal{H}_B$, which we denote by $\mathcal{H}_{AB}$, and to operators acting on it, denoted as X_{AB}. We also denote by

$$\mathrm{Pos}(\mathcal{H}_A) = \{P \in \mathcal{L}(\mathcal{H}_A) | \, \langle x| \, P \, |x\rangle \geq 0 \quad \forall \, |x\rangle \in \mathcal{H}_A\}$$

the set of positive semidefinite operators on $\mathcal{H}_A$. By strengthening the inequality to strict positive, we analogously define the set of positive definite operators $\mathrm{Pd}(\mathcal{H}_A)$,

$$\mathrm{Pd}(\mathcal{H}_A) = \{R \in \mathcal{L}(\mathcal{H}_A) | \, \langle x| \, R \, |x\rangle > 0 \quad \forall \, |x\rangle \neq 0\}.$$

Throughout the text, for any operator $P \in \mathrm{Pos}(\mathcal{H}_A)$ and $R \in \mathrm{Pd}(\mathcal{H}_A)$, we will use the symbols $\succeq$ and $\succ$ to represent them respectively as $P \succeq 0$ and $R \succ 0$. Also, for any $X, Y \in \mathcal{L}(\mathcal{H}_A)$, we will write $X \succeq Y$ to indicate the so-called Löwner partial order (32) (or, equivalently, $Y \preceq X$), meaning that $X - Y \succeq 0$. Moreover, the set of all density operators on $\mathcal{H}_A$ will be denoted by

$$\mathcal{D}(\mathcal{H}_A) = \{\rho \in \mathcal{L}(\mathcal{H}_A) | \rho \succeq 0, \mathrm{Tr}(\rho) = 1\}.$$

This set is also referred to as the set of quantum states of the quantum system A.

The set of Hermitian operators on $\mathcal{H}_A$ will be denoted by $\mathrm{Herm}(\mathcal{H}_A) = \{H \in \mathcal{L}(\mathcal{H}_A) | H = H^\dagger\}$. We will usually denote linear maps of operators by calligraphic letters (e.g., $\mathcal{E}, \mathcal{N}, \mathcal{M}, \mathcal{U}$) and capital Greek letters (e.g., Λ, Γ, Ω). For a given operator $A \in \mathcal{L}(\mathcal{H}_A)$, the trace norm, denoted in this work as $\| \cdot \|_1$, is given by $\|A\|_1 = \mathrm{Tr}\Big(\sqrt{A^\dagger A}\Big)$, which is equal to the sum of the singular values of A (49). Also, for any choice of complex Hilbert space $\mathcal{H}_A$, we denote the Hilbert-Schmidt inner product on the space $\mathcal{L}(\mathcal{H}_A)$ as $\langle A, B\rangle_{HS} = \mathrm{Tr}\Big(A^\dagger B\Big)$ for all $A, B \in \mathcal{L}(\mathcal{H}_A)$. The identity operator on $\mathcal{H}_A$ is denoted by

[1] After chapter 4, it will also be used to denote quantum regions, and such a transition will be indicated later.

$\mathbb{I}_A$, and the identity superoperator on $\mathcal{L}(\mathcal{H}_A)$ is denoted by id_A. For convenience, we write $\mathcal{L}(A,B) = \{\Phi : \mathcal{L}(\mathcal{H}_A) \to \mathcal{L}(\mathcal{H}_B) | \Phi \text{ is linear}\}$ to denote the space of all linear maps from $\mathcal{L}(\mathcal{H}_A)$ to $\mathcal{L}(\mathcal{H}_B)$, and $\mathcal{C}(A,B) = \{\Phi : \mathcal{L}(\mathcal{H}_A) \to \mathcal{L}(\mathcal{H}_B) | \Phi \text{ is CPTP}\}$ to denote the space of all CPTP linear maps from $\mathcal{L}(\mathcal{H}_A)$ to $\mathcal{L}(\mathcal{H}_B)$, and we inform the reader that a more detailed exposition of these maps will be presented below. We say that a map $\Phi \in \mathcal{L}(A,B)$ is Hermicity preserving if it holds that $\Phi(X_A) \in \mathrm{Herm}(\mathcal{H}_B)$ for all $X_A \in \mathrm{Herm}(\mathcal{H}_A)$. Finally, for a given $\Phi \in \mathcal{L}(A,B)$, the dual map associated to it is defined to be the unique map $\Phi^\dagger \in \mathcal{L}(B,A)$ that satisfies

$$\langle \Phi^\dagger(Y), X\rangle_{HS} = \langle Y, \Phi(X)\rangle_{HS}$$

for all $X \in \mathcal{L}(\mathcal{H}_A)$ and $Y \in \mathcal{L}(\mathcal{H}_B)$. In what follows, we present a specific class of linear maps of operators—extensively approached throughout this work—which are known in the literature to represent a general quantum evolution (20).

2.2 COMPLETELY POSITIVE AND TRACE PRESERVING MAPS

Before introducing, in more detail, the coarse-graining operations and the other elements that compose a general coarse-graining scenario, it is reasonable to briefly review and formally present the definition of CPTP linear maps, together with the very definition of quantum dynamics. In order to didactically review the motivations behind the definitions of general quantum evolutions and quantum channels, the construction of this section is mainly inspired by the axiomatic approach presented in Ref. (37).

As a starting point, let $\mathcal{E} : \mathcal{L}(\mathcal{H}_A) \to \mathcal{L}(\mathcal{H}_B)$ be a map that takes operators on $\mathcal{H}_A$ to operators on $\mathcal{H}_B$. We say that $\mathcal{E}$ is linear when, for any $X, Y \in \mathcal{L}(\mathcal{H}_A)$ and $\alpha, \beta \in \mathbb{C}$, $\mathcal{E}(\alpha X + \beta Y) = \alpha\mathcal{E}(X) + \beta\mathcal{E}(Y)$.

Having established the linearity of operator maps, and considering that quantum states, by their very definition, are positive operators, it is physically reasonable to assume that a quantum channel should take quantum states to quantum states. Furthermore, due to the structure of the set of quantum states, it must be closed to convex combinations; thus, for convenience, we definite it here as a linear map.[2] That is, in principle, they should be positive linear maps in accordance with the following definition.

Definition 1. *A linear map $\mathcal{E} : \mathcal{L}(\mathcal{H}_A) \to \mathcal{L}(\mathcal{H}_B)$ is positive when $\mathcal{E}(X)$ is a positive semidefinite operator on $\mathcal{H}_B$ for all $X \in Pos(\mathcal{H}_A)$.*

By the very structure of the tensor product and the mathematical representation of quantum systems—and also by the underlying physics—one is allowed to extend an initially prepared system A, described by $\rho_A \in \mathcal{D}(\mathcal{H}_A)$ and evolved by a positive linear

[2] A more detailed motivation for this requirement of linearity in quantum channels can be found in (37).

map $\mathcal{E} : \mathcal{L}(\mathcal{H}_A) \to \mathcal{L}(\mathcal{H}_A)$, to a composite system EA, described by $\rho_{EA} \in \mathcal{D}(\mathcal{H}_E \otimes \mathcal{H}_A)$, where $\mathcal{H}_E$ represents an auxiliary system E of arbitrary dimension. From this, one can notice that the notion of positivity of $\mathcal{E}$ alone does not adequately capture the evolution of the composite state ρ_{EA}. Thus, by allowing the map $\mathcal{E}$ to act only on the part A of the composite system while leaving the auxiliary part untouched—in such a way that the result remains a positive operator—the definition of completely positive maps must be incorporated into this construction.

Definition 2. *A linear map $\mathcal{E} : \mathcal{L}(\mathcal{H}_A) \to \mathcal{L}(\mathcal{H}_B)$ is said to be completely positive if $id_E \otimes \mathcal{E}$ is positive for every choice of auxiliary Hilbert space $\mathcal{H}_E$ of arbitrary size.*

After considering how such general quantum processes must deal with the positive semidefinite nature of quantum states, we now turn our attention to the other constraint imposed on these operators: the unity of the trace. Based on this, it is also physically reasonable to assume that if $\mathcal{E}$ represents the physical evolution of any quantum state $\rho \in \mathcal{D}(\mathcal{H}_A)$, then the equality $\mathrm{Tr}(\rho) = \mathrm{Tr}[\mathcal{E}(\rho)] = 1$ must hold. This trace-preservation aspect motivates us to bring to our construction the very definition of trace-preserving maps.

Definition 3. *A linear map $\mathcal{E} : \mathcal{L}(\mathcal{H}_A) \to \mathcal{L}(\mathcal{H}_B)$ is said to be trace-preserving if $\mathrm{Tr}(X) = \mathrm{Tr}[\mathcal{E}(X)]$ for all $X \in \mathcal{H}_A$.*

In summary, the above definition ensures that the probability assignments of $\mathcal{E}(\rho)$ remain consistent, while the completely positivity condition, Definition 2, guarantees that positive operators are mapped to positive operators even if the map acts only on a specific subsystem of the whole quantum system. Therefore, binding together all the above definitions, we are in a position to formally define a quantum channel.

Definition 4. *A quantum channel (also referred to as quantum evolution or quantum dynamics) is a linear, completely positive, and trace-preserving map that represents the most general evolution of a quantum system.*

Upon such a definition of quantum channels, in the following subsection, we present a characterization of these physically relevant objects in terms of positive operators, which turns out to be, as subsequently mentioned, one of the building blocks of the conditional states formalism—adopted in this work to frame the coarse-graining problem.

2.2.1 The Choi-Jamiołkowski isomorphism

From a straightforward examination, one can see that for any finite-dimensional Hilbert spaces $\mathcal{H}_A$ and $\mathcal{H}_B$, such that $dim(\mathcal{H}_A) = m$ and $dim(\mathcal{H}_B) = n$, with $m, n \in \mathbb{N}$, it holds that $dim(\mathcal{L}(\mathcal{H}_A, \mathcal{H}_B)) = dim(\mathcal{L}(\mathcal{H}_A \otimes \mathcal{H}_B)) = m^2n^2$, indicating, in this way, the

existence of an isomorphic connection between $\mathcal{L}(\mathcal{H}_A, \mathcal{H}_B)$ and $\mathcal{L}(\mathcal{H}_A \otimes \mathcal{H}_B)$. Building upon this fact, there exist in the literature two equivalent versions of such a connection, proposed by Jamiołkowski in (13) and also by Choi in (12), which—due to this very equivalence—are usually referred to, within the quantum information literature (50), as the Choi-Jamiołkowski isomorphism.

Since the equivalence between them is promoted by a partial transpose operation, and given that the partial transposition is not a positive map (49), the Jamiołkowski's version of the isomorphism does not directly connect quantum dynamics to positive semidefinite operators. Thus, motivated by the fact that, in this work, we are interested in engaging with semidefinite programming evaluations of the quantum dynamics that compose a coarse-graining scenario, the Choi's version of this isomorphism has been adopted. In this line, here we define the Choi(-Jamiołkowski) isomorphism, which, for the purposes of this work, assumes the following form.

Definition 5 (Choi Isomorphism)**.** *Let $\mathcal{H}_A$ and $\mathcal{H}_B$ be two Hilbert spaces. Let*

$$\mathcal{E} : \mathcal{L}(\mathcal{H}_A) \to \mathcal{L}(\mathcal{H}_B) \tag{2.1}$$

be a linear map. The Choi image of $\mathcal{E}$ is given by an operator $\rho \in \mathcal{L}(\mathcal{H}_A \otimes \mathcal{H}_B)$ such that

$$\rho := (id_A \otimes \mathcal{E}) |\Omega\rangle \langle\Omega| = (id_A \otimes \mathcal{E})(\sum_{i,j=0}^{d-1} |i\rangle \langle j| \otimes |i\rangle \langle j|), \tag{2.2}$$

where $d := dim(\mathcal{H}_A)$, $|\Omega\rangle = \sum_{i=0}^{d-1} |i\rangle \otimes |i\rangle$ is an unnormalized maximally entangled state on $\mathcal{H}_A \otimes \mathcal{H}_A$ with respect to some preferred orthonormal basis $\{|k\rangle\}_{k=0}^{d-1}$ of $\mathcal{H}_A$ and id_A is the identity map on $\mathcal{L}(\mathcal{H}_A)$. Also, for some $\sigma \in \mathcal{L}(\mathcal{H}_A)$, the action of $\mathcal{E}$ on $\mathcal{L}(\mathcal{H}_A)$ is given by

$$\mathcal{E}(\sigma) = \mathrm{Tr}_A[\rho(\sigma^T \otimes \mathbb{I}_B)] \in \mathcal{L}(\mathcal{H}_B). \tag{2.3}$$

From this definition, one can notice that the isomorphic connection between the Choi state ρ and $\mathcal{E}$ can be easily checked, given that

$$\begin{aligned} &\mathrm{Tr}_A[\rho(\sigma^T \otimes \mathbb{I}_B)] = \\ &= \mathrm{Tr}_A[(id_A \otimes \mathcal{E})(|\Omega\rangle \langle\Omega|)(\sigma^T \otimes \mathbb{I}_B)] \\ &= \mathrm{Tr}_A[(id_A \otimes \mathcal{E})(\sum_{i,j=0}^{d-1} |i\rangle \langle j| \otimes |i\rangle \langle j|)(\sigma^T \otimes \mathbb{I}_B)] \\ &= \mathrm{Tr}_A[\sum_{i,j=0}^{d-1} |i\rangle \langle j| \sigma^T \otimes \mathcal{E}(|i\rangle \langle j|)] = \sum_{i,j=0}^{d-1} \langle j| \sigma^T |i\rangle \mathcal{E}(|i\rangle \langle j|) \\ &= \sum_{i,j=0}^{d-1} (\sigma^T)_{j,i} \mathcal{E}(|i\rangle \langle j|) = \sum_{i,j=0}^{d-1} (\sigma)_{i,j} \mathcal{E}(|i\rangle \langle j|) = \mathcal{E}(\sigma). \end{aligned} \tag{2.4}$$

One relevant application of the Choi isomorphism, which is one of the cornerstones of the conditional states formalism enunciated later in this work, is that it maps any

quantum channel to a positive semidefinite operator. This fact is highlighted in the following theorem. We remark that this is a standard result in literature and can be found in (49).

Theorem 1. *Let $\mathcal{E} : \mathcal{L}(\mathcal{H}_A) \to \mathcal{L}(\mathcal{H}_B)$ be a linear map and let $\rho \in \mathcal{L}(\mathcal{H}_A \otimes \mathcal{H}_B)$ be its Choi-isomorphic operator. Then, it follows that ρ satisfies:*

1. $\rho \succeq 0$;
2. $\mathrm{Tr}_B(\rho) = \mathbb{I}_A$,

if, and only if, $\mathcal{E}$ is CPTP.

Proof. Suppose that ρ is positive and $\mathrm{Tr}_B(\rho) = \mathbb{I}_A$. Let $X \in \mathcal{L}(\mathcal{H}_A)$ be an arbitrary operator on $\mathcal{H}_A$. Then, first, to show that $\mathcal{E}$ is trace preserving, it proceeds as follows:

$$\begin{aligned} \mathrm{Tr}_B[\mathcal{E}(X)] &= \mathrm{Tr}_B\{\mathrm{Tr}_A[\rho(X^T \otimes \mathbb{I}_B)]\} \\ &= \mathrm{Tr}_A[\mathrm{Tr}_B(\rho)X^T] \\ &= \mathrm{Tr}_A(\mathbb{I}_A X^T) \\ &= \mathrm{Tr}_A(X). \end{aligned} \tag{2.5}$$

To show that $\mathcal{E}$ is completely positive, considering a positive operator $P \in \mathcal{L}(\mathcal{H}_C \otimes \mathcal{H}_A)$, where $\mathcal{H}_C$ is any finite-dimensional Hilbert space, we need to show that

$$(\mathrm{id}_C \otimes \mathcal{E})(P) \succeq 0. \tag{2.6}$$

To do this, first, as P is positive, consider its spectral decomposition

$$P = \sum_{i=1}^{d_A \cdot d_C} p_i \left|\psi_i\right\rangle \left\langle\psi_i\right|_{CA}, \tag{2.7}$$

where $d_A := dim(\mathcal{H}_A)$, $d_C := dim(\mathcal{H}_C)$, $\{|\psi_i\rangle_{CA}\}_{i=1}^{d_A \cdot d_C}$ is some orthonormal basis for $\mathcal{H}_C \otimes \mathcal{H}_A$ and $p_i \in spec(P)$. Thus,

$$(\mathrm{id}_C \otimes \mathcal{E})(P) = \sum_{i=1}^{d_A d_C} p_i[\mathrm{id}_C \otimes \mathcal{E}(\left|\psi_i\right\rangle \left\langle\psi_i\right|_{CA})]. \tag{2.8}$$

Since each eigenvalue p_i of P is non-negative, it is sufficient to prove that

$$\mathrm{id}_C \otimes \mathcal{E}(\left|\psi_i\right\rangle \left\langle\psi_i\right|_{CA}) \succeq 0 \tag{2.9}$$

for a given $i \in \{1, ..., d_A d_C\}$. For this, letting $\alpha := \{|j\rangle_A\}_{j=0}^{d_A - 1}$ and $\gamma := \{|k\rangle_C\}_{k=0}^{d_C - 1}$ be orthonormal basis of $\mathcal{H}_A$ and $\mathcal{H}_C$, respectively, we can expand each $|\psi_i\rangle_{CA}$ as:

$$\left|\psi_i\right\rangle_{CA} = \sum_{k=0}^{d_C - 1} \sum_{j=0}^{d_A - 1} (\Psi_i)_{kj} \left|k\right\rangle_C \left|j\right\rangle_A. \tag{2.10}$$

Then, one notes that:

$$\begin{aligned}\mathrm{id}_C \otimes \mathcal{E}(|\psi_i\rangle\langle\psi_i|_{CA}) &= \mathrm{id}_C \otimes \mathcal{E}[\sum_{k,m=0}^{d_C-1}\sum_{j,n=0}^{d_A-1}(\Psi_i)_{kj}(\Psi_i)^*_{mn}|k\rangle_C|j\rangle_A\langle m|_C\langle n|_A] \\ &= \sum_{k,m=0}^{d_C-1}\sum_{j,n=0}^{d_A-1}(\Psi_i)_{kj}(\Psi_i)^*_{mn}|k\rangle\langle m|_C \otimes \mathcal{E}(|j\rangle\langle n|_A). \end{aligned} \tag{2.11}$$

By the very definition 5, we have that

$$\begin{aligned}\mathcal{E}(|j\rangle\langle n|_A) &= (\langle j|_A \otimes \mathbb{I}_B)[\sum_{j,n=0}^{d_A-1}|j\rangle\langle n|_A \otimes \mathcal{E}(|j\rangle\langle n|_A)](|n\rangle_A \otimes \mathbb{I}_B) \\ &= (\langle j|_A \otimes \mathbb{I}_B)(\mathrm{id}_A \otimes \mathcal{E})(|\Omega\rangle\langle\Omega|)(|n\rangle_A \otimes \mathbb{I}_B) \\ &= (\langle j|_A \otimes \mathbb{I}_B)(\rho)(|n\rangle_A \otimes \mathbb{I}_B), \end{aligned} \tag{2.12}$$

where $|\Omega\rangle = \sum_{i=0}^{d_A-1} = |ii\rangle_{AA}$ is the unnormalized maximally entangled state with respect to the basis α. Replacing (2.12) in (2.11), we arrive at

$$\mathrm{id}_C \otimes \mathcal{E}(|\psi_i\rangle\langle\psi_i|_{CA}) = \sum_{k,m=0}^{d_C-1}\sum_{j,n=0}^{d_A-1}(\Psi_i)_{kj}(\Psi_i)^*_{mn}|k\rangle\langle m|_C \otimes [(\langle j|_A \otimes \mathbb{I}_B)(\rho)(|n\rangle_A \otimes \mathbb{I}_B)]. \tag{2.13}$$

Now, since ρ is positive, by the spectral theorem (49), there exists a orthonormal basis $\{|x_l\rangle_{AB}\}_{l=1}^{d_Ad_B}$ of $\mathcal{H}_A \otimes \mathcal{H}_B$ such that

$$\rho = \sum_{l=1}^{d_Ad_B}\lambda_l|x_l\rangle\langle x_l|_{AB}, \tag{2.14}$$

where λ_l are the (non-negative) eigenvalues of ρ and $d_B = dim(\mathcal{H}_B)$. From this, defining, for each $l \in \{1, ..., d_Ad_B\}$, $|\phi_l\rangle_{AB} := \sqrt{\lambda_l}|x_l\rangle_{AB}$, we can write ρ solely as

$$\rho = \sum_{l=1}^{k}|\phi_l\rangle\langle\phi_l|_{AB}, \tag{2.15}$$

where $k \leq d_Ad_B$ is the rank of ρ, and $\{|\phi_l\rangle\}_{l=1}^k$ constitute a set of orthogonal vectors of $\mathcal{H}_A \otimes \mathcal{H}_B$. For a given $l \in \{1, ..., k\}$, consider the following expansion of the vector $|\phi_l\rangle_{AB}$ in terms of the basis α of $\mathcal{H}_A$ and a given orthonormal basis $\beta := \{|i\rangle_B\}_{i=0}^{d_B-1}$ of $\mathcal{H}_B$ as:

$$|\phi_l\rangle_{AB} = \sum_{j=0}^{d_A-1}\sum_{n=0}^{d_B-1}(\Phi_l)_{jn}|j\rangle_A \otimes |n\rangle_B, \tag{2.16}$$

where, for each $l \in \{1, ..., k\}$, Φ_l denotes the $d_A \times d_B$ matrix whose entries are the coefficients of $|\phi_l\rangle_{AB}$ in the product basis $\{|j\rangle_A \otimes |n\rangle_B\}$.

Let $V_l : \mathcal{H}_A \to \mathcal{H}_B$ denote linear operators of the form:

$$V_l := \sum_{j=0}^{d_A-1}\sum_{n=0}^{d_B-1}(\Phi_l^T)_{nj}|n\rangle_B\langle j|_A = \sum_{j=0}^{d_A-1}\sum_{n=0}^{d_B-1}(\Phi_l)_{jn}|n\rangle_B\langle j|_A. \tag{2.17}$$

From this definition, one sees that:

$$\begin{aligned}(\mathbb{I}_A \otimes V_l)\,|\Omega\rangle &= \sum_{k=0}^{d_A-1} |k\rangle_A \otimes V_l\,|k\rangle_A \\ &= \sum_{k,j=0}^{d_A-1}\sum_{n=0}^{d_B-1} (\Phi_l)_{jn}\,|k\rangle_A \otimes |n\rangle_B \langle j|k\rangle_A \\ &= \sum_{k,j=0}^{d_A-1}\sum_{n=0}^{d_B-1} (\Phi_l)_{jn}\,|k\rangle_A \otimes |n\rangle_B\,\delta_{jk} \\ &= \sum_{j=0}^{d_A-1}\sum_{n=0}^{d_B-1} (\Phi_l)_{jn}\,|j\rangle_A \otimes |n\rangle_B = |\phi_l\rangle_{AB}\,.\end{aligned} \tag{2.18}$$

In other words, for each l, it is possible to find a linear operator V_l, as given in Eq. (2.17), such that every bipartite state $|\phi_l\rangle_{AB}$ can be written in the form $|\phi_l\rangle_{AB} = (\mathbb{I}_A \otimes V_l)\,|\Omega\rangle$. Besides this, note that:

$$\begin{aligned}(\langle j|_A \otimes \mathbb{I}_B)\,|\phi_l\rangle_{AB} &= \langle j|_A \otimes \mathbb{I}_B \left[\sum_{k=0}^{d_A-1}\sum_{n=0}^{d_B-1} (\phi_l)_{kn}\,|k\rangle_A \otimes |n\rangle_B\right] \\ &= \sum_{k=0}^{d_A-1}\sum_{n=0}^{d_B-1} (\phi_l)_{kn}\,|n\rangle_B\,\delta_{jk} \\ &= \left(\sum_{k=0}^{d_A-1}\sum_{n=0}^{d_B-1} (\phi_l)_{kn}\,|n\rangle_B \langle k|_A\right)|j\rangle_A = V_l\,|j\rangle_A\,.\end{aligned} \tag{2.19}$$

With the above observation and considering the decomposition shown in Eq. (2.15), we can rewrite the right-hand side of the Eq. (2.12) as follows:

$$\begin{aligned}(\langle j|_A \otimes \mathbb{I}_B)(\rho)(|n\rangle_A \otimes \mathbb{I}_B) &= (\langle j|_A \otimes \mathbb{I}_B)\left(\sum_{l=1}^{k} |\phi_l\rangle\langle\phi_l|_{AB}\right)(|n\rangle_A \otimes \mathbb{I}_B) \\ &= \sum_{l=1}^{k} \left[(\langle j|_A \otimes \mathbb{I}_B)\,|\phi_l\rangle_{AB}\right]\left[\langle\phi_l|_{AB}\,(|n\rangle_A \otimes \mathbb{I}_B)\right] \\ &= \sum_{l=1}^{k} V_l\,|j\rangle\langle n|_A\,V_l^\dagger\end{aligned} \tag{2.20}$$

Thus, replacing the result of Eq. (2.20) in Eq. (2.13), we have that,

$$\begin{aligned}\mathrm{id}_C \otimes \mathcal{E}(|\psi_i\rangle\langle\psi_i|_{CA}) &= \sum_{k,m=0}^{d_C-1}\sum_{j,n=0}^{d_A-1} (\Psi_i)_{kj}(\Psi_i)^*_{mn}\,|k\rangle\langle m|_C \otimes [(\langle j|_A \otimes \mathbb{I}_B) \\ &\quad \left(\sum_{l=1}^{k} |\phi_l\rangle\langle\phi_l|_{AB}\right)(|n\rangle_A \otimes \mathbb{I}_B)] \\ &= \sum_{k,m=0}^{d_C-1}\sum_{j,n=0}^{d_A-1} (\Psi_i)_{kj}(\Psi_i)^*_{mn}\,|k\rangle\langle m|_C \otimes \left(\sum_{l=1}^{k} V_l\,|j\rangle\langle n|_A\,V_l^\dagger\right) \\ &= \sum_{l=1}^{k}\left\{\mathrm{id}_C \otimes V_l\left[\sum_{k,m=0}^{d_C-1}\sum_{j,n=0}^{d_A-1} (\Psi_i)_{kj}(\Psi_i)^*_{mn}\,|k\rangle\langle m|_C \otimes |j\rangle\langle n|_A\right]\mathrm{id}_C \otimes V^\dagger\right\} \\ &= \sum_{l=1}^{k} \mathrm{id}_C \otimes V_l(|\psi_i\rangle\langle\psi_i|_{CA})\mathrm{id}_C \otimes V^\dagger{}_l.\end{aligned} \tag{2.21}$$

Finally, defining $K_l := \mathrm{id}_C \otimes V_l$ for all $l \in \{1, ..., k\}$, we can rewrite

$$\mathrm{id}_C \otimes \mathcal{E}(|\psi_i\rangle \langle\psi_i|_{CA}) = \sum_{l=1}^{k} K_l(|\psi_i\rangle \langle\psi_i|_{CA})K_l^\dagger \succeq 0, \tag{2.22}$$

where this follows from the fact that, for any $|\omega\rangle_{CB} \in \mathcal{H}_C \otimes \mathcal{H}_B$, we have, for each l, that

$$\langle\omega|_{CB} K_l(|\psi_i\rangle \langle\psi_i|_{CA})K_l^\dagger |\omega\rangle_{CB} = |\langle\omega|_{CB} K_l |\psi_i\rangle_{CA}|^2 \geq 0. \tag{2.23}$$

Concluding, in that way, the first half of the proof.

On the other side, suppose that $\mathcal{E}$ is CPTP. Then, it follows that, by the very definition of its Choi state ρ and by the fact that $\mathcal{E}$ is trace preserving,

$$\begin{aligned} \mathrm{Tr}_B(\rho) &= \mathrm{Tr}_B[\sum_{i,j=0}^{d_A-1} |i\rangle \langle j| \otimes \mathcal{E}(|i\rangle \langle j|)] \\ &= \sum_{i,j=0}^{d_A-1} |i\rangle \langle j| \otimes \mathrm{Tr}_B[\mathcal{E}(|i\rangle \langle j|)] \\ &= \sum_{i,j=0}^{d_A-1} |i\rangle \langle j| \otimes \mathrm{Tr}_A(|i\rangle \langle j|) \\ &= \sum_{i,j=0}^{d_A-1} |i\rangle \langle j| \, \delta_{ij} = \sum_{i=0}^{d_A-1} |i\rangle \langle i| = \mathbb{I}_A. \end{aligned} \tag{2.24}$$

Also, again by the very definition of the Choi state ρ, and using that $\mathcal{E}$ is completely positive, it follows that

$$\rho = (\mathrm{id}_A \otimes \mathcal{E}) |\Omega\rangle \langle\Omega| \succeq 0, \tag{2.25}$$

since it is a completely positive map acting on a positive operator of $\mathcal{L}(\mathcal{H}_A \otimes \mathcal{H}_A)$. ■

From the above connection between quantum channels and positive semidefinite operators, one can directly acknowledge that the set of quantum channels is also a convex set. This is one of the facts that, together with Choi's version of the aforementioned isomorphism, will allow us, as shown subsequently in this work, to frame the quantum channels employed in coarse-graining scenarios within a convex optimization and semidefinite programming perspective. Before digging into this, we show below another useful—and equivalent to this first one (49)—characterization of quantum channels in terms of a set of linear operators.

2.2.2 Kraus representation

Given that the Choi-Jamiołkowski isomorphism establishes a connection between a quantum channel and a positive semidefinite operator, there is another useful characterization of quantum channels in terms of a set of operators that obey specific constraints. Known as the Kraus representation (49, 37), in what follows, this characterization is presented through the so-called Kraus theorem.

Theorem 2 (Kraus theorem (37))**.** *A linear map $\mathcal{E} : \mathcal{L}(\mathcal{H}_A) \to \mathcal{L}(\mathcal{H}_B)$ is completely positive and trace preserving if and only if there exists a finite set of linear operators $\{K_i\}_{i=1}^r$, with each $K_i : \mathcal{H}_A \to \mathcal{H}_B$ known as a Kraus operator, such that, for all $X_A \in \mathcal{L}(\mathcal{H}_A)$, it holds:*

1. $\mathcal{E}(X_A) = \sum_{i=1}^r K_i X_A K_i^\dagger$;
2. $\sum_{i=1}^r K_i^\dagger K_i = \mathbb{I}_A$,

where r is the rank of the Choi operator associated with $\mathcal{E}$.

Proof. Firstly, suppose that $\mathcal{E}$ is a completely positive and trace preserving linear map. Then, by Theorem 1, it follows that its Choi-isomorphic operator $\rho \in \mathcal{L}(\mathcal{H}_A \otimes \mathcal{H}_B)$ is a positive semidefinite operator that obeys $\mathrm{Tr}_B(\rho) = \mathbb{I}_A$. Since ρ is positive semidefinite, it can be decomposed as

$$\rho = \sum_{i=1}^{r} |\omega_i\rangle \langle\omega_i|_{AB} , \tag{2.26}$$

where r is the rank of ρ and $\{|\omega_i\rangle_{AB}\}_{i=1}^r \subset \mathcal{H}_A \otimes \mathcal{H}_B$ is a set of orthogonal vectors. Then, considering the orthonormal basis α of $\mathcal{H}_A$, it follows, from Eq. (2.12), that

$$\begin{aligned}\mathcal{E}(|j\rangle \langle n|_A) &= (\langle j|_A \otimes \mathbb{I}_B)(\rho)(|n\rangle_A \otimes \mathbb{I}_B) \\ &= (\langle j|_A \otimes \mathbb{I}_B)(\sum_{i=1}^{r} |\omega_i\rangle \langle\omega_i|_{AB})(|n\rangle_A \otimes \mathbb{I}_B).\end{aligned} \tag{2.27}$$

Now, we can expand each $|\omega_i\rangle_{AB}$ in terms of the basis α and β as:

$$|\omega_i\rangle_{AB} = \sum_{j=0}^{d_A-1} \sum_{n=0}^{d_B-1} (\Omega_i)_{jn} |j\rangle_A \otimes |n\rangle_B . \tag{2.28}$$

Similar to the proof strategy used around Eq. (2.17), define $K_i : \mathcal{H}_A \to \mathcal{H}_B$ linear operators of the form:

$$K_i := \sum_{j=0}^{d_A-1} \sum_{n=0}^{d_B-1} (\Phi_i^T)_{nj} |n\rangle_B \langle j|_A = \sum_{j=0}^{d_A-1} \sum_{n=0}^{d_B-1} (\Omega_i)_{jn} |n\rangle_B \langle j|_A . \tag{2.29}$$

Moreover, by a similar result obtained in Eq. (2.17), it follows that

$$(\langle j|_A \otimes \mathbb{I}_B) |\omega_i\rangle_{AB} = K_i |j\rangle_A . \tag{2.30}$$

Thus, returning in Eq. (2.27), we have that

$$\begin{aligned}\mathcal{E}(|j\rangle \langle n|_A) &= (\langle j|_A \otimes \mathbb{I}_B)(\sum_{i=1}^{r} |\omega_i\rangle \langle\omega_i|_{AB})(|n\rangle_A \otimes \mathbb{I}_B) \\ &= \sum_{i=1}^{r} [(\langle j|_A \otimes \mathbb{I}_B) |\omega_i\rangle][\langle\omega_i|_{AB} (|n\rangle_A \otimes \mathbb{I}_B)] \\ &= \sum_{i=1}^{r} K_i |j\rangle \langle n|_A K_i^\dagger .\end{aligned} \tag{2.31}$$

Then, for any $X_A \in \mathcal{L}(\mathcal{H}_A)$, it follows by linearity of $\mathcal{E}$ that

$$\begin{aligned}\mathcal{E}(X_A) &= \mathcal{E}(\sum_{j,n=0}^{d_A-1}(X_A)_{jn}\left|j\right\rangle\left\langle n\right|_A) \\ &= \sum_{j,n=0}^{d_A-1}(X_A)_{jn}\mathcal{E}(\left|j\right\rangle\left\langle n\right|_A) \\ &= \sum_{i=1}^{r}\sum_{j,n=0}^{d_A-1}(X_A)_{jn}K_i(\left|j\right\rangle\left\langle n\right|_A)K_i^\dagger \\ &= \sum_{i=1}^{r}K_i(\sum_{j,n=0}^{d_A-1}(X_A)_{jn}\left|j\right\rangle\left\langle n\right|_A)K_i^\dagger \\ &= \sum_{i=1}^{r}K_iX_AK_i^\dagger. \end{aligned} \tag{2.32}$$

Furthermore, once $\mathcal{E}$ is trace preserving, it follows that

$$\begin{aligned}\mathrm{Tr}[\mathcal{E}(\left|j\right\rangle\left\langle k\right|_A)] &= \mathrm{Tr}\left[\sum_{i=1}^{r}K_i(\left|j\right\rangle\left\langle k\right|_A)K_i^\dagger\right] \\ &= \mathrm{Tr}\left[\left(\sum_{i=1}^{r}K_i^\dagger K_i\right)\left|j\right\rangle\left\langle k\right|_A\right] \\ &= \mathrm{Tr}(\left|j\right\rangle\left\langle k\right|_A) \\ \implies \sum_{i=1}^{r}K_i^\dagger K_i &= \mathbb{I}_A, \end{aligned} \tag{2.33}$$

and that concludes the first half of the proof.

Conversely, suppose that *1.* and *2.* hold true. Then, it follows that $\mathcal{E}$ is completely positive because, for any auxiliary Hilbert space $\mathcal{H}_C$ and $X_{CA} \in \mathcal{L}(\mathcal{H}_C \otimes \mathcal{H}_A)$ such that $X_{CA} \succeq 0$, it holds that

$$\begin{aligned}\mathrm{id}_C \otimes \mathcal{E}(X_{CA}) &= \sum_{i=1}^{r}(\mathbb{I}_C \otimes K_i)X_{CA}(\mathbb{I}_C \otimes K_i^\dagger) \\ &= \sum_{i=1}^{r}(\mathbb{I}_C \otimes K_i)X_{CA}(\mathbb{I}_C \otimes K_i)^\dagger \succeq 0, \end{aligned} \tag{2.34}$$

due to the fact that, for any $\left|\phi\right\rangle_{CB} \in \mathcal{H}_C \otimes \mathcal{H}_B$,

$$\left\langle\phi\right|_{CB}(\mathbb{I}_C \otimes K_i)X_{CA}(\mathbb{I}_C \otimes K_i)^\dagger\left|\phi\right\rangle_{CB} \geq 0. \tag{2.35}$$

Lastly, trace preservation follows because, for any $X_A \in \mathcal{L}(\mathcal{H}_A)$,

$$\begin{aligned}\mathrm{Tr}[\mathcal{E}(X_A)] &= \mathrm{Tr}\left(\sum_{i=1}^{r}K_iX_AK_i^\dagger\right) \\ &= \sum_{i=1}^{r}\mathrm{Tr}\left(K_i^\dagger K_iX_A\right) \\ &= \mathrm{Tr}\left(\sum_{i=1}^{r}K_i^\dagger K_iX_A\right) \\ &= \mathrm{Tr}(\mathbb{I}_AX_A) = \mathrm{Tr}(X_A). \end{aligned} \tag{2.36}$$

■

From the above characterization of quantum channels, it is instructive to highlight the conventional time evolution of a closed quantum system in the Schrödinger picture (31). Namely, an evolution dictated by a unitary dynamics,

$$\begin{aligned} \mathcal{U} : \mathcal{L}(\mathcal{H}_A) &\to \mathcal{L}(\mathcal{H}_A) \\ \rho &\mapsto U_t \rho U_t^\dagger, \end{aligned} \tag{2.37}$$

where $U_t = e^{-\frac{i}{\hbar}Ht}$ is the unitary time-evolution operator generated by a given Hamiltonian H, is a particular case of the Kraus representation with a single Kraus operator, that is, the unitary U_t itself. Upon this, we can observe that a given quantum channel $\mathcal{U}$ is unitary if and only if its Choi-isomorphic operator has rank equal to 1.

2.3 SEMIDEFINITE PROGRAMMING AND ELEMENTS OF CONVEXITY

After establishing two equivalent characterizations of quantum channels, we now give a glimpse of some key concepts of convex analysis, as well as promoting a brief introduction on semidefinite programming. Most of the following exposition can be found in textbooks such as (9), (38), (39), and also in the review paper (40). Following (49), throughout this section, we will use $\mathcal{X}$ and $\mathcal{Y}$ to denote finite-dimensional complex Euclidean spaces.

2.3.1 Convex sets

Let $\{x_1, ..., x_n\}$ be a finite set of vectors from $\mathcal{X}$. A vector

$$v = \sum_{i=1}^{n} \lambda_i x_i \quad \text{where} \quad \sum_{i=1}^{n} \lambda_i = 1 \quad \text{and} \quad \lambda_i \geq 0 \quad \text{for} \quad i = 1, ..., n$$

is called a *convex combination* of the vectors $x_1, ..., x_n$. This motivates the following definition of convexity for sets.

Definition 6. *A set $C \subseteq \mathcal{X}$ is convex if for any $x, y \in C$ and any $\lambda \in [0, 1]$, it holds that*

$$\lambda x + (1 - \lambda) y \in C.$$

In other words, a set C is convex if any line segment between two points in C lies entirely in C. Loosely speaking, a convex set is a set with "no holes", and this illustrate why a circle, a rectangle and a triangle are, intuitively, examples of convex sets in $\mathbb{R}^2$.

Having established a basic notion of convexity, an important class of convex sets are *convex cones*.

Definition 7. *A convex cone is a set $K \subseteq \mathcal{X}$ such that, for any two points $x, y \in \mathcal{X}$ and any two numbers $\alpha, \beta \geq 0$, it holds that $\alpha x + \beta y \in K$.*

A relevant example of convex cones for this work is the set of positive semidefinite operators. In fact, for any $P_1, P_2 \in \mathrm{Pos}(\mathcal{X})$ and for all $\alpha_1, \alpha_2 \geq 0$, it is straightforward to see, for any $|u\rangle \in \mathcal{X}$, that

$$\begin{aligned} \langle u| \left[\alpha_1 P_1 + \alpha_2 P_2\right] |u\rangle = \alpha_1 \langle u| P_1 |u\rangle + \alpha_2 \langle u| P_2 |u\rangle \geq 0 \\ \implies \alpha_1 P_1 + \alpha_2 P_2 \in \mathrm{Pos}(\mathcal{X}). \end{aligned}$$

In line with this, one can notice that both the set of quantum states $\mathcal{D}(\mathcal{X})$ and quantum channels $\mathcal{C}(\mathcal{X}, \mathcal{Y})$—the former being composed of positive semidefinite operators of unit trace, and the latter being isomorphically connected to positive semidefinite operators by Theorem 1—are valuable examples of convex sets.

2.3.2 An overview of semidefinite programming

The reason for beginning with the presentation of convex sets and convex cones is that semidefinite programming—one of the three pillars of this manuscript—is a branch of convex optimization concerned with optimization problems in which a linear objective function is maximized (or minimized) over the cone of positive semidefinite operators, subject to linear equality and inequality constraints. Within the field of mathematical programming, semidefinite programming is a relatively recent subfield, with its primordial roots traced back to the 1960s (23). Since that decade, interest in the field has grown substantially, giving rise to fruitful applications in a variety of areas of knowledge, such as combinatorial optimization, engineering, control theory, and optimal experiment design (16, 17, 15, 18, 19).

This amount of applications and studies directly involving semidefinite programming is mostly explained by the fact that most complex convex optimization problems handled in *semidefinite programs*—the name given to the class of optimization problems studied in semidefinite programming—can be efficiently solved, both in theory and in practice, by interior-point methods in polynomial time (14). Besides this, nowadays, efficient solvers and open source libraries have been widely used to disseminate and evaluate semidefinite programs on modern computers (10, 60).

In the context of quantum information, as mentioned previously, convexity and positive semidefinite objects arise naturally within the theory itself. As a consequence, many problems in the field involving finding optimal values—whether through minimization or maximization—can be cast directly as semidefinite programs. Its application landscape within quantum information science ranges from broadcasting (51) and the study of quantum correlations (57) to the derivation of bounds on entanglement distillation (55), a geometrical analysis of the stabilizer polytope (54), and the formulation of efficient methods to calculate and evaluate some useful norms of quantum channels (58). For more details and additional applications, we strongly recommend consulting Refs. (41, 40).

In what follows, we present the fundamental aspects of semidefinite programming, formalizing its main concepts, and discussing some of its properties. Most of the exposition is based on John Watrous' book (49), with some passages and insights drawn from the book by P. Skrzypczyk and D. Cavalcanti (41). We advise the reader that there are several formulations of the concept of semidefinite programming and semidefinite programs in the literature, each with definitions that may differ from one another. However, as noted in (49), even though they may appear different in essence, the underlying theory is the same. We choose to follow this particular formulation because it seems a bit more formal than the others.

We present below a definition of a semidefinite program.

Definition 8. *A semidefinite program is defined as a triple* (Φ, A, B)*, where* $\Phi : \mathcal{L}(\mathcal{X}) \to \mathcal{L}(\mathcal{Y})$ *is a Hermicity preserving linear map,* $A \in Herm(\mathcal{X})$ *and* $B \in Herm(\mathcal{Y})$*. Associated to this triple are two optimization problems. The first, referred to as the primal problem, is given by*

Primal Problem

$$\begin{aligned} &\textit{Given } A, B, \Phi \\ &\textit{Maximize} \quad \mathrm{Tr}(AX) \\ &\\ &\textit{Subject to} \quad \Phi(X) = B; \\ &\qquad\qquad\quad X \succeq 0. \end{aligned} \tag{2.38}$$

The second, referred to as the dual problem, is given by

Dual Problem

$$\begin{aligned} &\textit{Given } A, B, \Phi \\ &\textit{Minimize} \quad \mathrm{Tr}(BY) \\ &\\ &\textit{Subject to} \quad \Phi^{\dagger}(Y) \succeq A; \\ &\qquad\qquad\quad Y \in Herm(\mathcal{Y}). \end{aligned} \tag{2.39}$$

From this definition, and in view of the forms of the primal and the dual problems stated above, an important remark is that many semidefinite programs found in applications are typically presented without an explicit specification of a triple (Φ, A, B), as required by the definition above. Some of them—including those that we will address later in this work— are stated directly in a simplified form and require tedious algebraic manipulation of

the variables and the constraints in order to fit the standard definitional format. We advise the reader that the general method for formulating a triple (Φ, A, B) and establishing such an equivalence will not be covered here; instead, we refer to (49).

With these two problems in mind, we define the *primal feasible* set $\mathcal{A}$ as

$$\mathcal{A} := \{X \in \mathrm{Pos}(\mathcal{X}) : \Phi(X) = B\}, \tag{2.40}$$

and the *dual feasible* set $\mathcal{B}$ as

$$\mathcal{B} := \{Y \in \mathrm{Herm}(\mathcal{Y}) : \Phi^\dagger(Y) \succeq A\}. \tag{2.41}$$

In these problems, the function $X \mapsto \mathrm{Tr}(AX)$, from $\mathrm{Pos}(\mathcal{X})$ to $\mathbb{R}$, is called the *primal objective function*, and the function $Y \mapsto \mathrm{Tr}(BY)$, from $\mathrm{Herm}(\mathcal{Y})$ to $\mathbb{R}$, is the *dual objective function*. From these, we associate two *optimum values*—one for the primal problem and the other for the dual problem—defined[3], respectively, as

$$\alpha := \max_{X \in \mathcal{A}} \mathrm{Tr}(AX) \quad \text{and} \quad \beta := \min_{Y \in \mathcal{B}} \mathrm{Tr}(BY). \tag{2.42}$$

On one hand, if $\mathcal{A} \neq \emptyset$ and $\mathcal{B} \neq \emptyset$, both problems are called *feasible*. Moreover, if an operator $X \in \mathcal{A}$ satisfies $\alpha = \mathrm{Tr}(AX)$, it is called the *optimal primal variable*, and we will use the superscript "opt" to denote it as X^{opt}. Similarly, if there exists an operator $Y \in \mathcal{B}$ such that $\beta = \mathrm{Tr}(BY)$, it is called the *optimal dual variable* and will be denoted by Y^{opt}. On the other hand, if is the case that $\mathcal{A} = \emptyset$ and $\mathcal{B} = \emptyset$, then the SDP is said to be *infeasible*, and we define, by convention, $\alpha = -\infty$ and $\beta = \infty$. Based on the feasibility or infeasibility of an SDP, there exists an alternative formulation of semidefinite programs—which we will use in subsequent chapters of this work—that is concerned solely with finding, if it exists, a variable belonging to $\mathcal{A}$ or $\mathcal{B}$. That is, taking the primal problem as a reference, an *feasibility problem* is given, in its general form, by

Feasibility SDP

$$\begin{aligned} &\text{Given } B, \Phi \\ &\text{Find} \quad X \\ &\\ &\text{Subject to} \quad \Phi(X) = B; \\ &\qquad\qquad\quad X \succeq 0. \end{aligned} \tag{2.43}$$

This problem is equivalent to solving the primal problem (2.38) by defining A to be the null operator on $\mathcal{X}$, thereby yielding a constant (and thus omitted) primal objective function for any $X \in \mathcal{A}$.

[3] Here, without loss of generality, we have assumed the existence of the maximum and the minimum. An alternative definition, involving sup and inf, can be found in (49).

2.3.3 Duality in semidefinite programs

The concept of *duality* is one of the most relevant properties in semidefinite programming. It lies in the close relationship that exists between the primal and the dual problem of an SDP, particularly concerning the existence of general bounds—and, in specific cases, equivalence—between the optimal values α and β. Before delving into these aspects of duality involving the optimal values, we first showcase a Lagrange multiplier method for obtaining the dual problem of a general SDP starting from the primal problem, thereby highlighting the narrow connection between these two formulations. Since this procedure will be used in the next section only to pragmatically derive the formulation of the diamond norm adopted throughout this work, we omit some of its general properties and focus exclusively on its practical use. We also note that this method is based on, and described in more detail in Refs. (41, 39).

From the general primal problem shown in (2.38), the method begins attaching arbitrary Hermitian variables[4]—or, the so called *Lagrange multipliers*—for each equality and inequality constraint. More specifically, in order to become evident which dual variable correspond to each constraint, we rewrite (2.38) with the associate Lagrange multiplier side-by-side:

$$\begin{aligned} &\text{Given } A, B, \Phi \\ &\text{Maximize} \quad \mathrm{Tr}(AX) \end{aligned} \tag{2.44}$$

$$\begin{aligned} \text{Subject to} \quad \Phi(X) &= B \quad : Y \in \mathrm{Herm}(\mathcal{Y}) \\ X &\succeq 0 \quad : Z \in \mathrm{Herm}(\mathcal{X}) \end{aligned}$$

From the above designation, we thus define the *Lagrangian function* $\mathcal{L} : \mathcal{A} \times \mathrm{Herm}(\mathcal{Y}) \times \mathrm{Herm}(\mathcal{X}) \to \mathbb{R}$ as

$$\mathcal{L} = \mathcal{L}(X, Y, Z) := \mathrm{Tr}(AX) + \mathrm{Tr}[(B - \Phi(X))Y] + \mathrm{Tr}(XZ). \tag{2.45}$$

The logic behind this construction of the Lagrangian function can be split into two steps: (i) first, each constraint is multiplied by its respective dual variable and a trace is taken, yielding new terms; and (ii) if the initial problem is a maximization, these new terms are added to the original objective function, whereas if the initial problem is a minimization, they are subtracted from it. The reason why these new terms added (or subtracted) in a form proportional to traces is that, for SDPs, the trace[5] of an operator plays the same

[4] In the case of operator equality or inequality, the dual variables designated are Hermitian operators; however, in cases where the equality or inequality constraints are scalar, real numbers are used as dual variables.

[5] To make this clear, the trace terms could be viewed as the Hilbert-Schimidt inner products between the Hermitian dual variables and the corresponding constraints operators.

role as the inner products of vectors does for linear programs (41): it defines the most general linear function of the constraints that can be added.

From these observations, and by inspecting the right-hand side of (2.45), we now impose constraints on the dual variables in order to the Lagrangian $\mathcal{L}$ to upper bound the original objective function. Since the first term in the sum following the primal objective function vanishes for any $X \in \mathcal{A}$, in order to have $\mathcal{L} \geq \mathrm{Tr}(AX)$ for all $X \in \mathcal{A}$ we must require that $\mathrm{Tr}(ZX) \geq 0$. This conduction holds for all $X \in \mathcal{A}$ if and only if Z is also a positive semidefinite operator (49). Therefore, the first constraint on the dual variables is

$$Z \succeq 0. \tag{2.46}$$

Now, rearranging the terms on the right-hand side of (2.45), we obtain

$$\begin{aligned}\mathcal{L} &= \mathrm{Tr}(AX) + \mathrm{Tr}(YB) + \mathrm{Tr}(ZX) - \mathrm{Tr}[Y\Phi(X)] \\ &= \mathrm{Tr}(AX) + \mathrm{Tr}(YB) + \mathrm{Tr}(ZX) - \mathrm{Tr}\Big[\Phi^\dagger(Y)X\Big] \\ &= \mathrm{Tr}\Big[X(A + Z - \Phi^\dagger(Y))\Big] + \mathrm{Tr}(BY). \end{aligned} \tag{2.47}$$

From this expression,we see that the Lagrangian $\mathcal{L}$ can be made independent of the primal variable X by imposing a second constraint on the dual variable Z, namely,

$$Z = \Phi^\dagger(Y) - A. \tag{2.48}$$

Consequently, when the dual variables satisfy the constraints (2.46) and (2.48), the Lagrangian reduces, for all $X \in \mathcal{A}$, to

$$\mathcal{L} = \mathrm{Tr}(BY). \tag{2.49}$$

From this, by recognizing that Z is a slack variable—that is, a variable that does not appear in the objective function or, in this case, in the resulting Lagrangian—and by combining (2.46) and (2.48), we arrive at

$$Z = \Phi^\dagger(Y) - A \succeq 0 \Leftrightarrow \Phi^\dagger(Y) \succeq A, \tag{2.50}$$

which is the final constraint imposed on the dual variables. Finally, with the final observation that the tightest upper bound on the primal objective function is obtained by minimizing the Lagrangian (41), shown in (2.49), over the Hermitian dual variable Y and the slack variable Z subject to the imposed constraints (2.46), (2.48), and (2.50), we thus arrive at

$$\begin{aligned} &\text{Given } A, B, \Phi \\ &\text{Minimize} \quad \mathcal{L} = \mathrm{Tr}(BY) \\ \\ &\text{Subject to} \quad \Phi^\dagger(Y) \succeq A; \\ &\qquad\qquad\quad Y \in \mathrm{Herm}(\mathcal{Y}), \end{aligned}$$

which is precisely the dual problem stated earlier in (2.39).

2.3.3.1 Weak duality

Having uncovered the direct connection between the primal and the dual problems of a general SDP, we will now return to the important properties relating the primal optimum value, α, and the dual optimum value, β. The first of these, called *weak duality*, states that $\alpha \leq \beta$ for any semidefinite program (Φ, A, B). For the cases where $\mathcal{P} = \emptyset$ (which implies that $\alpha = -\infty$) or $\mathcal{B} = \emptyset$ (which implies that $\beta = \infty$), weak duality holds trivially. However, when we restrict to the case in which both $\mathcal{A}$ and $\mathcal{B}$ are nonempty, weak duality follows by observing that

$$\begin{aligned} \alpha = \mathrm{Tr}\Big(AX^{\mathrm{opt}}\Big) &\leq \mathrm{Tr}\Big[\Phi^\dagger(Y^{\mathrm{opt}})X^{\mathrm{opt}}\Big] \qquad (2.51) \\ &= \mathrm{Tr}\Big[Y^{\mathrm{opt}}\Phi(X^{\mathrm{opt}})\Big] \\ &= \mathrm{Tr}\Big(Y^{\mathrm{opt}}B\Big) \\ &= \mathrm{Tr}\Big(BY^{\mathrm{opt}}\Big) = \beta, \qquad (2.52) \end{aligned}$$

where we used, for any $Y \in \mathcal{B}$, the fact that

$$\begin{aligned} \Phi^\dagger(Y) - A \succeq 0 &\implies \mathrm{Tr}\{[\Phi^\dagger(Y) - A]X\} \geq 0 \quad \text{for all } X \succeq 0 \\ &\implies \mathrm{Tr}\Big[\Phi^\dagger(Y)X\Big] \geq \mathrm{Tr}(AX). \end{aligned}$$

2.3.3.2 Strong duality

The other property, called *strong duality* and expressed as $\alpha = \beta$, is, as the name suggests, a stronger condition that may hold between the primal and dual optimum values. While weak duality holds for every semidefinite program (Φ, A, B), strong duality is guaranteed only for semidefinite programs that satisfy the conditions of Slater's theorem for semidefinite programs.

Theorem 3 (Slater's theorem)**.** *Let (Φ, A, B) be a semidefinite program, and let $\mathcal{A}, \mathcal{B}, \alpha$ and β be defined as above. Then, the following two implications hold:*

1. *If $\mathcal{A} \neq \emptyset$ and there exists $Y \in Herm(\mathcal{Y})$ such that $\Phi^\dagger(Y) \succ A$, then strong duality holds, $\alpha = \beta$, and there exists an optimal primal variable X^{opt}.*
2. *If $\mathcal{B} \neq \emptyset$ and there exists $X \in Pos(\mathcal{X})$ such that $\Phi(X) = B$ and $X \succ 0$, then strong duality holds, $\alpha = \beta$, and there exists an optimal dual variable Y^{opt}.*

Proof. See (49, Theorem 7.6) for a complete proof. ■

From this remarkable theorem, an important note is that, in practice, various problems in quantum information that can be cast as a semidefinite program satisfy the conditions above, and strong duality holds (41). Moreover, as pinpointed in (49),"if one does not *try* to make strong duality fail, it will probably hold", referring to the fact

that semidefinite programs for which strong duality does not hold are typically explicitly handcrafted to show that exceptions exist to the conditions enunciated in the Slater's theorem, as also mentioned in (41). All in all, strong duality is basically the rule.

2.4 THE DIAMOND NORM

Once we have explored the formal definition of quantum channels as well as its the main characterizations that we are going to employ, it is reasonable—for the purposes of this work—to introduce a paradigmatic function designed to measure distances between quantum channels: the diamond norm (44) (also commonly referred to as the completely bounded trace norm). When approached in the quantum information realm, its domain of applicability ranges from: (i) a quantitative characterization of non-physical linear maps via the distance with quantum channels (46) to (ii) an efficient way to quantify the divisibility aspects of quantum dynamics, as seen in Ref. (47), and (iii) an operational tool to unveil how well a quantum channel can detect coherence (48).

Because we are interested in an operational use of the diamond norm to study a restricted type of linear maps, namely, completely positive and trace preserving maps, which are a special case of Hermitian preserving maps, to start our construction, the following characterization needs to be considered (49, 46).

Definition 9 (Diamond norm for CPTP maps)**.** *Let $\Phi \in \mathcal{C}(A, B)$. We define the diamond norm of Φ as*

$$\|\Phi\|_\diamond = \max_{\rho_{DA} \in \mathcal{D}(\mathcal{H}_D \otimes \mathcal{H}_A)} \|id_D \otimes \Phi(\rho_{DA})\|_1, \tag{2.53}$$

where $\mathcal{H}_D$ is any Hilbert space isomorphic to $\mathcal{H}_A$.

By considering the formulation of the trace norm shown in ref. (41), for any $\mathcal{H}_C$ and any $X \in \mathcal{L}(\mathcal{H}_C)$, given by

$$\|X\|_1 = \max_{-\mathbb{I}_C \preceq Z_C \preceq \mathbb{I}_C} \mathrm{Tr}(Z_C X), \tag{2.54}$$

we can straightforwardly use it to rewrite the trace norm on right-hand side of Eq. (2.53), thereby yielding another useful formulation of the diamond norm,

$$\|\Phi\|_\diamond = \max_{\substack{-\mathbb{I}_{DB} \preceq Z_{DB} \preceq \mathbb{I}_{DB}; \\ \rho_{DA} \in \mathcal{D}(\mathcal{H}_D \otimes \mathcal{H}_A)}} \mathrm{Tr}\{Z_{DB}[(\mathrm{id}_D \otimes \Phi)(\rho_{DA})]\}, \tag{2.55}$$

which is a formulation that also appears in (41) and in (46), for any Hilbert space $\mathcal{H}_D$ that is a copy of the space $\mathcal{H}_A$.

Although the expression in Eq. (2.55) may not look like a primal SDP problem, in the next section, we derive a characterization in terms of a semidefinite program for the diamond norm. We advise the reader that most of the construction that follows is

borrowed from Section 7.7 of Ref. (41) and has been adapted only to match the notations and the formulation of the Choi-isomorphism (Definition 5) adopted throughout this work. Besides this, although the primal and the dual SDP characterizations that follow are very well known in the literature, we claim that the step-by-step calculation we present to derive them—which, usually, does not appear explicitly in textbooks in the area—has a meaningful didactic value for a first contact by an inexperienced reader in the following topics. For experienced readers, we strongly recommend to skip to the next chapter.

2.4.1 SDP characterizations

As previously mentioned, the formulation (2.55) of the diamond norm shows nonlinearity in terms of the variables in the main expression on the right-hand side, making it unsuitable for a direct SDP formulation. In order to circumvent this issue, we present below a construction that, by a clever change of variables, indeed makes it possible to state this formulation as a primal problem of a semidefinite program.

To do so, and in order to explicitly expose the objective function (namely, the expression on the right-hand side of Eq. (2.55)) and the variables' constraints that will be manipulate throughout the remainder of this section, we adopt the format employed to display the semidefinite programs in Section 2.3 to rewrite the formulation (2.55). We emphasize, however, that the resulting expression does not yet constitute a semidefinite program. That is, letting $\Phi : \mathcal{L}(\mathcal{H}_A) \to \mathcal{L}(\mathcal{H}_B)$ be a quantum channel, we consider henceforward that its diamond norm is given by the program:

$$\begin{aligned} &\text{Given } \Phi \\ &||\Phi||_\diamond = \text{Maximize} \quad \text{Tr}\{Z_{DB}[(\text{id}_D \otimes \Phi)(\rho_{DA})]\} \qquad (2.56) \\ &\text{Subject to} \quad -\mathbb{I}_{DB} \preceq Z_{DB} \preceq \mathbb{I}_{DB}; \qquad (2.57) \\ &\qquad\qquad \rho_{DA} \succeq 0, \quad \text{Tr}(\rho_{DA}) = 1. \qquad (2.58) \end{aligned}$$

2.4.1.1 Primal formulation

To begin with, we will reformulate the objective function (2.56) in terms of the Choi isomorphism (Definition 5). Namely, letting $X_\Phi \in \mathcal{L}(\mathcal{H}_A \otimes \mathcal{H}_B)$ be the Choi-isomorphic operator associated with Φ, and extending by linearity the result of expression (2.3) to a tensor product space, we can rewrite the expression between the square brackets on the right-hand side of (2.56) as

$$\begin{aligned} \text{id}_D \otimes \Phi(\rho_{DA}) &= \text{Tr}_A[(\mathbb{I}_D \otimes X_\Phi)(\rho_{DA}^{T_A} \otimes \mathbb{I}_B)] \\ &= \text{Tr}_A[(\rho_{DA}^{T_A} \otimes \mathbb{I}_B)(\mathbb{I}_D \otimes X_\Phi)], \qquad (2.59) \end{aligned}$$

where the last equality follows from a direct calculation and the respective products by identities. From this, we can rewrite the entire objective function (right-hand side of (2.56)) as

$$\mathrm{Tr}\{Z_{DB}[(\mathrm{id}_D \otimes \Phi)(\rho_{DA})]\} = \mathrm{Tr}\Big[(\mathbb{I}_A \otimes Z_{DB})(\rho_{DA}^{T_A} \otimes \mathbb{I}_B)(\mathbb{I}_D \otimes X_\Phi)\Big]. \tag{2.60}$$

Defining

$$Y_{AB} := \mathrm{Tr}_D[(\mathbb{I}_A \otimes Z_{DB})(\rho_{DA}^{T_A} \otimes \mathbb{I}_B)] \in \mathcal{L}(\mathcal{H}_A \otimes \mathcal{H}_B), \tag{2.61}$$

we can combine the two variables, Z_{DB} and ρ_{DA}, into a single operator variable $Y_{AB} \in \mathcal{L}(\mathcal{H}_A \otimes \mathcal{H}_B)$. With this in hands, we can thus write the objective function given in (2.60) solely as

$$\mathrm{Tr}(Y_{AB} X_\Phi). \tag{2.62}$$

At this point, our goal will be to characterize, based on the constraints (2.57) and (2.58) of the initial variables Z_{DB} and ρ_{DA}, respectively, the constraints that are satisfied by the new variable Y_{AB} and to show that they are, at first glance, linear equality (and inequality) constraints. The latter, as shown below, will allow us to directly embed it inside a semidefinite program.

Before discussing this in detail, it is reasonable to first consider the following auxiliary lemma, whose proof will give us a tool to remove the partial transpose of ρ_{DA} on the right-hand side of expression (2.61) by performing a partial trace and introducing an unnormalized maximally entangled state.

Lemma 1. *Let $\mathcal{H}_A$ and $\mathcal{H}_D$ be finite-dimensional isomorphic Hilbert spaces, and let $K_{DA} \in \mathcal{L}(\mathcal{H}_D \otimes \mathcal{H}_A)$ be any linear operator. Let $\mathcal{H}_{A'} \simeq \mathcal{H}_A$ be a copy of $\mathcal{H}_A$. Fix (preferred) orthonormal bases $\{|k\rangle_A\}_{k=1}^{d_A}$ of $\mathcal{H}_A$, and the corresponding orthonormal basis $\{|k\rangle_{A'}\}_{k=1}^{d_A}$ of $\mathcal{H}_{A'}$, where $d_A = dim(\mathcal{H}_A) = dim(\mathcal{H}_{A'})$. Define $|\Omega\rangle_{AA'} = \sum_{k=1}^{d_A} |k\rangle_A \otimes |k\rangle_{A'}$, so that $|\Omega\rangle\langle\Omega|_{AA'} = \sum_{k,r=1}^{d_A} |k\rangle\langle r|_A \otimes |k\rangle\langle r|_{A'}$. Then, it holds that*

$$\mathrm{Tr}_A[(K_{DA} \otimes \mathbb{I}_{A'})(\mathbb{I}_D \otimes |\Omega\rangle\langle\Omega|_{AA'})] = K_{DA}^{T_A}. \tag{2.63}$$

Proof. Let $d_D = \dim(\mathcal{H}_D)$ and $\{j\}_{j=1}^{d_D}$ be a basis of $\mathcal{H}_D$. In terms of this basis and the basis $\{k\}_{k=1}^{d_A}$ of $\mathcal{H}_A$, we can expand K_{AD} explicitly as

$$K_{DA} = \sum_{i,j=1}^{d_D} \sum_{l,m=1}^{d_A} (K)_{ijlm} |i\rangle\langle j|_D \otimes |l\rangle\langle m|_A, \tag{2.64}$$

where K denotes the $d_D^2 \times d_A^2$ matrix whose entries are the coefficients of the operator K_{DA} in these bases. Upon this, we have explicitly that

$$\begin{aligned}
&\mathrm{Tr}_A[(K_{DA}\otimes \mathbb{I}_{A'})(\mathbb{I}_D \otimes |\Omega\rangle\langle\Omega|_{AA'}]) = \\
&= \mathrm{Tr}_A\left[\left(\sum_{i,j=1}^{d_D}\sum_{l,m=1}^{d_A}(K)_{ijlm}\,|i\rangle\langle j|_D \otimes |l\rangle\langle m|_A \otimes \mathbb{I}_{A'}\right)\left(\mathbb{I}_D \otimes \sum_{k,r=1}^{d_A}|k\rangle\langle r|_A \otimes |k\rangle\langle r|_{A'}\right)\right] \\
&= \mathrm{Tr}_A\left(\sum_{i,j=1}^{d_D}\sum_{l,m=1}^{d_A}\sum_{k,r=1}^{d_A}(K)_{ijlm}\delta_{mk}\,|i\rangle\langle j|_D \otimes |l\rangle\langle r|_A \otimes |k\rangle\langle r|_{A'}\right) \\
&= \sum_{l=1}^{d_A}\sum_{i,j=1}^{d_D}\sum_{k,r=1}^{d_A}(K)_{ijlk}\delta_{lr}\,|i\rangle\langle j|_D \otimes |k\rangle\langle r|_{A'} = \sum_{i,j=1}^{d_D}\sum_{k,r=1}^{d_A}(K)_{ijrk}\,|i\rangle\langle j|_D \otimes |k\rangle\langle r|_{A'}\,.
\end{aligned} \tag{2.65}$$

Since the space $\mathcal{H}_{A'}$ is a copy of $\mathcal{H}_A$ and A' in this expression is a dummy label, it can be changed to A. We then conclude that

$$\begin{aligned}
\mathrm{Tr}_A[(K_{DA}\otimes \mathbb{I}_{A'})(\mathbb{I}_D \otimes |\Omega\rangle\langle\Omega|_{AA'}]) &= \sum_{i,j=1}^{d_D}\sum_{k,r=1}^{d_A}(K)_{ijrk}\,|i\rangle\langle j|_D \otimes |k\rangle\langle r|_A \\
&= \sum_{i,j=1}^{d_D}\sum_{k,r=1}^{d_A}(K^{T_A})_{ijkr}\,|i\rangle\langle j|_D \otimes |k\rangle\langle r|_A \\
&= K_{DA}^{T_A}. \qquad \blacksquare
\end{aligned}$$

Using the result of Lemma 1, we can rearrange the right-hand side of expression (2.61) to write Y_{AB} as

$$\begin{aligned}
Y_{AB} &= \mathrm{Tr}_D[(\mathbb{I}_A \otimes Z_{DB})(\rho_{DA}^{T_A}\otimes \mathbb{I}_B)] \\
&= \mathrm{Tr}_D\{(\mathbb{I}_A \otimes Z_{DB})\{\mathrm{Tr}_A[(\rho_{DA}\otimes \mathbb{I}_{A'})(\mathbb{I}_D \otimes |\Omega\rangle\langle\Omega|_{AA'})]\}\otimes \mathbb{I}_B\} \\
&= \mathrm{Tr}_{AD}\{(\mathbb{I}_{AA'} \otimes Z_{DB})[(\rho_{DA}\otimes \mathbb{I}_{A'})(\mathbb{I}_D \otimes |\Omega\rangle\langle\Omega|_{AA'})]\otimes \mathbb{I}_B\} \\
&= \mathrm{Tr}_{AD}[(\mathbb{I}_{AA'} \otimes Z_{DB})(\rho_{DA}\otimes \mathbb{I}_{A'B})(\mathbb{I}_D \otimes |\Omega\rangle\langle\Omega|_{AA'}\otimes \mathbb{I}_B)] \\
&= \mathrm{Tr}_{AD}[(|\Omega\rangle\langle\Omega|_{AA'} \otimes Z_{DB})(\rho_{DA}\otimes \mathbb{I}_{A'B})].
\end{aligned} \tag{2.66}$$

Now, based on the last expression obtained for Y_{AB}, by defining a class of maps

$$\begin{aligned}
\Gamma_\sigma : \mathcal{L}(\mathcal{H}_D \otimes \mathcal{H}_B) &\to \mathcal{L}(\mathcal{H}_A \otimes \mathcal{H}_B) \\
M_{DB} &\mapsto \mathrm{Tr}_{AD}[(|\Omega\rangle\langle\Omega|_{AA'} \otimes M_{DB})(\sigma \otimes \mathbb{I}_{A'B})],
\end{aligned} \tag{2.67}$$

where σ is a positive operator on $\mathcal{H}_D \otimes \mathcal{H}_A$, we can directly recognize, from the right-hand side of (2.66), that

$$Y_{AB} = \Gamma_{\rho_{DA}}(Z_{DB}). \tag{2.68}$$

In other words, we have shown that there exists a map $\Gamma_{\rho_{DA}}(\cdot)$ that maps the initial variable Z_{DB} to the new one, Y_{AB}. Since our goal is, to recapitulate, to characterize the

constraints on the new variable based on the constraints (2.57) and (2.58) over the old ones, we can thus use the fact that $\Gamma_{\rho_{DA}}$ is a map between these variables and apply it to deal with the constraints themselves.

Before doing so, it is useful to highlight some properties of the map $\Gamma_{\rho_{DA}}$. By the very linearity of the partial trace and the tensor product operation, we can conclude that Γ_σ is a linear map for any positive operator $\sigma \in \mathcal{L}(\mathcal{H}_D \otimes \mathcal{H}_A)$. Moreover, letting $M_{DB} \in \mathcal{L}(\mathcal{H}_D \otimes \mathcal{H}_B)$ and $N_{A'B} \in \mathcal{L}(\mathcal{H}_{A'} \otimes \mathcal{H}_B)$ be positive semidefinite operators, one observes that

$$\begin{aligned}
\langle N_{A'B}, \Gamma_\sigma(M_{DB})\rangle_{HS} &= \mathrm{Tr}\Big[N_{A'B}^\dagger \Gamma_\sigma(M_{DB})\Big] \\
&= \mathrm{Tr}\{N_{A'B}\,\mathrm{Tr}_{AD}[(|\Omega\rangle\langle\Omega|_{AA'} \otimes M_{DB})(\sigma \otimes \mathbb{I}_{A'B})]\} \\
&= \mathrm{Tr}[(|\Omega\rangle\langle\Omega|_{AA'} \otimes M_{DB})(\sigma \otimes \mathbb{I}_{A'B})(\mathbb{I}_{DA} \otimes N_{A'B})] \\
&= \mathrm{Tr}[(|\Omega\rangle\langle\Omega|_{AA'} \otimes M_{DB})(\sigma \otimes N_{A'B})] \\
&= \langle |\Omega\rangle\langle\Omega|_{AA'} \otimes M_{DB}, \sigma \otimes N_{A'B}\rangle_{HS} \geq 0,
\end{aligned} \tag{2.69}$$

because both $|\Omega\rangle\langle\Omega|_{AA'} \otimes M_{DB}$ and $\sigma \otimes N_{A'B}$ are positive semidefinite, and the Hilbert-Schimidt inner product of two positive semidefinite operators is always non-negative (49). Based on this, we can conclude that

$$\langle N_{A'B}, \Gamma_\sigma(M_{DB})\rangle_{HS} \succeq 0 \quad \text{for all } N_{A'B} \succeq 0, \tag{2.70}$$

which implies that $\Gamma_\sigma(M_{DB})$ is a positive semidefinite operator on $\mathcal{H}_A \otimes \mathcal{H}_B$ for every positive semidefinite operator $M_{DB} \in \mathcal{L}(\mathcal{H}_D \otimes \mathcal{H}_B)$. Hence, by Definition 1, Γ_σ is a positive (linear) map.

Now, with these two properties of the map Γ_σ in hand, together with the identity (2.66), we are in a position to carefully examine the constraints satisfied by the variable Z_{DB} and thereby derive the corresponding constraints on the variable Y_{AB}. Firstly, from the left-hand side of (2.57), we have that

$$Z_{DB} + \mathbb{I}_{DB} \succeq 0. \tag{2.71}$$

Since $\Gamma_{\rho_{DA}}$ is a positive map, it implies that

$$\Gamma_{\rho_{DA}}(Z_{DB} + \mathbb{I}_{DB}) \succeq 0. \tag{2.72}$$

Explicitly, exploring the linearity of $\Gamma_{\rho_{DA}}$ on the left-hand side of the above expression gives

$$\Gamma_{\rho_{DA}}(Z_{DB} + \mathbb{I}_{DB}) = \Gamma_{\rho_{DA}}(Z_{DB}) + \Gamma_{\rho_{DA}}(\mathbb{I}_{DB}) = Y_{AB} + \Gamma_{\rho_{DA}}(\mathbb{I}_{DB}). \tag{2.73}$$

Denoting the reduction of ρ_{DA} on $\mathcal{D}(\mathcal{H}_A)$ as $\rho_A = \mathrm{Tr}_D(\rho_{DA})$, one can verify by direct calculation that

$$\begin{aligned}\Gamma_{\rho_{DA}}(\mathbb{I}_{DB}) &= \mathrm{Tr}_{AD}[(|\Omega\rangle\langle\Omega|_{AA'} \otimes \mathbb{I}_{DB})(\rho_{DA} \otimes \mathbb{I}_{A'B})] \\ &= \mathrm{Tr}_D\{\mathrm{Tr}_A[(\rho_{DA} \otimes \mathbb{I}_{A'})(\mathbb{I}_D \otimes |\Omega\rangle\langle\Omega|_{AA'})]\} \otimes \mathbb{I}_B \\ &= \mathrm{Tr}_D(\rho_{DA}^{T_A}) \otimes \mathbb{I}_B \\ &= [\mathrm{Tr}_D(\rho_{DA})]^T \otimes \mathbb{I}_B = \rho_A^T \otimes \mathbb{I}_B, \end{aligned} \tag{2.74}$$

where the last equalities follow from a direct use of Lemma 1 and from the fact that the partial trace and the partial transposition operation, when acting on different subsystems, do commute. Then, returning with this result on the right-hand side of Eq. (2.73) and together with expression (2.72), by defining a second new variable as $\omega_A := \rho_A^T$, we can conclude that

$$\Gamma_{\rho_{DA}}(Z_{DB} + \mathbb{I}_{DB}) = Y_{AB} + \omega_A \otimes \mathbb{I}_B \succeq 0 \implies Y_{AB} \succeq -(\omega_A \otimes \mathbb{I}_B), \tag{2.75}$$

thus establishing the first constraint satisfied by Y_{AB}. Regarding the other constraint imposed on it, now looking at the right-hand side of (2.57), we have that

$$\mathbb{I}_{DB} - Z_{DB} \succeq 0, \tag{2.76}$$

and, by a similar argument, we obtain

$$\Gamma_{\rho_{DA}}(\mathbb{I}_{DB} - Z_{DB}) = \omega_A \otimes \mathbb{I}_B - Y_{AB} \succeq 0 \implies Y_{AB} \preceq (\omega_A \otimes \mathbb{I}_B).$$

Moreover, since by the constraints in (2.58) the initial variable ρ_{DA} is a valid density operator on $\mathcal{H}_D \otimes \mathcal{H}_A$, and the second new variable ω_A has been defined as the transpose of its reduction to A, it also implies that ω_A is itself a density operator.

To summarize, from the initial pair of variables (Z_{DB}, ρ_{DA}) satisfying the constraints (2.57) and (2.58), by the action of the map $\Gamma_{\rho_{DA}}$, we have obtained a new pair of variables, (Y_{AB}, ω_A), satisfying

$$-(\omega_A \otimes \mathbb{I}_B) \preceq Y_{AB} \preceq (\omega_A \otimes \mathbb{I}_B) \tag{2.77}$$

and

$$\mathrm{Tr}(\omega_A) = 1, \quad \omega_A \succeq 0. \tag{2.78}$$

To end this construction, with the purpose of demonstrating the equivalence between these two pairs of variables, we will show how to recover the pair (Z_{DB}, ρ_{DA}), which obey the constraints (2.57) and (2.58), when one starts from the pair (Y_{AB}, ω_A), obeying (2.77) and (2.78). For this, first, given ω_A obeying (2.78), by defining $\rho_{DA} \in \mathcal{D}(\mathcal{H}_D \otimes \mathcal{H}_A)$ as any bipartite density operator extension of ω_A^T such that $\mathrm{Tr}_D(\rho_{DA}) = \omega_A^T$, the initial constraint (2.58) is recovered. In line with this but now regarding the variable Z_{DB}, given Y_{AB}, define it as

$$Z_{DB} := (\omega_A^{-\frac{1}{2}} \otimes \mathbb{I}_B) Y_{AB} (\omega_A^{-\frac{1}{2}} \otimes \mathbb{I}_B) \in \mathcal{L}(\mathcal{H}_D \otimes \mathcal{H}_B), \tag{2.79}$$

where $\omega_A^{-\frac{1}{2}}$ is defined only upon the support of ω_A, and it was used explicitly the fact that $\mathcal{H}_D \simeq \mathcal{H}_A$.

Next, given $\beta_D \in \mathcal{L}(\mathcal{H}_D)$ such that $\beta_D \succeq 0$, define the map $\mathcal{O}_\beta$ as

$$\begin{aligned} \mathcal{O}_\beta :& \mathcal{L}(\mathcal{H}_A \otimes \mathcal{H}_B) \to \mathcal{L}(\mathcal{H}_D \otimes \mathcal{H}_B) \\ & M_{AB} \mapsto (\beta_D^{-\frac{1}{2}} \otimes \mathbb{I}_B) M_{AB} (\beta_D^{-\frac{1}{2}} \otimes \mathbb{I}_B). \end{aligned} \tag{2.80}$$

Since this a conjugation, the map is linear and positive, and one can notice that

$$Z_{DB} = \mathcal{O}_{\omega_A}(Y_{AB}). \tag{2.81}$$

Then, by a similar line of reasoning pursued around Eq. (2.72), by first examining the left-hand side of (2.77), we have that

$$\begin{aligned} \mathcal{O}_{\omega_A}(Y_{AB} + \omega_A \otimes \mathbb{I}_B) &= \mathcal{O}_{\omega_A}(Y_{AB}) + \mathcal{O}_{\omega_A}(\omega_A \otimes \mathbb{I}_B) \\ &= Z_{DB} + (\omega_A^{-\frac{1}{2}} \otimes \mathbb{I}_B)(\omega_A \otimes \mathbb{I}_B)(\omega_A^{-\frac{1}{2}} \otimes \mathbb{I}_B) \\ &= Z_{DB} + \mathbb{I}_{DB} \succeq 0 \\ &\implies Z_{DB} \succeq -\mathbb{I}_{DB}, \end{aligned} \tag{2.82}$$

and, by looking at the right-hand side of (2.77), an analogous calculation shows that

$$\begin{aligned} \mathcal{O}_{\omega_A}(\omega_A \otimes \mathbb{I}_B - Y_{AB}) &= \mathcal{O}_{\omega_A}(\omega_A \otimes \mathbb{I}_B) - \mathcal{O}_{\omega_A}(Y_{AB}) \\ &= \mathbb{I}_{DB} - Z_{DB} \succeq 0 \\ &\implies Z_{DB} \preceq \mathbb{I}_{DB}. \end{aligned} \tag{2.83}$$

Taken together with (2.82), this precisely recovers the constraints shown in (2.57), and therefore establishes the equivalence between these two pairs of variables.

Recapitulating, from the above calculations we have shown that: (i) any pair of variables (Z_{DB}, ρ_{DA}), where $\rho_{DA} \in \mathcal{D}(\mathcal{H}_D \otimes \mathcal{H}_A)$ and $-\mathbb{I}_{DB} \preceq Z_{DB} \preceq \mathbb{I}_{DB}$, is mapped, via $\Gamma_{\rho_{DA}}$, to a new pair of variables (Y_{AB}, ω_A) such that $-(\omega_A \otimes \mathbb{I}_B) \preceq Y_{AB} \preceq (\omega_A \otimes \mathbb{I}_B)$ and $\omega_A \in \mathcal{D}(\mathcal{H}_A)$; and (ii) any pair of variables (Y_{AB}, ω_A), using the (inverse) map $\mathcal{O}_{\omega_A}$, is mapped back to the original pair (Z_{DB}, ρ_{DA}), with both pairs satisfying their respective constraints. Thus, this shows—together with the expression of the objective function presented in (2.62)—that the initial non-linear formulation (2.55) of the diamond norm can now be cast into a (primal) SDP form, in terms of the variables Y_{AB} and ω_A, as

Primal formulation of the diamond norm

$$\begin{aligned} &\text{Given } X_\Phi \simeq \Phi \\ &||\Phi||_\diamond = \text{Maximize} \quad \text{Tr}(Y_{AB} X_\Phi) \\ &\text{Subject to} \quad -(\omega_A \otimes \mathbb{I}_B) \preceq Y_{AB} \preceq \omega_A \otimes \mathbb{I}_B; \\ &\omega_A \succeq 0, \quad \text{Tr}(\omega_A) = 1. \end{aligned} \tag{2.84}$$

2.4.1.2 Dual formulation

Having established the primal SDP formulation of the diamond norm, we will now show—using the Lagrange multiplier procedure discussed in section **2.3.3**—how to derive the dual SDP formulation of the primal stated in (2.84). Since this dual formulation is the one we will employ in later sections to evaluate distances between the dynamics that compose coarse-graining scenarios, the exposition presented here not only has a conceptual character for readers who are not familiar with the semidefinite programming derivations of the diamond norm, but also sheds light on the consistency of the mathematical methods that we will later employ to develop our main contributions.

To do so, let us associate Hermitian dual variables (Lagrange multipliers) to each equality and inequality constraint of (2.84). That is, the primal SDP under consideration—now equipped with its dual variables, written explicitly alongside each constraint—is given by:

$$\begin{aligned} &\text{Given } X_\Phi \simeq \Phi \\ &||\Phi||_\diamond = \text{Maximize} \quad \text{Tr}(Y_{AB} X_\Phi) \\ &\text{Subject to} \quad -(\omega_A \otimes \mathbb{I}_B) \preceq Y_{AB}, \quad : Z_1 \in \text{Herm}(\mathcal{H}_A \otimes \mathcal{H}_B) \\ &Y_{AB} \preceq \omega_A \otimes \mathbb{I}_B, \quad : Z_2 \in \text{Herm}(\mathcal{H}_A \otimes \mathcal{H}_B) \\ &\omega_A \succeq 0, \quad : Z_3 \in \text{Herm}(\mathcal{H}_A) \\ &\text{Tr}(\omega_A) = 1, \quad : \mu \in \mathbb{R} \end{aligned} \tag{2.85}$$

From this, we then define the Lagrangian function $\mathcal{L} = \mathcal{L}(Y_{AB}, \omega_A, Z_1, Z_2, Z_3, \mu)$ for this

problem as

$$\mathcal{L} := \mathrm{Tr}(Y_{AB}X_\Phi) + \mathrm{Tr}[Z_1(Y_{AB} + \omega_A \otimes \mathbb{I}_B)] + \mathrm{Tr}[Z_2(\omega_A \otimes \mathbb{I}_B - Y_{AB})] \\ + \mathrm{Tr}(\omega_A Z_3) + \mu[1 - \mathrm{Tr}(\omega_A)]. \tag{2.86}$$

Since the primal problem is a maximization, $\mathcal{L}$ must upper bound the primal objective function for all Y_{AB} and ω_A feasible. For this, we need to identify the specific constraints the dual variables must satisfy so that this upper-bound is achieved and $\mathcal{L}$ becomes independent of the old variables Y_{AB} and ω_A. That is, by looking at the second, third, and fourth terms on the right-hand side of (2.86) and requiring each of them to be nonnegative—which directly implies that $\mathcal{L} \geq \mathrm{Tr}(Y_{AB}X_\Phi)$—we can conclude that Z_1, Z_2 and Z_3 must be positive semidefinite operators. Moreover, by setting $d_B = \dim(\mathcal{H}_B)$, we can rearrange (2.86) as

$$\mathcal{L} = \mathrm{Tr}[Y_{AB}(X_\Phi + Z_1 - Z_2)] + \mathrm{Tr}\{(\omega_A \otimes \mathbb{I}_B)[Z_1 + Z_2 + Z_3 \otimes \frac{\mathbb{I}_B}{d_B} - (\mu \mathbb{I}_A \otimes \frac{\mathbb{I}_B}{d_B})]\} + \mu, \tag{2.87}$$

where we have explicitly used the fact that, for any $X_A \in \mathcal{L}(\mathcal{H}_A)$,

$$\mathrm{Tr}_A(X_A) = \mathrm{Tr}_{AB}\left(X_A \otimes \frac{\mathbb{I}_B}{d_B}\right). \tag{2.88}$$

By inspecting the right-hand side of (2.87), in order to the Lagrangian $\mathcal{L}$ to become independent of the primal variables Y_{AB} and ω_A, we observe that the constraints:

$$X_\Phi + Z_1 - Z_2 = 0; \tag{2.89}$$

$$Z_1 + Z_2 + Z_3 \otimes \frac{\mathbb{I}_B}{d_B} - (\mu \mathbb{I}_A \otimes \frac{\mathbb{I}_B}{d_B}) = 0, \tag{2.90}$$

must be imposed. Thus, with these constraints taken into account, returning to (2.87), the expression for the Lagrangian reduces simply to

$$\mathcal{L} = \mu. \tag{2.91}$$

Since, in this problem, the dual variable Z_3 is a slack variable, the constraint (2.90) can be simplified. In particular, we can solve it for Z_3, giving

$$Z_3 \otimes \frac{\mathbb{I}_B}{d_B} = \mu \mathbb{I}_A \otimes \frac{\mathbb{I}_B}{d_B} - (Z_1 + Z_2). \tag{2.92}$$

Under the assumption that $Z_3 \succeq 0$, we can directly conclude from the above expression that

$$Z_3 = \mathrm{Tr}_B\left(Z_3 \otimes \frac{\mathbb{I}_B}{d_B}\right) = \mathrm{Tr}_B\left(\mu \mathbb{I}_A \otimes \frac{\mathbb{I}_B}{d_B}\right) - \mathrm{Tr}_B(Z_1 + Z_2) \succeq 0 \implies \mu \mathbb{I}_A \succeq \mathrm{Tr}_B(Z_1 + Z_2). \tag{2.93}$$

Therefore, combining (2.91) with the constraints (2.89), (2.93), and the fact that $Z_1 \succeq 0, Z_2 \succeq 0$, we arrive to the following dual SDP formulation for the diamond norm:

Dual formulation of the diamond norm

$$\begin{aligned} &\text{Given } X_\Phi \simeq \Phi \\ &||\Phi||_\diamond = \text{Minimize} \quad \mu \\ &\\ &\text{Subject to} \quad X_\Phi = Z_2 - Z_1; \\ &\\ &\qquad\qquad Z_1 \succeq 0, \quad Z_2 \succeq 0; \\ &\\ &\qquad\qquad \mu \mathbb{I}_A \succeq \text{Tr}_B(Z_1 + Z_2), \end{aligned} \tag{2.94}$$

which is the main formulation that we will employ in later sections of this work. We emphasize that we have implicitly used the fact that strong duality holds for the diamond norm (41). This explains, in parallel with the primal problem (2.84), why the equality in the dual problem (2.94) holds.

To conclude this rather technical section, based on the diamond norm formulation (2.94), we define a set $\mathcal{B}_\diamond^{\epsilon,\Phi}$—referred to here as the *diamond norm ball* of radius ϵ around a given channel Φ—consisting of quantum channels $\Gamma \in \mathcal{C}(A,B)$ that are ϵ–close to Φ. Since this set will be used in later sections within semidefinite programs to evaluate distances between Bayesian solutions to the coarse-graining problem, we define it explicitly as

$$\begin{aligned} \mathcal{B}_\diamond^{\epsilon,\Phi} &:= \{\Gamma \in \mathcal{C}(A,B) : \|\Phi - \Gamma\|_\diamond \leq \epsilon\} \\ &= \left\{ \Gamma \in \mathcal{C}(A,B) : \begin{array}{l} X_\Phi - X_\Gamma = Z_2 - Z_1, \\ Z_1 \succeq 0, \quad Z_2 \succeq 0, \\ \epsilon\, \mathbb{I}_A \succeq \text{Tr}_B(Z_1 + Z_2), \\ X_\Gamma \succeq 0, \quad \text{Tr}_B(X_\Gamma) = \mathbb{I}_A \end{array} \right\}. \end{aligned} \tag{2.95}$$

3 THE COARSE-GRAINING PROBLEM

3.1 OVERVIEW

From a numerical perspective, dealing with descriptions of arbitrarily large many-body quantum systems that account for the degree of freedom of each of its individual subsystems seems computationally intractable (21, 22). Since the complexity and the number of parameters of such descriptions grow exponentially with the number of constituents (namely, their degrees of freedom), a typical simulation of a system containing 6×10^{23} particles, which takes into account all particle-particle interactions and does not leverage any approximation methods (e.g., mean-field approximations and Monte Carlo methods), would take an entire lifetime to be executed on a classical computer.

One way to deal with this limitation within the quantum information paradigm—without resorting directly to quantum computation and quantum computers—is to work with effective descriptions (24, 25, 27, 30). These effective dynamical descriptions, when they do exist, may be seen as the result of passing the microscopic system we are unable to have a full account for through a coarse-graining map. Such a map, which is defined as a CPTP map (24), is not only used to reduce the dimensionality of the system—bypassing our incapacity to access at all such degrees of freedom of the microscopic system—but it also is usually employed to model the effect of a measurement performed by a non-ideal measuring device (24). Reflecting, in that way, the shortcomings of the measurement apparatus on the effective state of the system.

Before proceeding with this discussion, it is reasonable to formally define what we refer to as a coarse-graining map (24, 64).

Definition 10 (Coarse-graining map)**.** *Let $\mathcal{H}_D \simeq \mathbb{C}^D$ and $\mathcal{H}_d \simeq \mathbb{C}^d$ be Hilbert spaces assigned, respectively, to a $D-$dimensional and a $d-$dimensional quantum system. Let $\mathcal{L}(\mathcal{H}_D)$ and $\mathcal{L}(\mathcal{H}_d)$ be the sets of linear operators acting on $\mathcal{H}_D$ and $\mathcal{H}_d$, respectively. A coarse-graining map Λ_{CG} is defined to be a CPTP linear map that reduces the dimensionality of the system:*

$$\Lambda_{CG} : \mathcal{L}(\mathcal{H}_D) \to \mathcal{L}(\mathcal{H}_d), \tag{3.1}$$

such that $D > d$.

Therefore, the Λ_{CG} map defined in this way, as pinpointed by the previous works in literature—and also pursued in this one—is a reasonable choice to obtain macroscopic, less complex, and yet informative descriptions of quantum systems, when we start with the description of the microscopic ones.

Letting this discussion aside for a moment and going deep into the microscopic description when one works with closed quantum systems, it is reasonable to assume, under the postulates of quantum mechanics, that the system evolves unitarily (31). In

other words, there is some unitary quantum channel $\mathcal{U}_t : \mathcal{D}(\mathcal{H}_D) \to \mathcal{D}(\mathcal{H}_D)$ that we can assign to carry the evolution of the system.

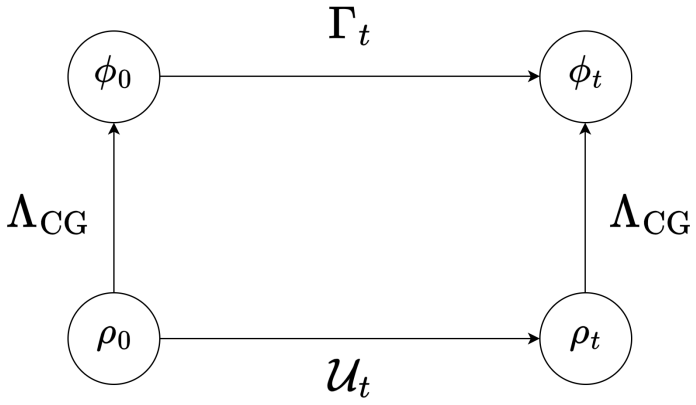

Figure 1 - A general coarse-graining problem scenario. The horizontal arrow at the bottom represents the unitary evolution of a closed many-body quantum system. Vertical arrows represent information loss, noise, or lack of access to all degrees of freedom, while the horizontal arrow at the top represent the emergent, less complex and macroscopic dynamics.

Connecting the coarse-grained description of a quantum system and its unitary evolution, one question that naturally arises from the aforementioned exposition is: Given a closed microscopic quantum system in a state described by the density operator $\rho_0 \in \mathcal{D}(\mathcal{H}_D)$, which evolves under a unitary dynamics $\mathcal{U}_t$, what is its effective dynamics $\Gamma_t : \mathcal{D}(\mathcal{H}_d) \to \mathcal{D}(\mathcal{H}_d)$ that emerges from a coarse-grained description—dictated by a coarse-graining map Λ_{CG}—of the underlying microscopic system? Such a question, presented primarily in Ref. (24), is known as the *coarse-graining problem*. This problem can be translated as seeking the necessary and sufficient conditions for the existence of the emergent dynamics Γ_t that commutes the diagram of Fig. 1. Mathematically, the latter reads as the commutativity relation:

$$\Gamma_t \circ \Lambda_{\mathrm{CG}} = \Lambda_{\mathrm{CG}} \circ \mathcal{U}_t. \tag{3.2}$$

One of the key aspects of the problem, which lies behind the commutativity relation seen in Eq. (3.2), is the fact that, if such emergent dynamics Γ_t exist—a property that does not hold in general—one can describe the evolution of the underlying many-body quantum system through a less complex and accessible framework, rather than the $\mathcal{U}_t$ itself. In other words, looking again at the diagram of Fig. 1, this regards obtaining the effective quantum state ϕ_t either by $\Lambda_{\mathrm{CG}} \circ \mathcal{U}_t(\rho_0) = \Lambda_{\mathrm{CG}}(\rho_t)$ or by $\Gamma_t \circ \Lambda_{\mathrm{CG}}(\rho_0) = \Gamma_t(\phi_0)$, interchangeably.

Upon this exposition, we define the notion of compatibility in a coarse-graining scenario.

Definition 11 (Compatibility in a coarse-graining scenario)**.** *Let $\mathcal{H}_D$ be a $D-$dimensional Hilbert space and let $\mathcal{H}_d$ be a $d-$dimensional Hilbert space, with $D > d$. Let $\mathcal{U}_t : \mathcal{L}(\mathcal{H}_D) \to \mathcal{L}(\mathcal{H}_D)$ be a unitary dynamics and let $\Lambda_{CG} : \mathcal{L}(\mathcal{H}_D) \to \mathcal{L}(\mathcal{H}_d)$ be a coarse-graining map. We say that $\mathcal{U}_t$ is compatible with Λ_{CG} (or, equivalently, that the coarse-graining scenario itself is compatible) if there exists a CPTP emergent dynamics $\Gamma_t : \mathcal{L}(\mathcal{H}_d) \to \mathcal{L}(\mathcal{H}_d)$ such that*

$$\Gamma_t \circ \Lambda_{CG} = \Lambda_{CG} \circ \mathcal{U}_t.$$

This is the core of the coarse-graining problem advanced in (24): the second conceptual pillar of this thesis. More details, as well as some specific examples of applications of the formalism of coarse-graining maps, can be found in Refs. (24, 34, 35). In what follows, we present some concrete examples of coarse-graining maps which we will consider in this work.

3.2 EXAMPLES

The first one represents the most common coarse-grained description, usually employed in scenarios of open quantum systems (33), when we are only interested in a subsystem and do not want to keep handling with unnecessary information about the environment. That is, the coarse-graining map responsible for throwing away the environment degrees of freedom and reducing the description to only the subsystem of interest is the partial trace, denoted by $\Lambda_{\mathrm{Tr}} : \mathcal{L}(\mathcal{H}_S \otimes \mathcal{H}_E) \to \mathcal{L}(\mathcal{H}_S)$, where $\mathcal{H}_S$ and $\mathcal{H}_E$ are supposed to be the Hilbert spaces associated with the subsystem of interest and the environment, respectively. Here, we will retain the partial trace over the subsystem on the right, i.e, the second entry of the tensor product.

Lastly, the other coarse-grained description that we aim to explore subsequently in this contribution relies on modeling the effect of a measurement conducted by a non-ideal detector. Proposed primarily in (24) and also approached in (25, 28), the blurred and saturated detector coarse-graining map $\Lambda_{\mathrm{BnS}} : \mathcal{L}(\mathbb{C}^2 \otimes \mathbb{C}^2) \to \mathcal{L}(\mathbb{C}^2)$, whose Kraus operators are given explicitly by

$$K_1 = \begin{pmatrix} 1 & 0 & 0 & 0 \\ 0 & 1/\sqrt{3} & 1/\sqrt{3} & 1/\sqrt{3} \end{pmatrix}, K_2 = \begin{pmatrix} 0 & 0 & 0 & 0 \\ 0 & 1/\sqrt{3} & 0 & -1/\sqrt{3} \end{pmatrix},$$
$$K_3 = \begin{pmatrix} 0 & 0 & 0 & 0 \\ 0 & 1/\sqrt{3} & -1/\sqrt{3} & 0 \end{pmatrix}, K_4 = \begin{pmatrix} 0 & 0 & 0 & 0 \\ 0 & 0 & 1/\sqrt{3} & -1/\sqrt{3} \end{pmatrix},$$

is employed to model the scenario of an alleged fluorescence detection of two neighboring atoms by a detector which has not good enough lens and saturates the light scattered by the atoms (see Fig. 2). Both coarse-graining maps, Λ_{Tr} and Λ_{BnS}, are going to be used to construct the coarse-graining scenarios addressed in our numerical benchmarking in Chapter 6.

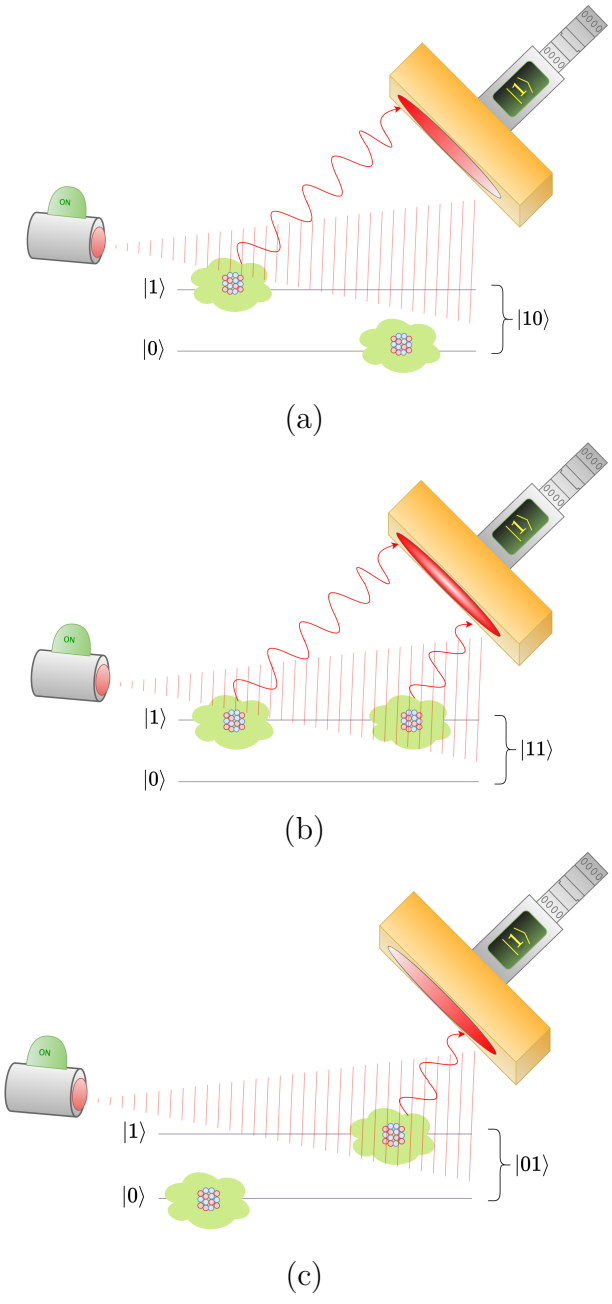

Figure 2 - Schematic representation of the blurred and saturated detector. Two atoms are measured using a fluorescence technique in a regime where the ground state and the first excited state of each atom can be represented as a qubit. The measurement apparatus does not have a sufficiently good lens to distinguish between the states $|01\rangle$ and $|10\rangle$. Furthermore, the amount of light scattered by a single atom is already sufficient to saturate the detector; therefore, whether there are two excitations, $|11\rangle$, or a single excitation, $|01\rangle$ or $|10\rangle$, the apparatus registers the same signal, $|1\rangle$.

4 CONDITIONAL QUANTUM STATES

4.1 OVERVIEW

Regarding the final main ingredient of this work, in this section, an adapted [1] version of the conditional states formalism (CSF) developed in Ref. (5) will be briefly reviewed. Before delving into the formalism itself, and establishing the connection with the result of the Theorem 1, first, we bring the notion—borrowed from Ref. (5)—of *elementary regions*. An elementary region is designed to denote any space-time domain where an agent might possibly make a single intervention on a quantum system through an experiment, either by making a measurement or by preparing a state. Henceforth, the term *region* (also refereed to as a *quantum region*) denotes a collection of elementary regions.

Until here in our construction, we assigned Hilbert spaces to describe a quantum system—with channels and composite systems being described by two different structures; however, from now on, each Hilbert space will be labeled and assigned to a respective region, as $\mathcal{H}_A$ for a region A, for instance. Composite regions, labeled by AB, with $\mathcal{H}_A$ assigned to A and $\mathcal{H}_B$ to B, will be represented by a tensor product space $\mathcal{H}_{AB} := \mathcal{H}_A \otimes \mathcal{H}_B$ and described by a positive semidefinite operator ρ_{AB} on $\mathcal{H}_{AB}$, dubbed the *joint state*. In this case, the reduced states yielded by ρ_{AB} represent the agents' beliefs about each region, A or B (5).

Since one of the goals of the conditional state formalism was to formulate a (causally neutral) quantum generalization of classical probability theory, it incorporates classical probability formulae into a unified framework within the conventional formalism of quantum theory. In that sense, a classical random variable X (or any other uppercase Latin letter near the end of the alphabet) finds its counterpart within the formalism through a quantum region that encodes its values. These regions are called *classic regions* and their associated Hilbert spaces come equipped with a preferred basis $\{|x\rangle\}_{x\in \mathrm{Out}(X)}$ where every positive semidefinite operator in question is diagonal on that basis.

Regarding the usual expressions in classical probability theory, which is also widely treated within the formalism, the CSF depicts the marginalization of a joint probability distribution

$$P(X) = \sum_{y\in \mathrm{Out}(Y)} P(X, Y = y) \tag{4.1}$$

as partial traces:

$$\rho_X = \mathrm{Tr}_Y(\rho_{XY}) = \sum_{x\in \mathrm{Out}(X)} P(X = x)\, |x\rangle \langle x| \in \mathcal{D}(\mathcal{H}_X). \tag{4.2}$$

[1] The main difference between the two formulations was just a matter of choice. Here, we choose the Choi isomorphism, as in Definition 5, instead of the Jamiołkowski's adopted in (5).

Analogously, but, in the fully quantum case, if $\rho_{AB} \in \mathcal{L}(\mathcal{H}_{AB})$ describes the knowledge, beliefs or information that an agent has about a composite quantum region AB, then the information about only the region A is obtained by tracing out the region we do not care about:

$$\rho_A = \mathrm{Tr}_B(\rho_{AB}) \in \mathcal{D}(\mathcal{H}_A). \tag{4.3}$$

This operation plays the same role as a marginal probability distribution.

We are now in a position to delve into the Bayesian conditioning aspect of the formalism, which, as shown in the subsequent section, allow us to fit the coarse-graining problem into a Bayesian inference's scenario. In that context, we will adopt the "given" notation—the same used in the context of conditional probabilities—to refer, in the appropriate context, to regions, quantum channels and their corresponding isomorphic state. Therefore, when any linear map is written as $\mathcal{M}_{B|A}$, it means that

$$\mathcal{M}_{B|A} : \mathcal{L}(\mathcal{H}_A) \to \mathcal{L}(\mathcal{H}_B). \tag{4.4}$$

Extending by analogy, its associated Choi state will be denoted by $\sigma_{B|A} \in \mathcal{L}(\mathcal{H}_A \otimes \mathcal{H}_B)$. With this notation in hand, we are equipped to define our *causal conditional states*, which differs a little from the one properly defined in Ref. (5).

Definition 12. *A causal conditional state $\rho_{B|A}$ for B given A is a positive semidefinite operator on $\mathcal{H}_{AB}$ that satisfies*

$$\mathrm{Tr}_B(\rho_{B|A}) = \mathbb{I}_A. \tag{4.5}$$

Thus, inheriting from the result exposed in Theorem 1, together with the above definition, we have in hands a framework to characterize quantum channels by causal conditional states. In other words, given an arbitrary linear map $\mathcal{E}_{B|A} : \mathcal{L}(\mathcal{H}_A) \to \mathcal{L}(\mathcal{H}_B)$, it will be a quantum channel if, and only if, its Choi-isomorphic state $\rho_{B|A}$ is a causal conditional state. We emphasize that because $\rho_{B|A}$ is a causal conditional state, Choi-isomorphic to a quantum channel $\mathcal{E}_{B|A}$, it will carry the *causal* connection between the regions A and B. Roughly speaking, the latter means that B is in the causal future of A and $\rho_{B|A}$ will be the propagator of agent's beliefs between the two regions; a fact that can be made explicit by looking at the action of $\mathcal{E}_{B|A}$—dubbed *belief propagation*—over a state $\rho_A \in \mathcal{D}(\mathcal{H}_A)$ of the region A, obtaining a state $\rho_B \in \mathcal{D}(\mathcal{H}_B)$ in terms of $\rho_{B|A}$:

$$\rho_B = \mathcal{E}_{B|A}(\rho_A) = \mathrm{Tr}_A[\rho_{B|A}(\rho_A^T \otimes \mathbb{I}_B)] \in \mathcal{D}(\mathcal{H}_B). \tag{4.6}$$

This picture of causal connections, as well as the distinction between quantum and classical regions, can be captured in a diagrammatic representation—also borrowed from Ref. (5), as shown in Fig. 3.

In what follows, another concept in the realm of classical probability has its counterpart within the formalism here discussed. If X and Y are two random variables,

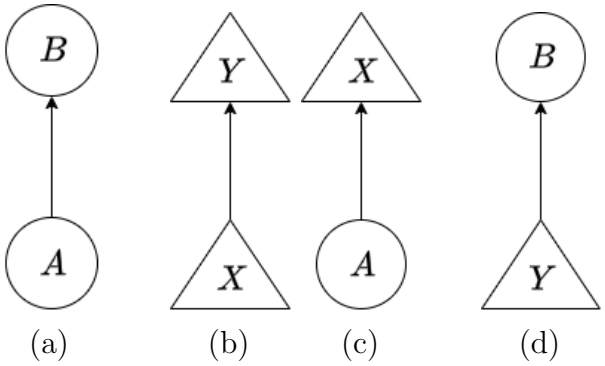

Figure 3 - Some diagrams of the formalism. Classical regions are denoted by triangles while quantum regions by circles. Arrows represents causal connections and the directions of causal influence. (a) A general quantum dynamics. Region A represents the input of a quantum channel $\mathcal{E}_{B|A}$ and B represents the output. A conditional state $\rho_{B|A}$ establishes the connection via the belief propagation rule. (b) A classical measurement. This process takes the random variable X as input and gives Y as output. The conditional state $\rho_{Y|X} \in \mathcal{L}(\mathcal{H}_X \otimes \mathcal{H}_Y)$ carries the conditional probability distribution $P(Y|X)$. (c) Representation of a quantum measurement. The hybrid operator $\rho_{X|A} \in \mathcal{L}(\mathcal{H}_A \otimes \mathcal{H}_X)$, designated to propagates beliefs in this case, carries a POVM $\{E_x^A\}_{x\in \mathrm{Out(X)}} \subset \mathcal{L}(\mathcal{H}_A)$ in its composition. (d) Quantum preparation procedures are also represented within the formalism. A hybrid operator $\rho_{B|Y} \in \mathcal{L}(\mathcal{H}_Y \otimes \mathcal{H}_B)$ carries a set $\{\rho_y^B\}_{y\in \mathrm{Out}(Y)} \subset \mathcal{D}(\mathcal{H}_B)$ in its definition.

then one can write a conditional probability distribution of X conditioned over Y, possessing the joint distribution $P(X, Y)$ and the marginal $P(Y)$, as:

$$P(X|Y) = \frac{P(X, Y)}{P(Y)}. \tag{4.7}$$

On the other hand, for any joint state $\rho_{AB} \in \mathcal{L}(\mathcal{H}_{AB})$ and reduced state $\rho_A = \mathrm{Tr}_B(\rho_{AB})$, a conditional state of B given A can be defined via

$$\rho_{B|A} = \rho_{AB} \star \rho_A^{-1}, \tag{4.8}$$

where the $\star-$product, presented in Ref. (5), is defined as:

$$M_{AB} \star N_A := (N_A^{\frac{1}{2}} \otimes \mathbb{I}_B) M_{AB} (N_A^{\frac{1}{2}} \otimes \mathbb{I}_B), \tag{4.9}$$

for any $M_{AB} \in \mathcal{L}(\mathcal{H}_{AB})$ and $N_A \in \mathrm{Pos}(\mathcal{H}_A)$.

A straightforward calculation shows that $\rho_{B|A}$, as given in Eq. (4.8), is indeed a valid conditional state in accordance with the Definition 12:

$$\mathrm{Tr}_B(\rho_{B|A}) = \mathrm{Tr}_B(\rho_{AB} \star \rho_A^{-1}) = \mathrm{Tr}_B(\rho_{AB}) \star \rho_A^{-1} = \rho_A \star \rho_A^{-1} = \mathbb{I}_A. \tag{4.10}$$

Positivity follows because the right-hand side of Eq. (4.8) is a conjugation of the positive operator ρ_{AB} by $\rho_A^{-\frac{1}{2}}$.

Moreover, in this classical Bayesian scenario, from the expression (4.7), one can apply Bayes' theorem in order to obtain $P(Y|X)$ as

$$P(Y|X) = \frac{P(X|Y)P(Y)}{P(X)}. \tag{4.11}$$

Through a direct analogy, from the expression (4.8), we can use the *quantum Bayes' theorem* (5) to obtain the conditional state $\rho_{A|B}$ of A given B as:

$$\rho_{A|B} = \rho_{B|A} \star (\rho_A \rho_B^{-1}), \tag{4.12}$$

where, to simplify the notation, for any $N_A \in \mathcal{L}(\mathcal{H}_A)$ and $N_B \in \mathcal{L}(\mathcal{H}_B)$, we write $N_A N_B = (N_A \otimes \mathbb{I}_B)(\mathbb{I}_A \otimes N_B)$. In this context, suppose that $\rho_{B|A}$ is Choi-isomorphic to a channel $\mathcal{E}_{B|A}$. If ρ_A is the state that describes the agent's knowledge of a region A and ρ_B is the result of the belief propagation from A to B determined by $\rho_B = \mathcal{E}_{B|A}(\rho_A) = \mathrm{Tr}_A(\rho_{B|A}\rho_A^T)$, then the operator $\rho_{A|B}$—dubbed the *quantum Bayesian inversion* of $\rho_{B|A}$—turns out to be the Choi state associated with a quantum channel $\mathcal{R}^{\mathrm{Petz}}_{A|B,\rho_A}$, whose expression is given explicitly by:

$$\mathcal{R}^{\mathrm{Petz}}_{A|B,\rho_A}(\cdot) = \rho_A^{\frac{1}{2}}\{\mathcal{E}^\dagger_{B|A}[\rho_B^{-\frac{1}{2}}(\cdot)\rho_B^{-\frac{1}{2}}]\}\rho_A^{\frac{1}{2}}, \tag{4.13}$$

where $\mathcal{E}^\dagger_{B|A} : \mathcal{L}(\mathcal{H}_B) \to \mathcal{L}(\mathcal{H}_A)$ is the adjoint of $\mathcal{E}_{B|A}$.

The map $\mathcal{R}^{\mathrm{Petz}}_{A|B,\rho_A}$, as given in the expression above, was discovered in Ref. (6) and is usually known as the Petz's recovery map. Such a map, which also appears in the literature of error correction (7), is recognizable to be a channel that achieves near-optimal quantum error correction in cases where the initial state and quantum channel are known. In parallel with that, we would like to highlight its emergence within the conditional state formalism: $\mathcal{R}^{\mathrm{Petz}}_{A|B,\rho_A}$ is the Choi-isomorphic map to the Bayesian inversion $\rho_{A|B}$. While $\rho_{B|A}$ is responsible for propagating beliefs from A to its causal future B, its Bayesian inversion $\rho_{A|B}$ retrospects beliefs from B to A. Although naive, this digression is fundamental. It emphasizes, in a natural way, the potential Bayesian character we can give to the coarse-graining formalism as a whole, as shown in more detail in the next section.

Ending this section, we present the channel composition rule viewed as an instance of belief propagation (5). Such a result, as seen in later sections, will be one of the key tools used to develop the operational aspect of the coarse-graining problem in the light of the conditional states paradigm.

Theorem 4. *Let $\mathcal{E}_{B|A}, \mathcal{E}_{C|B}$ and $\mathcal{E}_{C|A}$ be linear maps, and $\rho_{B|A}, \rho_{C|B}$ and $\rho_{C|A}$, their respective Choi isomorphic operators. Then, it holds that $\mathcal{E}_{C|A} = \mathcal{E}_{C|B} \circ \mathcal{E}_{B|A}$ if, and only if, the Choi isomorphic operators satisfy*

$$\rho_{C|A} = \mathrm{Tr}_B[(\mathbb{I}_A \otimes \rho_{C|B})(\rho_{B|A}^{T_B} \otimes \mathbb{I}_C)]. \tag{4.14}$$

Proof. Firstly, suppose that $\mathcal{E}_{C|A} = \mathcal{E}_{C|B} \circ \mathcal{E}_{B|A}$. Let $M_A \in \mathcal{L}(\mathcal{H}_A)$ be an arbitrary operator on $\mathcal{H}_A$. Then,

$$\begin{aligned}
\mathcal{E}_{C|A}(M_A) &= \mathrm{Tr}_A[\rho_{C|A}(M_A^{T_A} \otimes \mathbb{I}_C)] \\
&= \mathcal{E}_{C|B}[\mathcal{E}_{B|A}(M_A)] \\
&= \mathcal{E}_{C|B}\{\mathrm{Tr}_A[\rho_{B|A}(M_A^{T_A} \otimes \mathbb{I}_B)]\} \\
&= \mathrm{Tr}_B\{\rho_{C|B}[[\mathrm{Tr}_A(\rho_{B|A}(M_A^{T_A} \otimes \mathbb{I}_B))]^{T_B} \otimes \mathbb{I}_C]\} \\
&= \mathrm{Tr}_A\{\mathrm{Tr}_B[(\mathbb{I}_A \otimes \rho_{C|B})(\rho_{B|A}^{T_B} \otimes \mathbb{I}_C)](M_A^{T_A} \otimes \mathbb{I}_C)\} \\
\implies \rho_{C|A} &= \mathrm{Tr}_B[(\mathbb{I}_A \otimes \rho_{C|B})(\rho_{B|A}^{T_B} \otimes \mathbb{I}_C)].
\end{aligned} \tag{4.15}$$

Conversely, suppose that

$$\rho_{C|A} = \mathrm{Tr}_B[(\mathbb{I}_A \otimes \rho_{C|B})(\rho_{B|A}^{T_B} \otimes \mathbb{I}_C)]. \tag{4.16}$$

Then,

$$\begin{aligned}
\mathcal{E}_{C|A}(M_A) &= \mathrm{Tr}_A[\rho_{C|A}(M_A^{T_A} \otimes \mathbb{I}_C)] \\
&= \mathrm{Tr}_A\{\mathrm{Tr}_B[(\mathbb{I}_A \otimes \rho_{C|B})(\rho_{B|A}^{T_B} \otimes \mathbb{I}_C)](M_A^{T_A} \otimes \mathbb{I}_C)\} \\
&= \mathrm{Tr}_B\{\rho_{C|B}[[\mathrm{Tr}_A(\rho_{B|A}(M_A^{T_A} \otimes \mathbb{I}_B))]^{T_B} \otimes \mathbb{I}_C]\} \\
&= \mathrm{Tr}_B\{\rho_{C|B}[[\mathcal{E}_{B|A}(M_A)]^{T_B} \otimes \mathbb{I}_C]\} \\
&= \mathcal{E}_{C|B}[\mathcal{E}_{B|A}(M_A)] \\
\implies \mathcal{E}_{C|A} &= \mathcal{E}_{C|B} \circ \mathcal{E}_{B|A}.
\end{aligned} \tag{4.17}$$

■

This is the essence of the conditional state formalism: the last of three conceptual pillars of the present manuscript. In the next section, we show how this formalism can be used to reframe the coarse-graining problem and discuss in more detail the solution proposed by Brugger et al. (29) within this framework.

4.2 A BAYESIAN PERSPECTIVE OF THE COARSE-GRAINING PROBLEM

In chapter 3, we first introduced the coarse-graining problem in its conventional standpoint: as a question about the existence of a completely positive, trace-preserving map satisfying a certain commutativity relation—see Fig. 1. In other words, whether an appropriate (CPTP) emergent dynamics Γ_t can simulate or not an underlying unitary evolution $\mathcal{U}_t$ of a quantum system, subjected to a lack or loss of information represented by Λ_{CG}, is directly tied to the conventional commutativity relation shown in Eq. (3.2).

In this perspective, as proposed originally in Ref. (24) and pursued in this work, the Λ_{CG} map is intended to model faulty detector apparatuses or situations where one cannot account for all degrees of freedom of the system of interest. Although this point of view prevails in this work, we begin to advance an alternative view of this problem. By strolling

in the same direction partially addressed in (30), explored in (27) and heavily approached in (29), we will assume that quantum theory is but another theory of probabilistic assignments (42, 5, 43) and approach the coarse-graining problem with the standpoint of the conditional state formalism shown so far. In doing so, it allows us to reframe—without losing its standard characteristics—the original coarse-graining scenario as a problem of (subjective) Bayesian inference,[2] as seen illustratively in Fig. 4.

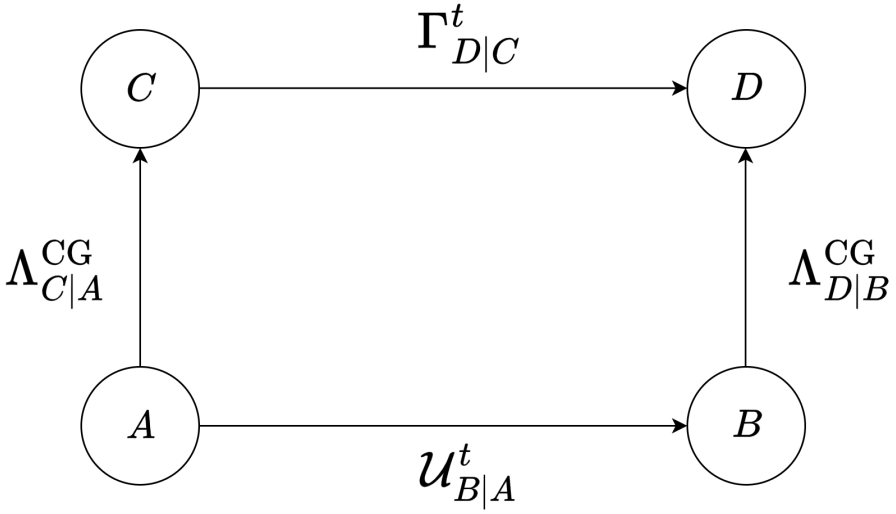

Figure 4 - The coarse-graining problem from the point of view of the conditional states formalism. Letting $\rho_{D|C}, \rho_{B|A}$ and $\rho_{C|A}(\rho_{D|B})$ be the causal conditional states associated to $\Gamma^t_{D|C}, \mathcal{U}^t_{B|A}$ and $\Lambda^{\mathrm{CG}}_{C|A}(\Lambda^{\mathrm{CG}}_{D|B})$, respectively; then, the conventional commutativity relation, $\Gamma^t_{D|C} \circ \Lambda^{\mathrm{CG}}_{C|A} = \Lambda^{\mathrm{CG}}_{D|B} \circ \mathcal{U}^t_{B|A}$, can be expressed in terms of its respective causal conditional states (Theorem 4) as $\mathrm{Tr}_C[(\mathbb{I}_A \otimes \rho_{D|C})(\rho^{T_C}_{C|A} \otimes \mathbb{I}_D)] = \mathrm{Tr}_B[(\mathbb{I}_A \otimes \rho_{D|B})(\rho^{T_B}_{B|A} \otimes \mathbb{I}_D)]$.

This Bayesian and agent-centric point of view forces us to interpret quantum states as the proxy of an agent's beliefs about the outcome of a quantum experiment (42), and quantum dynamics (CPTP maps) as mechanisms of belief propagation (5). Also, the very use of the coarse-graining map—from now on denoted by $\Lambda^{\mathrm{CG}}_{C|A}(\Lambda^{\mathrm{CG}}_{D|B})$—assumes a direct interpretation in this picture as being the map that expresses the experimentalist' (fragmentary) knowledge of their non-ideal detection apparatus. The emergent dynamics $\Gamma^t_{D|C}$ is now the agent's effective (accessible) description—based on their knowledge—and the standard commutativity relation,

$$\Gamma^t_{D|C} \circ \Lambda^{\mathrm{CG}}_{C|A} = \Lambda^{\mathrm{CG}}_{D|B} \circ \mathcal{U}^t_{B|A}, \tag{4.18}$$

[2] This terminology needs a brief clarification. We say this perspective is "subjective" mainly because it is agent-centric; it sees probabilities and, consequently, density states (from our standpoint) as measuring agents' degrees of belief. Also, we classify it as "Bayesian" because the belief update rule of X given the acquiring of new information Y, $P(X) \mapsto P_Y(X)$, is given by the usual conditioning: $P(X) \mapsto P_Y(X) = P(X|Y)$—when the agent is certain of Y. An extensive discussion of this point can be found in (52).

now can be re-written in terms of the causal conditional states associated with each quantum channel and its respective belief propagation rules (Theorem 4) as

$$\mathrm{Tr}_C[(\mathbb{I}_A \otimes \rho_{D|C})(\rho_{C|A}^{T_C} \otimes \mathbb{I}_D)] = \mathrm{Tr}_B[(\mathbb{I}_A \otimes \rho_{D|B})(\rho_{B|A}^{T_B} \otimes \mathbb{I}_D)], \tag{4.19}$$

thereby imposing an operational restriction on which types of emergent description the experimentalist is able to handle.

Within this paradigm, and to propose an emergent dynamics rooted in this quantum Bayesian inference ground, Brugger et al. (29) have devised a protocol to obtain an emergent dynamics by addressing the reversion of the first vertical arrow (see Fig. 5) in the diagram of Fig. 4 as a special case of the very quantum Bayesian inversion. Specifically, by letting ρ_A be the initial state of the region A, $\rho_C = \Lambda_{C|A}^{\mathrm{CG}}(\rho_A)$ be the result of propagating beliefs from A to C, and $\rho_{C|A}$ be the causal conditional state associated with the coarse-graining map $\Lambda_{C|A}^{\mathrm{CG}}$, they made use of the already discussed quantum Bayes's theorem (Eq. (4.12)) to define the causal conditional state

$$\rho_{A|C} := \rho_{C|A} \star (\rho_A \rho_C^{-1}), \tag{4.20}$$

which is the conditional state isomorphic to the Petz recovery map given by

$$\mathcal{R}_{A|C,\rho_A}^{\mathrm{Petz}}(\cdot) = \rho_A^{\frac{1}{2}}\{(\Lambda_{C|A}^{\mathrm{CG}})^\dagger[\rho_C^{-\frac{1}{2}}(\cdot)\rho_C^{-\frac{1}{2}}]\}\rho_A^{\frac{1}{2}}. \tag{4.21}$$

Finally, with $\rho_{A|C}$ on hand, making use of the channel composition rule in terms of the respective causal conditional states (Theorem 4), they obtained

$$\rho_{D|C}^{\mathrm{Petz}} := \mathrm{Tr}_B\{(\mathbb{I}_C \otimes \rho_{D|B})[\mathrm{Tr}_A[(\mathbb{I}_C \otimes \rho_{B|A})(\rho_{A|C}^{T_A} \otimes \mathbb{I}_B)]^{T_B} \otimes \mathbb{I}_D]\}, \tag{4.22}$$

thereby yielding the causal conditional state isomorphic to their proposed solution

$$\Gamma_{D|C,\rho_A}^{\mathrm{Petz}} := \Lambda_{D|B}^{\mathrm{CG}} \circ \mathcal{U}_{B|A}^t \circ \mathcal{R}_{A|C,\rho_A}^{\mathrm{Petz}}. \tag{4.23}$$

Nevertheless, despite such a proposed solution being indeed a CPTP map—as it is isomorphic to a valid causal conditional state and the necessary and sufficient conditions of Theorem 1 hold—it is guaranteed to satisfy the commutativity relation, Eq. (4.18), for the same initial ρ_A contained in Petz' recovery map expression (Eq. (4.21))—although one cannot rule out from the outset that the commutativity might hold also for other ρ_A'. Evidently, one can verify this fact directly by

$$\begin{aligned}
\Gamma_{D|C,\rho_A}^{\mathrm{Petz}} \circ \Lambda_{C|A}^{\mathrm{CG}}(\rho_A) &= \Gamma_{D|C,\rho_A}^{\mathrm{Petz}}(\rho_C) \\
&= \Lambda_{D|B}^{\mathrm{CG}} \circ \mathcal{U}_{B|A}^t \circ \mathcal{R}_{A|C,\rho_A}^{\mathrm{Petz}}(\rho_C) \\
&= \Lambda_{D|B}^{\mathrm{CG}}(\mathcal{U}_{B|A}^t(\rho_A^{\frac{1}{2}}\{(\Lambda_{C|A}^{\mathrm{CG}})^\dagger[\rho_C^{-\frac{1}{2}}(\rho_C)\rho_C^{-\frac{1}{2}}]\}\rho_A^{\frac{1}{2}}) \\
&= \Lambda_{D|B}^{\mathrm{CG}}(\mathcal{U}_{B|A}^t(\rho_A^{\frac{1}{2}}\{(\Lambda_{C|A}^{\mathrm{CG}})^\dagger[\mathbb{I}_C]\}\rho_A^{\frac{1}{2}}) \\
&= \Lambda_{D|B}^{\mathrm{CG}}(\mathcal{U}_{B|A}^t(\rho_A^{\frac{1}{2}}\mathbb{I}_A\rho_A^{\frac{1}{2}}) \\
&= \Lambda_{D|B}^{\mathrm{CG}} \circ \mathcal{U}_{B|A}^t(\rho_A),
\end{aligned} \tag{4.24}$$

where the last equality holds by the fact that the coarse-graining map is CPTP and the dual map of every CPTP map is unital[3] (49). From this, one can notice clearly that we cannot conclude the same analytical result for any $\rho'_A \in \mathcal{D}(\mathcal{H}_A)$ such that $\rho'_A \neq \rho_A$.

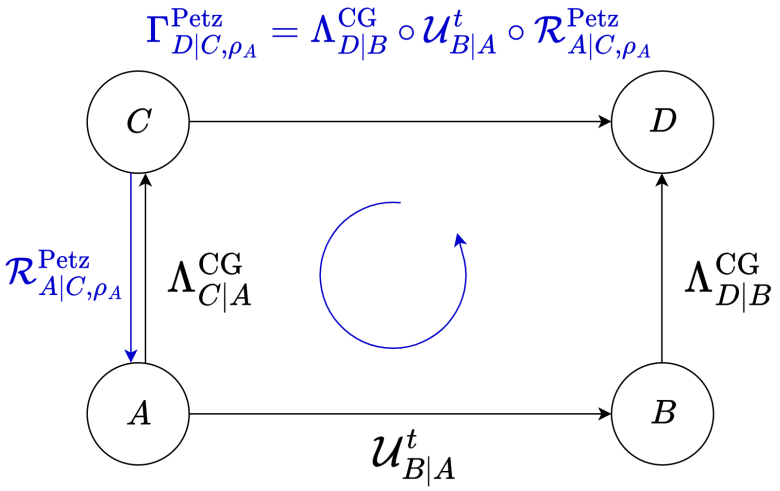

Figure 5 - The proposed solution by Brugger et al. of the coarse-graining problem within the conditional state formalism. By using the quantum Bayesian inversion to revert the first vertical arrow of the coarse-graining diagram, they proposed a solution that depends intrinsically of the Petz recovery map.

In other words, this potential lack of commutativity, except for ρ_A itself, imposes a hard and evident limitation of the solution advanced by Brugger et al. (29). Their framework fail to satisfy the commutativity relation of the coarse-graining problem for any ρ'_A different from the ρ_A state used in the very $\mathcal{R}^{\text{Petz}}_{A|C,\rho_A}$ definition. It is upon such a state-dependent limitation that the main contributions of the present manuscript are built. In the following chapters, we first propose convex optimization programs in order to analyze and circumvent this limitation, thereby studying the coarse-graining problem through the conditional state formalism lenses, but leaving aside its probabilistic character. We then carry out numerical benchmarking to understand where such a solution can be effectively employed to solve the coarse-graining problem in concrete two-qubit scenarios, as well as conduct numerical implementations of the proposed programs.

[3] A map $\mathcal{E} : \mathcal{L}(\mathcal{H}_C) \to \mathcal{L}(\mathcal{H}_A)$ is said to be unital when $\mathcal{E}(\mathbb{I}_C) = \mathbb{I}_A$.

5 SEMIDEFINITE PROGRAMMING ANALYSIS

As discussed in the previous chapter, the conditional states formalism, when adopted as an operational standpoint, gives to the coarse-graining problem a Bayesian inference character. Besides this, as noted in the discussions around Fig. 4, it becomes possible to look at the conventional commutativity relation (3.2) as a function of the causal conditional states associated with each quantum channel exhibited in the diagram of Fig. 4. Since, by Definition 12, such states are positive semidefinite operators, it gives the appropriate conditions to look at this problem through a semidefinite programming perspective. On this basis, in this section, we engage in some questions that arise from the proposed Bayesian, state-dependent solution to the coarse-graining problem shown in Eq. (4.23); addressing its limitations and exploring other aspects of this Bayesian point of view of the coarse-graining problem through semidefinite programs (SDPs) implementations. Such implementations will anchor the numerical calculations, conducted in more detail in the next chapter, of the proposed Bayesian solution when one employs it in concrete coarse-graining scenarios.

Before delving into this convex optimization exposition, it is reasonable—for the purposes of this work—to first introduce the characterization of the diamond norm adopted throughout this section. Since it can be cast as a semidefinite program, as previously discussed in Section **2.4.1**, we directly embed our following analysis with its (dual) SDP version—borrowed from the formulation shown in (2.94) and adapted to the notations of the conditional states formalism for characterizing quantum channels. Thus, letting $\rho_{B|A}$ be the causal conditional state associated with a given quantum channel $\mathcal{E}_{B|A} : \mathcal{L}(\mathcal{H}_A) \to \mathcal{L}(\mathcal{H}_B)$, this leads us to employ the following SDP formulation of the diamond norm:

$$
\begin{aligned}
&\text{Given } \rho_{B|A} \\
&||\mathcal{E}_{B|A}||_{\diamond} := \text{Minimize} \quad \epsilon \\
&\\
&\text{Subject to} \quad \rho_{B|A} = Z_{AB} - X_{AB}; \\
&\\
&\qquad\qquad Z_{AB} \succeq 0, \quad X_{AB} \succeq 0; \\
&\\
&\qquad\qquad \epsilon \mathbb{I}_A \succeq \text{Tr}_B(Z_{AB} + X_{AB}),
\end{aligned}
\tag{5.1}
$$

where we denote the SDP dual variables, such as $X_{AB}, Z_{AB} \in \text{Herm}(\mathcal{H}_{AB})$, with the same joint notation adopted in previous sections to refer to their respective Hilbert spaces.

Now, we are in a position to analyze the limitations of the proposed Bayesian solution $\Gamma^{\text{Petz}}_{D|C,\rho_A}$ for the coarse-graining problem. Since the $\Gamma^{\text{Petz}}_{D|C,\rho_A}$ depends intrinsically on an initial state ρ_A for its construction, it restricts our task to finding an emergent dynamics

that makes the diagram in Fig. 4 commute only in a state-by-state manner, at least for ρ_A itself. Therefore, in order to remove the ρ_A dependence out of the commutativity relation while maintaining it in the $\Gamma^{\text{Petz}}_{D|C,\rho_A}$ construction, we start to face this state-dependence limitation through the following crucial inquiry: Is there another quantum dynamics $\Gamma^t_{D|C}$, ϵ-close to $\Gamma^{\text{Petz}}_{D|C,\rho_A}$, that makes the diagram of Fig. 4 commute for any initial state? A direct and conventional SDP formulation of such a question assumes the following form:

$$\begin{aligned}
&\text{Given} \quad \Gamma^{\text{Petz}}_{D|C,\rho_A}, \mathcal{U}^t_{B|A}, \Lambda^{\text{CG}}_{C|A}(\Lambda^{\text{CG}}_{D|B}) \\
&\text{Minimize} \quad \epsilon \\
&\text{Subject to} \quad \Gamma^t_{D|C} \circ \Lambda^{\text{CG}}_{C|A} = \Lambda^{\text{CG}}_{D|B} \circ \mathcal{U}^t_{B|A}; \\
&\qquad\qquad ||\Gamma^{\text{Petz}}_{D|C,\rho_A} - \Gamma^t_{D|C}||_\diamond \leq \epsilon; \\
&\qquad\qquad \Gamma^t_{D|C} \quad \text{is CPTP.}
\end{aligned} \tag{5.2}$$

Alternatively, we can rewrite the SDP above entirely within the conditional state formalism. This is achieved by replacing the diamond norm constraint by its SDP characterization—corresponding to the minimization of the radius ϵ of the diamond norm ball (Eq. (2.95)) around $\Gamma^{\text{Petz}}_{D|C,\rho_A}$, expressed in accordance with the notations of the SDP in (5.1)—and by representing all quantum channels and the commutativity relation (Eq. (4.19)) through their respective conditional states. The resulting, equivalent SDP reads

Searching for state-independent solutions close to $\Gamma^{\text{Petz}}_{D|C,\rho_A}$

$$\begin{aligned}
&\text{Given} \quad \rho^{\text{Petz}}_{D|C,\rho_A}, \rho_{B|A}, \rho_{C|A}(\rho_{D|B}) \\
&\text{Minimize} \quad \epsilon \\
&\text{Subject to} \quad \text{Tr}_C[(\mathbb{I}_A \otimes \rho_{D|C})(\rho^{T_C}_{C|A} \otimes \mathbb{I}_D)] = \text{Tr}_B[(\mathbb{I}_A \otimes \rho_{D|B})(\rho^{T_B}_{B|A} \otimes \mathbb{I}_D)]; \\
&\qquad\qquad \rho^{\text{Petz}}_{D|C,\rho_A} - \rho_{D|C} = Z_{CD} - X_{CD}; \\
&\qquad\qquad Z_{CD} \succeq 0, \quad X_{CD} \succeq 0; \\
&\qquad\qquad \epsilon \mathbb{I}_C \succeq \text{Tr}_D(Z_{CD} + X_{CD}); \\
&\qquad\qquad \rho_{D|C} \succeq 0, \quad \text{Tr}_D(\rho_{D|C}) = \mathbb{I}_C,
\end{aligned} \tag{5.3}$$

thereby emphasizing the usefulness of the conditional state formalism in approaching the coarse-graining problem. We claim that, through the above SDP, we can start to

understand how distant the proposed state-dependent solution is from another effective solution—if the latter actually exists.

To find an emergent dynamics compatible to a given microscopic dynamics and coarse-grained description, regardless of whether it is close to $\Gamma^{\text{Petz}}_{D|C,\rho_A}$, we can reformulate the above problem. It suffices to remove the diamond distance constraints and raise it to a feasibility SDP:

Searching for state-independent solutions

$$\begin{aligned} &\text{Given} \quad \rho_{B|A}, \rho_{C|A}(\rho_{D|B}) \\ &\text{Find} \quad \rho_{D|C} \\ &\text{Subject to} \quad \text{Tr}_C[(\mathbb{I}_A \otimes \rho_{D|C})(\rho^{T_C}_{C|A} \otimes \mathbb{I}_D)] = \text{Tr}_B[(\mathbb{I}_A \otimes \rho_{D|B})(\rho^{T_B}_{B|A} \otimes \mathbb{I}_D)]; \\ &\qquad\qquad \rho_{D|C} \succeq 0, \quad \text{Tr}_D(\rho_{D|C}) = \mathbb{I}_C. \end{aligned} \tag{5.4}$$

The SDPs presented above concern the existence of an emergent dynamics, related or not to the solution proposed by Brugger et al. The questions raised by the SDPs (5.3) and (5.4)—and the answers thereon—provide an initial direction by which we start to understand: (i) where the state-dependent solution proposed by Brugger et al. is located in relation to a definitive solution, that is, an emergent dynamics which commutes the diagram for any initial state, and (ii) in what scenarios there exists such definitive solution, circumventing in that way the state-by-state limitation of the previous one. From this point onward, we put the solution proposed by Brugger et al. aside and concentrate our efforts to investigate some additional aspects of the coarse-graining problem in this Bayesian inference picture here sketched.

To do so, we need first to introduce the concept of *robustness*. Historically, the *robustness measure*, originally—up to our knowledge—proposed in Ref. (36), was a special case of an entanglement magnitude. Roughly speaking, it quantifies how much noise can be added to an entangled state in order to erase all entanglement contained in that state. Despite such a concept being first concerned about the quantum correlation properties of states, there are several other applications and variants of such a quantity proposed in the literature (46, 61, 62, 63, 65). Hence, inspired by such studies and in line with the concept of the (non-)compatibility between the quantum channels employed in a coarse-graining scenario, as discussed in Ref. (27) and stated here in Definition 11, we propose a new robustness measure that quantifies how much noise can be added to a unitary evolution—compatible with a given coarse-graining map—while still remaining compatible with the corresponding coarse-grained description.

Definition 13 (CG-compatibility robustness)**.** *Let $\mathcal{U}^t_{B|A}$ be a unitary dynamics compatible with a given coarse-graining map $\Lambda^{CG}_{C|A}(\Lambda^{CG}_{D|B})$, that is, there exists a CPTP emergent dynamics $\Gamma^t_{D|C}$ such that $\Gamma^t_{D|C} \circ \Lambda^{CG}_{C|A} = \Lambda^{CG}_{D|B} \circ \mathcal{U}^t_{B|A}$. We define the CG-compatibility robustness of $\mathcal{U}^t_{B|A}$ as*

$$r_c(\mathcal{U}^t_{B|A}) := 1 - \tilde{r}_c(\mathcal{U}_{B|A}), \tag{5.5}$$

where the quantity $\tilde{r}_c(\mathcal{U}_{B|A})$ is given explicitly by

$$\begin{aligned} &\tilde{r}_c(\mathcal{U}^t_{B|A}) := min\{\gamma \mid \gamma\mathcal{U}^t_{B|A} + (1-\gamma)\Phi^t_{B|A} =: \mathcal{N}^t_{B|A} \in \mathcal{C}(A,B), \\ &\Phi^t_{B|A} \in \mathcal{C}(A,B), \exists \Omega^t_{D|C} \in \mathcal{C}(C,D) : \Omega^t_{D|C} \circ \Lambda^{CG}_{C|A} = \Lambda^{CG}_{D|B} \circ \mathcal{N}^t_{B|A}\}. \end{aligned} \tag{5.6}$$

Intuitively, $r_c(\mathcal{U}^t_{B|A})$ quantifies how *robust* the microscopic dynamics $\mathcal{U}^t_{B|A}$ is—for a given coarse-grained description—in allowing the existence of another emergent dynamics $\Omega^t_{D|C}$, even in the presence of any microscopic noise. In other words, the value assumed by $r_c(\mathcal{U}^t_{B|A})$ refers to the maximal addition of noise (dictated by $\Phi^t_{B|A}$) to a compatible unitary dynamics $\mathcal{U}^t_{B|A}$, with a fixed coarse-grained description $\Lambda^{\mathrm{CG}}_{C|A}(\Lambda^{\mathrm{CG}}_{D|B})$, before its compatibility vanishes. In this sense, the smaller $\tilde{r}_c(\mathcal{U}^t_{B|A})$ is, the more $\mathcal{U}^t_{B|A}$ can be perturbed by the noise $\Phi^t_{B|A}$ while remaining compatible with the coarse-grained description $\Lambda^{\mathrm{CG}}_{C|A}(\Lambda^{\mathrm{CG}}_{D|B})$, and thus the greater its *CG*–compatibility robustness $r_c(\mathcal{U}_{B|A})$ is.

We can look at the respective conditional state associated with each aforementioned quantum channel in order to propose the following SDP characterization to the auxiliary quantity $\tilde{r}_c(\mathcal{U}_{B|A})$:

$$\begin{aligned} &\text{Given} \quad \rho_{B|A}, \phi_{B|A}, \rho_{C|A}(\rho_{D|B}) \\ &\tilde{r}_c(\mathcal{U}^t_{B|A}) = \text{Minimize} \quad \gamma \\ &\\ &\text{Subject to} \quad \sigma_{B|A} = \gamma\rho_{B|A} + (1-\gamma)\phi_{B|A}; \\ &\\ &\qquad \mathrm{Tr}_C[(\mathbb{I}_A \otimes \omega_{D|C})(\rho^{T_C}_{C|A} \otimes \mathbb{I}_D)] = \mathrm{Tr}_B[(\mathbb{I}_A \otimes \rho_{D|B})(\sigma^{T_B}_{B|A} \otimes \mathbb{I}_D)]; \\ &\\ &\sigma_{B|A} \geq 0, \quad \mathrm{Tr}_B(\sigma_{B|A}) = \mathbb{I}_A; \\ &\\ &\omega_{D|C} \geq 0, \quad \mathrm{Tr}_D(\omega_{D|C}) = \mathbb{I}_C, \end{aligned} \tag{5.7}$$

and, as consequence, efficiently compute $r_c(\mathcal{U}^t_{B|A})$ from it.

Note that, since we are interested in cases where the noisy, resultant microscopic dynamics $\mathcal{N}^t_{B|A}$ is CPTP, the very same constraints in the SDP which guarantee that its Choi-isomorphic state $\sigma_{B|A}$ is a valid acausal conditional state imply naturally that $r_c(\mathcal{U}^t_{B|A}) \in [0,1]$. Moreover, when $r_c(\mathcal{U}^t_{B|A}) = 0$, we say that the microscopic dynamics

$\mathcal{U}^t_{B|A}$ is not robust—relative to a given compatible coarse-grained description—against any noise $\Phi^t_{B|A}$.

Inspired by the discussions about the CG-compatibility robustness above we take now a subtly different path. There is one last question that we want to address in this contribution: Given a coarse-grained description, dictated by a coarse-graining map $\Lambda^{\text{CG}}_{C|A}(\Lambda^{\text{CG}}_{D|B})$, and an initial, non-compatible unitary dynamics $\mathcal{U}^t_{B|A}$, does there exist any microscopic dynamics $\Psi^t_{B|A} \in \mathcal{C}(A, B)$ such that, for some $\gamma \in [0, 1]$, the noised, resultant dynamics

$$\mathcal{J}^t_{B|A} := \gamma \mathcal{U}^t_{B|A} + (1 - \gamma)\Psi^t_{B|A} \tag{5.8}$$

is compatible with an emergent dynamics $\Theta^t_{D|C} \in \mathcal{C}(D, C)$, satisfying $\Theta^t_{D|C} \circ \Lambda^{\text{CG}}_{C|A} = \Lambda^{\text{CG}}_{D|B} \circ \mathcal{J}^t_{B|A}$? Put another way, is it possible to render a non-compatible unitary dynamics compatible? Such a question, when one lets $\rho_{B|A}$ and $\rho_{C|A}(\rho_{D|B})$ be the causal conditional states associated with $\mathcal{U}^t_{B|A}$ and $\Lambda^{\text{CG}}_{C|A}(\Lambda^{\text{CG}}_{D|B})$, respectively, could be reformulated as a feasibility problem, as shown in the SDP below.

Robustness inspired

$$\begin{aligned}
&\text{Given} \quad \rho_{B|A}, \rho_{C|A}(\rho_{D|B}), \gamma \\
&\text{Find} \quad \psi_{B|A} \\
&\\
&\text{Subject to} \quad \sigma_{B|A} = \gamma\rho_{B|A} + (1 - \gamma)\psi_{B|A}; \\
&\\
&\qquad \text{Tr}_C[(\mathbb{I}_A \otimes \theta_{D|C})(\rho^{T_C}_{C|A} \otimes \mathbb{I}_D)] = \text{Tr}_B[(\mathbb{I}_A \otimes \rho_{D|B})(\sigma^{T_B}_{B|A} \otimes \mathbb{I}_D)]; \\
&\\
&\qquad \psi_{B|A} \succeq 0, \quad \text{Tr}_B(\psi_{B|A}) = \mathbb{I}_A; \\
&\\
&\qquad \theta_{D|C} \succeq 0, \quad \text{Tr}_D(\theta_{D|C}) = \mathbb{I}_C.
\end{aligned} \tag{5.9}$$

In other words, the SDP above provides a yes/no answer to the following question: if the initial microscopic dynamics of a quantum system is non-compatible with a given coarse-grained description, does there exist any CPTP map such that their convex combination becomes compatible?

This question seems to be deeply in the core of the coarse-graining problem, because even if we are unable to describe the underlying microscopic dynamics of a quantum system through a less complex, effective dynamics—promoted by a given coarse-grained description—by solving the optimization problem stated in (5.9), one is able to check whether, at least, there exists some quantum dynamics whose combination with the initial ones makes it possible to operationally obtain such an effective description.

With the willingness to evaluate numerically the state-dependent solution proposed by Brugger et al.—via the SDPs proposed in this section—as well as some coarse-graining scenarios within this Bayesian framework, we implemented these optimization programs in Python language using the CVXPY (10) library, with MOSEK (60) as the solver. To instigate further research in this direction and promote reproducibility of our numerical findings, the data and implementation codes used here to generate our following numerical results are available on GitHub.[1]

[1] `https://github.com/thalesbsfr/CG-SDP-numerical-implementations`

6 NUMERICAL RESULTS

Although our SDPs were designed to work in full generality, to verify them against concrete benchmarks, we will focus on studying and analysis pairs of qubits. This way, we can determine interesting properties without having to care about the quirks of multipartite, high-dimensional quantum scenarios. To address this in detail, we begin by presenting two unitary dynamics which, when combined with the two paradigmatic coarse-graining maps Λ_{Tr} and Λ_{BnS} discussed at the end of chapter 3, allow us to build four concrete coarse-graining scenarios. In all cases, still resorting to the diagram of Fig. 4, both regions A and B are such that $\mathcal{H}_A \simeq \mathcal{H}_B \simeq \mathbb{C}^2 \otimes \mathbb{C}^2$, and the regions C and D will be such that $\mathcal{H}_C \simeq \mathcal{H}_D \simeq \mathbb{C}^2$.

To benchmark our work, the first underlying unitary dynamics we choose is the SWAP gate $\mathcal{U}^{\mathrm{SWAP}}_{B|A}(\cdot) := U_{\mathrm{swap}}(\cdot)U^{\dagger}_{\mathrm{swap}}$, where (31):

$$U_{\mathrm{swap}} := \begin{pmatrix} 1 & 0 & 0 & 0 \\ 0 & 0 & 1 & 0 \\ 0 & 1 & 0 & 0 \\ 0 & 0 & 0 & 1 \end{pmatrix}. \tag{6.1}$$

Although its action simply exchanges the quantum state of a two-qubit system, this gate has meaningful applications spread along the literature, one of them is its role as one of the building blocks of the SWAP test (66): the best tool in quantum computation used to estimate how close two given quantum states are (67). Besides this, when combined with the coarse-graining description dictated by the partial trace over the subsystem on the right, it yields a remarkable coarse-graining scenario in which the general emergent dynamics cannot even be defined, as elucidated in (29).

The second unitary evolution adopted here is based on an adapted version of the Hamiltonian used to model spin interactions of two neighboring particles in a quantum Ising model (68), in a region where the external magnetic field vanishes. More specifically, we employ the Hamiltonian $H = -J\hbar\sigma_z \otimes \sigma_z$, for a given coupling constant J in units of frequency, to model the interaction between the parts of a two-qubit system determined by the alignment (or anti-alignment) of its spin projections along the $z-$axis, where

$$\sigma_z = \begin{pmatrix} 1 & 0 \\ 0 & -1 \end{pmatrix}. \tag{6.2}$$

An important feature of such a Hamiltonian is that the unitary operator arising from it, denoted in this contribution by

$$U_{\sigma_z} := e^{-i\frac{Ht}{\hbar}} = e^{itJ\sigma_z\otimes\sigma_z} = \begin{pmatrix} e^{itJ} & 0 & 0 & 0 \\ 0 & e^{-itJ} & 0 & 0 \\ 0 & 0 & e^{-itJ} & 0 \\ 0 & 0 & 0 & e^{itJ} \end{pmatrix}, \tag{6.3}$$

models a quantum dynamics in which, for some initial states, entanglement is created (or annihilated) between the two parts of the system, depending intrinsically on the value of the time parameter t. Thus, with a motivation of bringing to our coarse-graining scenarios a quantum channel that addresses quantum correlation aspects between the subsystems, we define our last unitary dynamics approached, named $z-$interaction channel, by $\mathcal{U}^{\sigma_z}_{B|A}(\cdot) := U_{\sigma_z}(\cdot)\, U^{\dagger}_{\sigma_z}$.

Now, with these unitary dynamics above presented in hand, and together with the coarse-graining maps presented in Chapter 3, the coarse-graining scenarios we study are:

- Scenario 1: Blurred and saturated detector and SWAP channel;
- Scenario 2: Blurred and saturated detector and $z-$interaction channel;
- Scenario 3: Partial trace and SWAP channel;
- Scenario 4: Partial trace and $z-$interaction channel.

6.1 BENCHMARKING DIAGRAM COMMUTATIVITY

As a starting point, it was shown along this work, specifically, in Section 4.2, that the solution proposed by Brugger et al., $\Gamma^{\text{Petz}}_{D|C,\rho_A}$, for the coarse-graining problem (Fig. 4) has an intrinsic dependence on an initial state ρ_A. Moreover, as also discussed, for a given microscopic dynamics and coarse-grained description, it satisfies the commutativity relation at least for the same ρ_A adopted in its own construction—its *generator*. Nevertheless, fixing an initial generator ρ_A in the $\Gamma^{\text{Petz}}_{D|C,\rho_A}$ construction one might pragmatically ask: How robust is the $\Gamma^{\text{Petz}}_{D|C,\rho_A}$ solution in making the diagram of Fig. 4 commute for other states in the region A, not necessarily equal to its generator? In other words, letting $\rho'_A \in \mathcal{D}(\mathcal{H}_A)$ be any state of the initial region A, how close, in the trace norm, is

$$||\Gamma^{\text{Petz}}_{D|C,\rho_A} \circ \Lambda^{\text{CG}}_{C|A}(\rho'_A) - \Lambda^{\text{CG}}_{D|B} \circ \mathcal{U}^{t}_{B|A}(\rho'_A)||_1, \tag{6.4}$$

to zero? Or, equivalently, in terms of the conditional states, how close is

$$||\,\text{Tr}_C\{\rho^{\text{Petz}}_{D|C,\rho_A}[\text{Tr}_A(\rho_{C|A}\rho'^{T_A}_A)]^{T_C}\} - \text{Tr}_B\{\rho_{D|B}[\text{Tr}_A(\rho_{B|A}\rho'^{T_A}_A)]^{T_B}\}||_1 \tag{6.5}$$

to zero, for a given configuration of unitary dynamics $\mathcal{U}^{t}_{B|A}$ that is Choi-isomorphic to $\rho_{B|A}$ and coarse-graining map $\Lambda^{\text{CG}}_{C|A}(\Lambda^{\text{CG}}_{D|B})$ that is Choi-isomorphic to $\rho_{C|A}(\rho_{D|B})$?

Initially, we study four generators: (1) $\rho_{\text{ME}} := \frac{1}{2}\,|\Omega\rangle\,\langle\Omega| \in \mathcal{D}(\mathbb{C}^2 \otimes \mathbb{C}^2)$, representing the normalized maximally entangled state; (2) $\rho_{\text{MM}} := \frac{1}{4}\mathbb{I}_{4\times 4}$, the maximally mixed state; (3) a state ρ_{rand} generated randomly using a uniform random sampling method of the NumPy library (69); and (4) the two-qubit Werner state

$$\rho_{\text{W}} := \lambda \left|\Psi^-\right\rangle \left\langle\Psi^-\right| + \frac{1-\lambda}{4}\mathbb{I}_{4\times 4}, \tag{6.6}$$

for $|\Psi^-\rangle := \frac{1}{\sqrt{2}}(|01\rangle - |10\rangle)$ and $\lambda = 1/3$. Figures 6a, 6b, 6c and 6d contain our initial results. Because scenarios 2 and 4 are time dependent, we decided to show the results initially for $t = 1$—other time steps will be investigated later in this work.

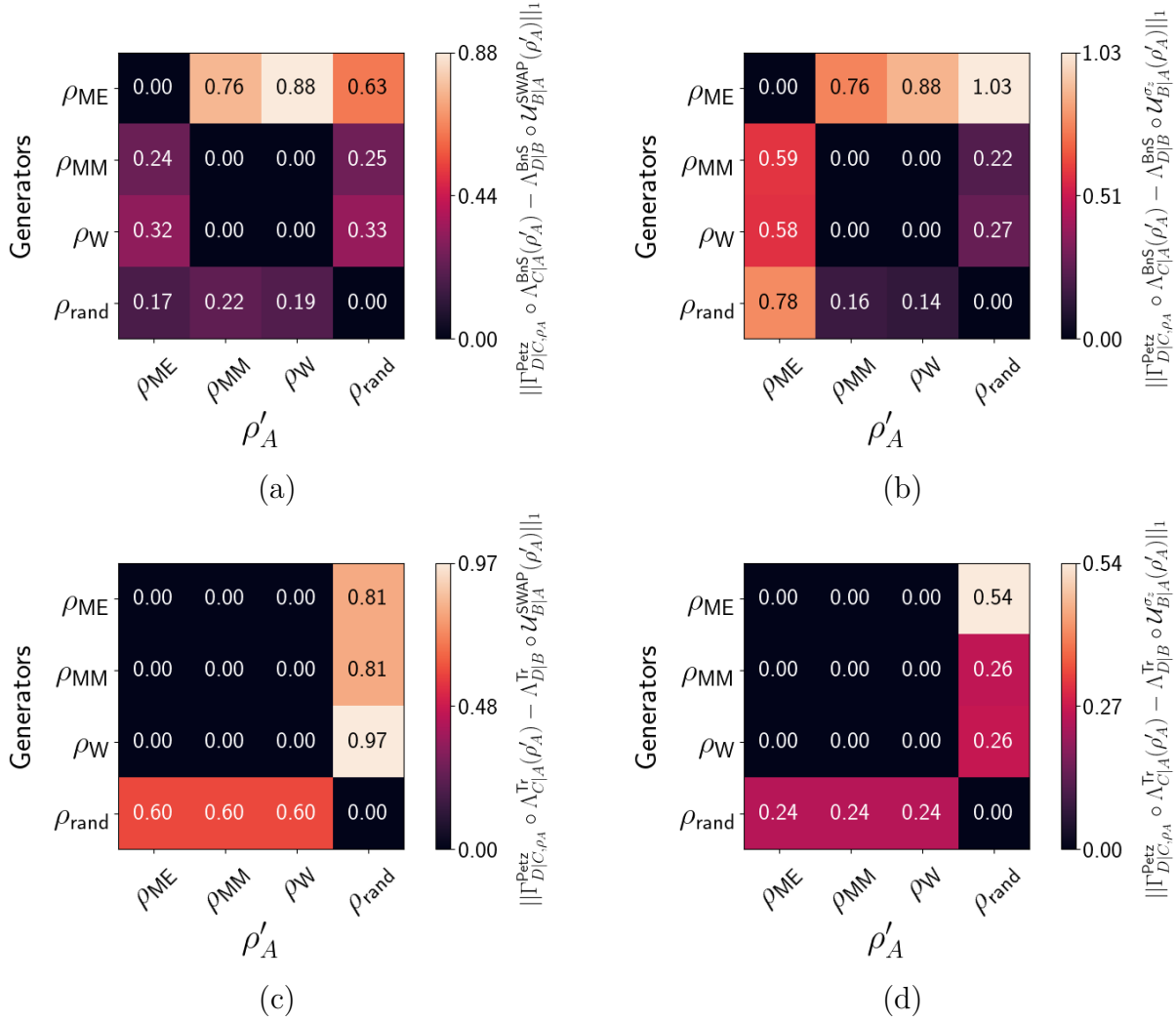

Figure 6 - Performance of the solution $\Gamma^{\mathbf{Petz}}_{D|C,\rho_A}$ in four different coarse-graining scenarios for four different generators. The states on the rows on the left represents the generators, while those on the bottom of the columns represents the ρ'_A states used in the commutativity relation displayed in (6.4). The performance of the solution $\Gamma^{\text{Petz}}_{D|C,\rho_A}$ in commuting the diagram, quantified by Eq. (6.4), is represented through a color-scale mapping. Image (a) shows the results for our scenario 1, while images (b), (c) and (d), for the scenarios 2, 3 and 4, respectively. One can see that, in general, even in the worst scenario (based on the mean value of all results) in this picture for the commutativity using the proposed $\Gamma^{\text{Petz}}_{D|C,\rho_A}$ solution, scenario 2, image (b), there are states different from the generator in which the diagram commutes.

From the results shown in Fig. 6, we observe that, in all four scenarios, deploying the solution $\Gamma^{\text{Petz}}_{D|C,\rho_A}$ as the emergent dynamics makes it possible to satisfy the commutativity relation for states different from its generators, as is the case, in all scenarios, when ρ_{W} is the generator and ρ_{MM} goes into the commutativity relation (or vice versa). In particular, for the scenario 4, Fig. 6d, we can also think that, for a given generator, the $\Gamma^{\text{Petz}}_{D|C,\rho_A}$

makes the diagram commute not only for the generator itself, but additionally, there exists a set of states which satisfy the desired commutativity relation, achieving zero in (6.4). This fact, concerning a pragmatic point of view of the coarse-graining problem as a role, emphasizes numerically that, even in some specific scenarios where there doesn't exist an emergent dynamics that commutes the diagram for all initial states, i.e., which satisfies Eq. (3.2), or its respective causal conditional state satisfies (4.19), the solution proposed by Brugger et al. can be employed for this task at least for a set of initial states.

For sustaining this last numerical statement, we also engage with several evaluations of the expression (6.4) through a uniform sample of 10^6 different random states as ρ'_A. Since ρ_{rand}, as shown in Fig. 6, is the generator for which $\Gamma^{\text{Petz}}_{D|C,\rho_A}$ yields the worst performance in commuting the diagram for states different from itself, we restrict our subsequent calculations of the expression (6.4) to the other three generators. The results are summarized in the histograms of Fig. 7.

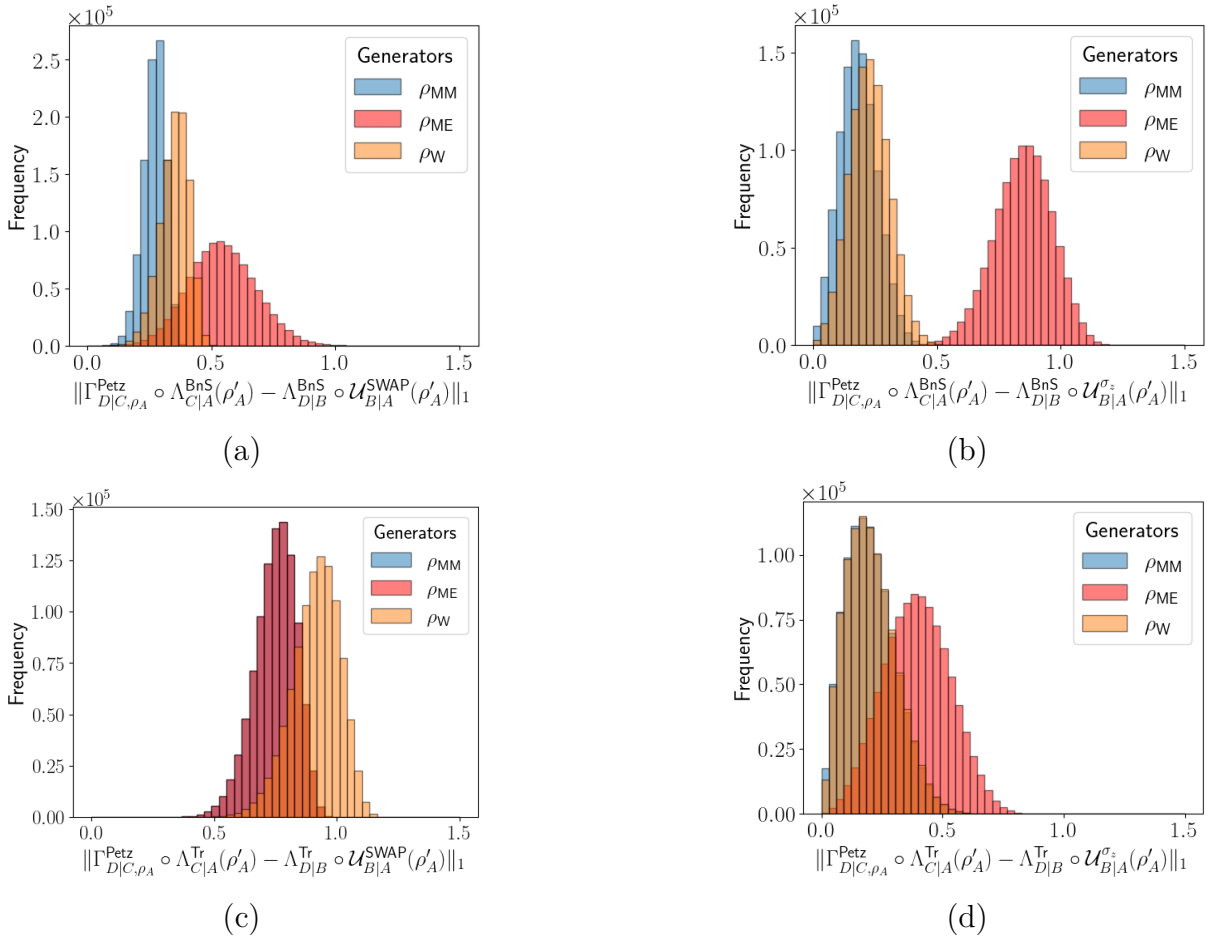

Figure 7 - Histograms showing the commutativity performance of $\Gamma^{\mathbf{Petz}}_{D|C,\rho_A}$ (Eq. (6.4)) for a sample of 10^6 random states in the four scenarios. For scenarios 1 and 2, shown in images (a) and (b), respectively, the generator in which the $\Gamma^{\text{Petz}}_{D|C,\rho_A}$ achieves the worst results was ρ_{ME}, while for the other two, their respective histograms present a similar behavior, with ρ_{MM} producing better results in general. In the last histograms—shown in images (c) and (d), corresponding to scenarios 3 and 4, respectively—a slightly different behavior emerges in comparison to the previously discussed histograms. In scenario 3, since the $\Gamma^{\text{Petz}}_{D|C,\rho_A}$ generated by ρ_{ME} and by ρ_{MM} are identical, both ρ_{ME} and ρ_{MM} yield similar results, whereas ρ_{W} performs worst in general. On the other hand, in scenario 4, ρ_{MM} and ρ_{W} achieve almost equal, best results, while ρ_{ME} shows the worst. Overall, scenario 4 distributions reach results closest to zero compared to the others, while scenario 3 is, on average, the most distant. Additionally, on average, the generator producing the worst results is ρ_{ME}.

From the above histograms, notably, one can see that there are some scenarios, such as scenario 2 and 4 shown in Fig.7b and Fig. 7d, respectively, in which the proposed solution $\Gamma^{\text{Petz}}_{D|C,\rho_A}$, with ρ_{MM} and ρ_{W} as generators, achieves results very close to zero for a considerable number of random states in the first bins of such histograms. Highlighting, in this way, our initial numerical statement that, from a pragmatic point of view, the solution proposed by Brugger et al. can be employed to commute the diagram in such scenarios, not only for the generator itself, but also for a set of distinct states of the initial region.

A more detailed view of the best results in the bin closest to zero in the histograms of scenarios 2 and 4 (Fig. 7b and Fig. 7d, respectively) is shown in Fig. 8.

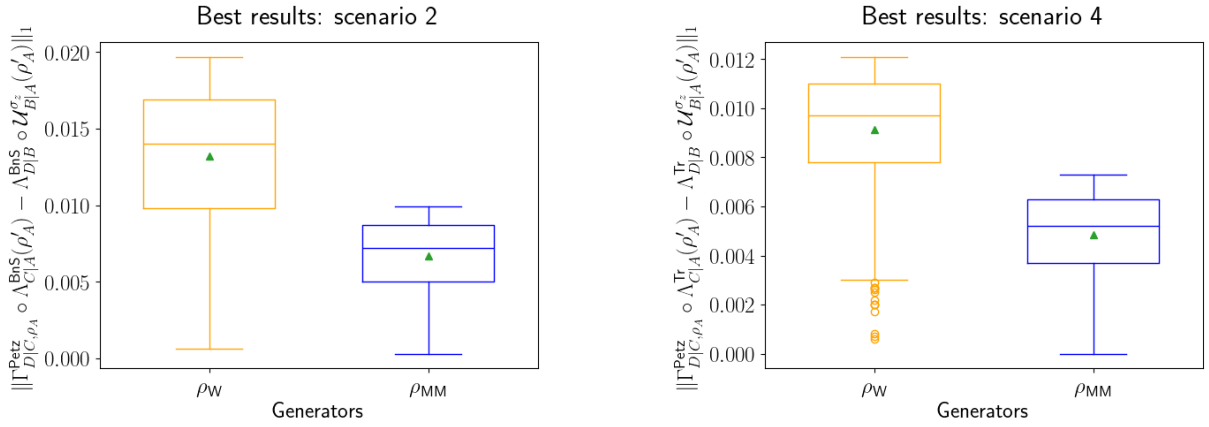

(a) (b)

Figure 8 - Boxplots of the best 10^3 results obtained in scenarios 2 and 4. Each box represents the interquartile range, the central line marks the median, green triangles indicate the mean values, and outliers are shown as individual circles. In general, ρ_{MM} as generator produces better results compared to ρ_{W}. For scenario 4, blue boxplot in image (b), the minimum result (zero) occurs for 28 different random states within the 10^3 analyzed.

As mentioned previously, the results for scenarios 2 and 4 in Figs. 6, 7 and 8 were generated by setting $t = 1$ in the unitary dynamics $\mathcal{U}^{\sigma_z}_{B|A}$. Since such dynamics, as discussed around Eq. (6.3), can create or annihilate correlations between the two parts of the initial system depending on the value of the parameter t, it is reasonable to also analyze numerically what this fact could imply to diagram commutativity involving our interested scenarios. Taking the random state which generates the best result in Fig. 7b and 7d for each generator, one can see, in Fig. 9, how varying the time parameter t of the microscopic dynamics directly affects the commutativity of the diagram of scenarios 2 and 4.

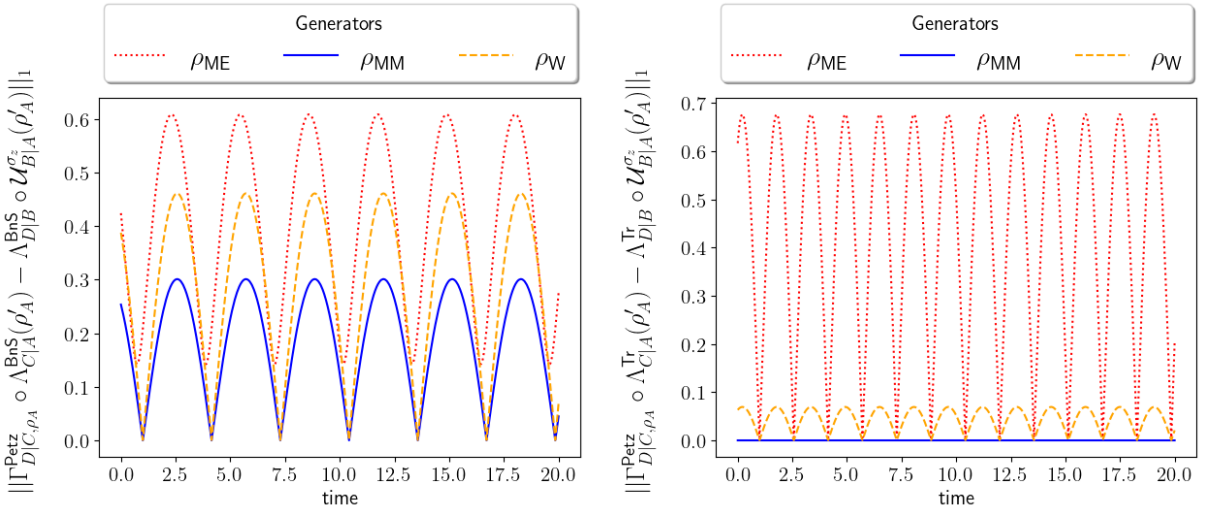

Figure 9 - Time varying effects on the commutativity performance of $\Gamma^{\mathbf{Petz}}_{D|C,\rho_A}$. Image (a) shows the results for scenario 2 and image (b) for the scenario 4. We can see, for scenario 2, changing the time t of the microscopic dynamics $\mathcal{U}^{\sigma_z}_{B|A}$ can improve the results obtained for ρ_{ME} generator; however, it neither approaches nor reaches zero as equal the results of the other generators. In general, it sustains the same behavior shown in Fig. 7b, with the ρ_{MM} achieving the best results, follows by the ρ_{W} and, despite in some time-steps its results has improved, ρ_{ME} remains the worst generator for this scenario. Regarding the scenario 4, the differences between the performance of each generator become highly evident through this time varying evaluation. ρ_{ME}, which achieves the worst results in Fig. 7d, here, for some timestep, it achieves results close to zero, in contrast to the results observed on image (a). Moreover, notably, the results for ρ_{W} for all timestep, even in some specific ones it gets a little worse, they revolved around values very close to zero. For the ρ_{MM} as the generator, we can see a very peculiar behavior in comparison to the others. The selected state, which commutes the diagram of scenario 4 for $t = 1$ in the microscopic dynamics $\mathcal{U}^{\sigma}_{B|A}$, remains commuting the diagram, i.e., achieving zero in the expression (6.4) for all the timestep in this analysis. Shining light to the usefulness, from a pragmatic point of view, of the ρ_{MM} as $\Gamma^{\text{Petz}}_{D|C,\rho_A}$ generator in this coarse-graining scenario.

From the results shown in Fig. 9, one can see that, in scenario 2 (Fig. 9a), the time dependence of the microscopic dynamics $\mathcal{U}^{\sigma_z}_{B|A}$ does really interfere in the commutativity performance of all generators. In particular, it is worth mentioning that, in comparison to the results depicted in Fig. 7b for $t = 1$, there are some values of t where the results produced with all generators were improved. Furthermore, regarding the results of scenario 4 (Fig. 9b), we would like to highlight that, performing the same analysis with the other 27 random states in which the diagram of scenario 4 commutes when one uses the ρ_{MM} as the $\Gamma^{\text{Petz}}_{D|C,\rho_A}$ generator and sets $t = 1$ in $\mathcal{U}^{\sigma_z}_{B|A}$, it also presents the same behavior and result observed in the blue-continuous line of Fig. 9b. Reinforcing, in that way, for this scenario, the usefulness of the $\Gamma^{\text{Petz}}_{D|C,\rho_A}$ generated by ρ_{MM} in commuting the diagram not only for the generator itself, but also for a set of random states, regardless of the value of t in the microscopic dynamics.

To conclude this numerical investigation of the diagram commutativity for the state-dependent solution $\Gamma^{\text{Petz}}_{D|C,\rho_A}$, we engage in a last but not least inquiry within this paradigm. The ρ_{W} generator here employed, in the way it was defined in Eq. (6.6), is a separable state for $\lambda \in [-1/3, 1/3]$ and entangled for $\lambda \in (1/3, 1]$ (56). Given that, in its very definition, we have set $\lambda = 1/3$ and conducted all of our above numerical evaluation with it being a separable state, one might ask what changing in the value[1] of the parameter λ could imply for the performance of ρ_{W} as a generator. Taking each random state which produces the best result in each of the four scenarios[2] depicted in Fig. 7 with ρ_{W} as generator, an enlightenment upon such a question can be seen in Fig. 10.

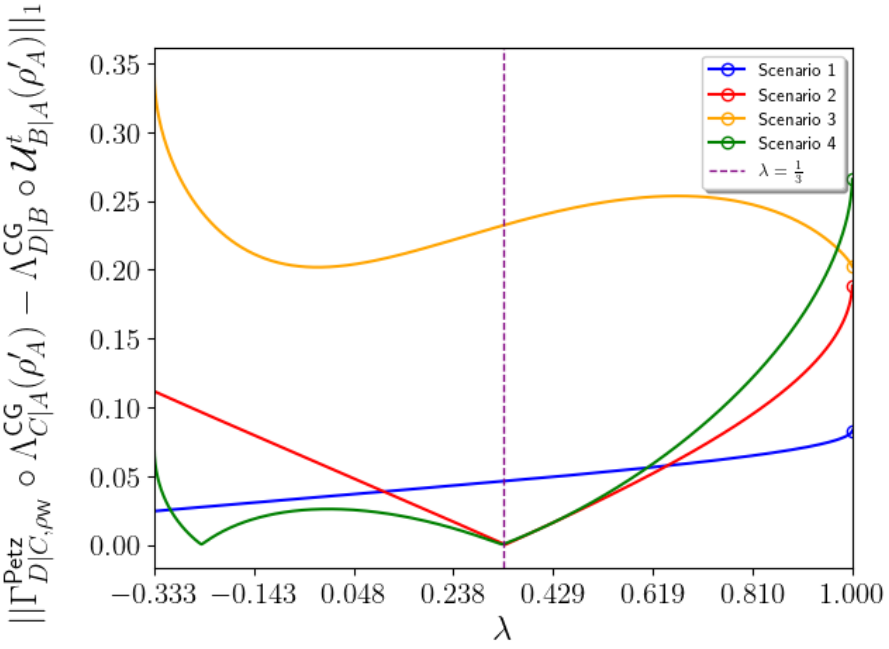

Figure 10 - Performance of $\Gamma^{\text{Petz}}_{D|C,\rho_{\text{W}}}$ as a function of the parameter λ in ρ_{W}. For each scenario, the random state ρ'_A that goes into (6.4) was the one that achieves the best results in Fig. 7 histograms of ρ_{W} generator for $\lambda = 1/3$. One can see that, with this vertical purple dashed line indicating where $\lambda = 1/3$, how changing this parameter affects the commutativity performance of ρ_{W} in all four scenarios. In particular, regarding the results of scenario 2 and scenario 4, one can see, notably, a inflection point and a worsening in the results displayed in their respective line graphs, right at $\lambda = 1/3$. Since for $\lambda > 1/3$ the ρ_{W} becomes entangled and the worst result for these scenarios occurred when $\lambda \approx 1$ (ρ_{W} approximately maximally entangled), drawing a parallel with the results of the maximally entangled generator ρ_{ME} shown in Fig. 7b and 7d, this might be an evidence that: the more entangled the $\Gamma^{\text{Petz}}_{D|C,\rho_A}$ generator is, the worse is the commutativity performance of $\Gamma^{\text{Petz}}_{D|C,\rho_A}$ in such scenarios.

---

[1] Given that, for $\lambda = 1$, $\Lambda_{\text{BnS}}(\rho_{\text{W}})$ is not invertible and, because of this, we cannot construct the $\Gamma^{\text{Petz}}_{D|C,\rho_A}$, the open circles highlight that we only consider λ values close to 1 at the end of $x-$axis of the following figure.

[2] As a remark, for generated this analysis with emphasis on the effect of changing the value of the parameter λ in the ρ_{W} generator, we consider $t = 1$ on the microscopic dynamics $\mathcal{U}^{\sigma_z}_{B|A}$ of scenarios 2 and 4.

6.2 SDP IMPLEMENTATIONS

After establishing the numerical evaluations of the solution proposed by Brugger et al., we now turn our attention to additional numerical inquiries raised by the semidefinite programs introduced throughout chapter 5, still concerning the four coarse-graining scenarios previously addressed.

6.2.1 Finding state-independent solutions

It was shown by the results displayed on Fig. 7 and along the discussions around Fig. 8 that, for a given coarse-graining scenario, the choice of the $\Gamma^{\text{Petz}}_{D|C,\rho_A}$ generators interferes directly in its commutativity performance. Besides this, we can claim from the aforementioned result that, for scenario 4, within a sample of 10^6 random states, the $\Gamma^{\text{Petz}}_{D|C,\rho_A}$ generated by ρ_{MM} can be employed as a candidate of macroscopic, emergent dynamics, in the formalism here carried, for only a set of 28 distinct states plus the generator itself. Aligned with that, in order to circumvent this limitation while pursuing a more general treatment of commutativity, we numerically solve the proposed SDP (5.3) for the four scenarios considered and the three generators depicted in Fig. 7. Among them, the only scenario in which it was possible to find an optimal emergent dynamics, $\Gamma^{\text{opt}}_{D|C}$, that commutates the diagram for all initial states was in scenario 1. We report in Table 1, for each generator, the optimal value achieved of ϵ which minimizes such an optimization program.

Generator	$\lVert\Gamma^{\text{Petz}}_{D\|C,\rho_A} - \Gamma^{\text{opt}}_{D\|C}\rVert_\diamond$
ρ_{ME}	1.66
ρ_{MM}	0.42
ρ_{W}	0.55

Table 1 – Optimum values achieved by solving SDP (5.3) for the three generators. The scenario 1 was the only scenario in which such a solution was feasible.

Additionally, in agreement with the above results, by solving numerically the feasibility SDP (5.4) for the four scenarios here approached, the only one for which the program was solvable was setup 1; with the optimal (feasible) solution given explicitly by

$$\rho^{\text{opt}}_{D|C} = \begin{pmatrix} 1 & 0 & 0 & 1 \\ 0 & 0 & 0 & 0 \\ 0 & 0 & 0 & 0 \\ 1 & 0 & 0 & 1 \end{pmatrix}. \tag{6.7}$$

Since this solution is the Choi-isomorphic operator to the identity channel, we can conclude that, among all the scenarios evaluated, the scenario in which the microscopic dynamics is compatible with the coarse-grained description is the one composed of the blurred

and saturated detector and the SWAP channel. Furthermore, tracing a parallel with the results displayed in Sec. 6.1, we would like to emphasize that, even in the scenarios where there is no general emergent dynamics—by the fact that the microscopic dynamics is not compatible with the coarse-grained description, such as scenarios 2, 3 and 4—the solution proposed by Brugger et al., $\Gamma^{\text{Petz}}_{D|C,\rho_A}$, with the right choice of its generator, can be employed pragmatically to solve the problem—at least for the generator itself and a limited number of states.

6.2.2 Robustness aspects

We now showcase the robustness aspect of such microscopic (compatible) dynamics. More specifically, given that from the above discussions we know that the SWAP channel is compatible with the coarse-grained description represented by the blurred and saturated detector map, we restrict our attention to the discussions around the proposed robustness measure and its SDP characterization displayed in Eq. (5.7). Essentially, since the microscopic dynamics $\mathcal{U}^{\sigma_z}_{B|A}$ is not compatible with the Λ_{BnS} map, we initially take it to be the added noise dynamics. By numerically solving the SDP enunciated in Eq. (5.7) with its respective causal conditional states, we obtain, for the CG-compatibility robustness of the SWAP channel with respect to Λ_{BnS} and this noise, that $r_c(\mathcal{U}^{\text{swap}}_{B|A}) \approx 0$. In other words, up to numerical imprecision, the compatibility of $\mathcal{U}^{\text{swap}}_{B|A}$ with the coarse-grained description Λ_{BnS} is not robust against the noise generated by $\mathcal{U}^{\sigma_z}_{B|A}$.

Moreover, conducting the same analysis except for changing the noise dynamics by: (1) a random unitary evolution $\mathcal{U}^{rand(1)}_{B|A}(\cdot) := U^{(1)}(\cdot)U^{(1)\dagger}$ where $U^{(1)}$ is some random element[3] of the group $U(4)$; and (2) a random product unitary evolution $\mathcal{U}^{rand(2)}_{B|A}(\cdot) := U^{(2)}(\cdot)U^{(2)\dagger}$ where $U^{(2)} := U_A \otimes U_B$ for some random elements U_A, U_B of the group $U(2)$, the results obtained are in agreement with the one shown previously; with the CG-compatibility robustness of the SWAP channel, up to numerical imprecision, being equal to zero. Therefore, at least for these three types of noise, we can conclude that: although the SWAP channel is compatible with the coarse-grained description raised by the blurred and saturated detector map, its compatibility is not robust.

This fact alone suggests how difficult the existence of a macroscopic, emergent dynamics is in the presence of any undesirable microscopic noise. It also suggests that, since we have chosen the noisy, resulting microscopic dynamics to be CPTP, even in this noisy scenario one is able to use the $\Gamma^{\text{Petz}}_{D|C,\rho_A}$ solution to solve the problem at least for the generator itself—or for a limited number of initial states. Thus, remarking a valuable property of the $\Gamma^{\text{Petz}}_{D|C,\rho_A}$ solution.

Implementing the robustness-inspired SDP proposed in Eq. (5.9), we now investi-

[3] The random unitary matrices used in this analysis were generated using SciPy's (53) `scipy.stats.unitary_group.rvs` method.

gate numerically, taking into account the previous verifications conducted above, whether there exists a microscopic dynamics which allows the existence of a general emergent dynamics for the non-compatible scenarios 2, 3, and 4. In particular, we are willing to answer whether there exists a microscopic dynamics such that its convex combination with the initial one becomes compatible with that coarse-grained description.

Letting our standpoint be the discussions around Eq. (5.8), with the convex combination parameter γ assuming 1.5×10^3 numerical values evenly spaced within the interval $[0, 1]$, we solve numerically the feasibility SDP proposed in (5.9) for the three aforementioned scenarios. In Table 2, we report the sub-intervals of γ in which, by solving such feasibility SDP, it was possible to find: (1) an (optimal) feasible microscopic dynamics $\Psi^t_{B|A}$ which, together with the respective initial (non-compatible) microscopic dynamics $\mathcal{U}^t_{B|A}$ of the scenario, allows us to construct the resultant dynamics $\mathcal{J}^t_{B|A}$ (Eq. (5.8)), compatible with the respective coarse-grained description; and (2) an effective macroscopic dynamics $\Theta^t_{D|C}$ that satisfies the commutativity relation (4.19) for this resultant configuration.

Scenarios	Solution ($\Theta^t_{D\|C}$) attainable
2 ($\mathcal{U}^t_{B\|A} = \mathcal{U}^{\sigma_z}_{B\|A}$)	$0 \leq \gamma \leq 0.557$
3 ($\mathcal{U}^t_{B\|A} = \mathcal{U}^{\text{swap}}_{B\|A}$)	$0 \leq \gamma \leq 0.249$
4 ($\mathcal{U}^t_{B\|A} = \mathcal{U}^{\sigma_z}_{B\|A}$)	$0 \leq \gamma \leq 0.524$

Table 2 – Sub-intervals of γ in which we can promote compatibility in the three non-compatible scenarios.

From these results, we can claim that, by running the proposed SDP (5.9) for the three non-compatible coarse-graining scenario, it was possible to find a resultant microscopic dynamics compatible with the given coarse-grained description—at least for a sub-interval of the parameter γ. Furthermore, from a pragmatic viewpoint, since the SDP (5.9) also returns an effective macroscopic dynamics for that resultant scenario, together with the results on the performance of $\Gamma^{\text{Petz}}_{D|C,\rho_A}$ discussed in Sec. 6.1, two conclusion can be drawn. First, the problem can be solved for all initial states whenever, for each non-compatible scenario considered, the parameter γ lies within the sub-intervals reported in Table 2. Second, for values of γ outside these intervals, given that the resultant microscopic dynamics remains CPTP, one is able to solve the problem in a state-by-state manner by using $\Gamma^{\text{Petz}}_{D|C,\rho_A}$, at least for its generator or for a limited number of underlying initial states.

7 CONCLUSION

In this work, motivated by the state-dependence limitation of the solution $\Gamma^{\text{Petz}}_{D|C,\rho_A}$ proposed by Brugger et al. (29) to the coarse-graining problem, we conducted a numerical evaluation in order to benchmark its performance in four concrete coarse-graining scenarios. Using the trace distance of the difference between the two sides of the conventional commutativity relation (Eq. (6.4)), we have analyzed its capacity in solve the problem, for a given coarse-graining scenario, in terms of different generator states in its construction. Our findings reveal a strong dependence in the choice of the generator state, with the solution performing better, in the four scenarios here approached, when it was generated from the maximally mixed state. Moreover, we observed that, in some cases, the solution can be employed, for a given coarse-graining scenario, not only for the generator-state itself but also for a limited number of random states. Note that throughout this work, we have picked up states randomly according to the uniform measure. In theory, we might have used a different form of sorting out random states, but since we are not investigating asymptotic behaviors (where concentration effects start to take place), nor are we circumscribed by an operational task demanding a more adapted measure (where measures should be compatible with allowed transformations), we have opted for a simpler random process.

Since the evaluated solution $\Gamma^{\text{Petz}}_{D|C,\rho_A}$ depends explicitly on the Petz recovery map, we claim that this finding might suggest a strong connection with the best performance observed for the Petz recovery map, as shown previously in Ref. (59), when it is generated from the maximally mixed state. This might constitute evidence, in parallel with that previous study, that the best choice of reference state for the Petz recovery map—not only for reverting the action of the dephasing and depolarizing channels, but also for the blurred and saturated detector coarse-graning map and for the partial trace—is the maximally mixed state. Additionally, we observed that, when varying the parameter of the Werner state taken as the generator state of the Petz recovery map in the solution, the more entangled this state is, the worse the results yielded become in reverting the coarse-graining maps. Suggesting, in that way, a fruitful direction for future investigations involving the role played by the reference state's quantum correlations—the generator of our solution, and consequently of the Petz recovery map—in coarse-graining scenarios beyond those addressed here.

Furthermore, in our semidefinite programming investigation, we have proposed novel convex-optimization strategies to overcome the state-dependence limitation of this previous Bayesian solution, such as searching for general, state-independent solutions, as shown in SDPs (5.2)-(5.4). We also address the coarse-graining problem from the perspective of the conditional state formalism as a whole. By viewing the compatibility of quantum dynamics in a coarse-graining scenario as a resource, we propose a new robustness measure (Definition

13) to quantify how much noise an initial compatible unitary dynamics can tolerate before its compatibility with a given coarse-grained description vanish. Additionally, drawing inspiration from it, we formulate a semidefinite program (SDP (5.9)) that searches for a compatible microscopic dynamics—and, consequently, a compatible macroscopic, emergent dynamics—for initially non-compatible coarse-graining scenarios. It should be remarked that this constitute a step toward a comprehensive computational study—in tandem with the ones approached in (30)—of the essence of the conventional coarse-graining problem, as stated in Ref. (24), within the quantum Bayesian framework for quantum theory.

Finally, since we have benchmarked and implemented numerically our proposed programs for only four concrete coarse-graining scenarios, we hope that they might serve as a basis for further research in these directions, especially in evaluating our proposed optimization routines across other coarse-graining scenarios.

REFERENCES

1 WANG, Yanzhi; WANG, Jianxiao; ZHANG, Haoran; SONG, Jie. Bridging prediction and decision: Advances and challenges in data-driven optimization. **Nexus**, v. 2, n. 1, p. 100057, 2025. Available at: <https://www.sciencedirect.com/science/article/pii/S295016012500004X>. DOI: https://doi.org/10.1016/j.ynexs.2025.100057.

2 SUN, Shiliang; CAO, Zehui; ZHU, Han; ZHAO, Jing. A survey of optimization methods from a machine learning perspective. **IEEE Transactions on Cybernetics**, v. 50, p. 3668–3681, 2019. Available at: <https://api.semanticscholar.org/CorpusID:189928307>.

3 GONÇALVES, G. C. *Abordagens matemática e estatística aplicadas a um modelo de dinâmica tumoral com células CAR-T*. 2025. Dissertação (Mestrado em Matemática) — Universidade Federal de Juiz de Fora, Instituto de Ciências Exatas, Juiz de Fora, 2025. Available at: <https://repositorio.ufjf.br/jspui/handle/ufjf/19415>.

4 YADAV, Km. Shveta; BHARDWAJ, Pooja; CHAUHAN, Ashirvad; MISHRA, Shweta. A review on optimization techniques used in pharmaceutical formulations. **International Journal of Pharmaceutical Sciences**, v. 3, n. 1, jan. 2025. DOI: 10.5281/zenodo.14749255. Available at: <https://doi.org/10.5281/zenodo.14749255>.

5 LEIFER, M. S.; SPEKKENS, R. W. Towards a formulation of quantum theory as a causally neutral theory of Bayesian inference. **Physical Review A**, v. 88, n. 5, p. 052130, 2013. DOI: 10.1103/PhysRevA.88.052130.

6 PETZ, D. Sufficient subalgebras and the relative entropy of states of a von Neumann algebra. **Communications in Mathematical Physics**, v. 105, p. 123-131, 1986. DOI: 10.1007/BF01212345.

7 BARNUM, H.; KNILL, E. Reversing quantum dynamics with near-optimal quantum and classical fidelity. **Journal of Mathematical Physics**, v. 43, n. 5, p. 2097-2106, 2002. DOI: 10.1063/1.1459754.

8 UOLA, R.; KRAFT, T.; SHANG, J.; YU, X.-D.; GÜHNE, O. Quantifying quantum resources with conic programming. **Physical Review Letters**, v. 122, n. 13, p. 130404, abr. 2019. DOI: 10.1103/PhysRevLett.122.130404.

9 DAHL, G. *An introduction to convexity*. Oslo: University of Oslo, Centre of Mathematics for Applications, 2010.

10 DIAMOND, S.; BOYD, S. *CVXPY: A Python-embedded modeling language for convex optimization*. Journal of Machine Learning Research, v. 17, n. 83, p. 1–5, 2016.

11 DA SILVA, R. A.; MARQUES, B. Semidefinite-programming-based optimization of quantum random access codes over noisy channels. **Physical Review A**, v. 107, n. 4, p. 042433, abr. 2023. DOI: 10.1103/PhysRevA.107.042433.

12 CHOI, M.-D. Completely positive linear maps on complex matrices. **Linear Algebra and its Applications**, v. 10, n. 3, p. 285–290, 1975. DOI: 10.1016/0024-3795(75)90075-0.

13 JAMIOŁKOWSKI, A. Linear transformations which preserve trace and positive semidefiniteness of operators. **Reports on Mathematical Physics**, v. 3, n. 4, p. 275–278, 1972. DOI: 10.1016/0034-4877(72)90011-0.

14 VANDENBERGHE, L.; BOYD, S. Semidefinite programming. *SIAM Review*, v. 38, n. 1, p. 49–95, 1996. DOI: 10.1137/1038003.

15 PUKELSHEIM, F. *Optimal design of experiments*. Philadelphia: SIAM, 2006.

16 ALIZADEH, F. Interior point methods in semidefinite programming with applications to combinatorial optimization. *SIAM Journal on Optimization*, v. 5, 1998. DOI: 10.1137/0805002.

17 BOYD, S.; EL GHAOUI, L.; FERON, E.; BALAKRISHNAN, V. *Linear matrix inequalities in system and control theory*. Philadelphia: Society for Industrial and Applied Mathematics (SIAM), 1994. DOI: 10.1137/1.9781611970777.

18 VANDENBERGHE, L.; BOYD, S. Applications of semidefinite programming. *Applied Numerical Mathematics*, v. 29, p. 283–299, 2000. DOI: 10.1016/S0168-9274(98)00098-1.

19 BOYD, S.; VANDENBERGHE, L.; GRANT, M. Efficient convex optimization for engineering design. In: *Proceedings of the IFAC Symposium on Robust Control Design*. 1994. p. 14–23.

20 KRAUS, K.; BÖHM, A.; DOLLARD, J. D.; WOOTTERS, W. H. **States, Effects, and Operations: Fundamental Notions of Quantum Theory**. Berlin: Springer Berlin Heidelberg, 1983. (Lecture Notes in Physics). ISBN 9780387127323.

21 FEYNMAN, R. P. Simulating physics with computers. **International Journal of Theoretical Physics**, v. 21, n. 6, p. 467-488, 1982. DOI: 10.1007/BF02650179.

22 PÉREZ-GARCÍA, D.; VERSTRAETE, F.; WOLF, M. M.; CIRAC, J. I. **Matrix product state representations**. Quantum Information & Computation, Paramus, NJ: Rinton Press, v. 7, n. 5, p. 401–430, Jul. 2007.

23 BELLMAN, R. E.; FAN, K. *On systems of linear inequalities in Hermitian matrix variables*. Santa Monica, CA: RAND Corporation, 1962.

24 DUARTE, C.; CARVALHO, G. D.; BERNARDES, N. K.; DE MELO, F. Emerging dynamics arising from coarse-grained quantum systems. **Phys. Rev. A**, v. 96, n. 3, p. 032113, 2017. DOI: 10.1103/PhysRevA.96.032113.

25 CORREIA, P. S.; OBANDO, P. C.; VALLEJOS, R. O.; DE MELO, F. Macro-to-micro quantum mapping and the emergence of nonlinearity. **Phys. Rev. A**, v. 103, n. 5, p. 052210, 2021. DOI: 10.1103/PhysRevA.103.052210.

26 CALLEN, Herbert B. **Thermodynamics and an introduction to thermostatistics**. New York: Wiley, 1985.

27 DUARTE, C. Compatibility between agents as a tool for coarse-grained descriptions of quantum systems. **Journal of Physics A: Mathematical and Theoretical**, v. 53, n. 39, p. 395301, 2020. DOI: 10.1088/1751-8121/aba574.

28 VALLEJOS, R. O.; CORREIA, P. S.; OBANDO, P. C.; O'NEILL, N. M.; TACLA, A. B.; DE MELO, F. Quantum state inference from coarse-grained descriptions: Analysis and an application to quantum thermodynamics. **Phys. Rev. A**, v. 106, n. 1, p. 012219, 2022. DOI: 10.1103/PhysRevA.106.012219.

29 BRUGGER, Lucas L.; DUARTE, Cristhiano; RIZZUTI, Bruno F. **Descrições efetivas em mecânica quântica: um problema de inferência bayesiana**. 2025. Dissertação (Mestrado em Física) – Universidade Federal de Juiz de Fora, Juiz de Fora.

30 DUARTE, C.; AMARAL, B.; CUNHA, M. T.; LEIFER, M. Investigating coarse-grainings and emergent quantum dynamics with four mathematical perspectives. **arXiv preprint** arXiv:2011.10349 [quant-ph], 2020. Available at: <https://arxiv.org/abs/2011.10349>.

31 NIELSEN, M. A.; CHUANG, I. L. Quantum computation and quantum information: 10th anniversary edition. Cambridge: Cambridge University Press, 2010.

32 ZHAN, X. **Matrix inequalities**. Berlin: Springer, 2004.

33 BREUER, H.-P.; PETRUCCIONE, F. The theory of open quantum systems. Oxford: Oxford University Press, 2007. DOI: 10.1093/acprof:oso/9780199213900.001.0001.

34 COSTA, P. C. S.; DE MELO, F. Coarse graining of partitioned cellular automata. **J. Cell. Autom.**, v. 15, n. 4, p. 305-311, 2020. Available in: <https://www.oldcitypublishing.com/journals/jca-home/jca-issue-contents/jca-volume-15-number-4-2020/jca-15-4-p-305-311/>.

35 CORREIA, P. S.; DE MELO, F. Spin-entanglement wave in a coarse-grained optical lattice. **Phys. Rev. A**, v. 100, n. 2, p. 022334, 2019. DOI: 10.1103/PhysRevA.100.022334.

36 VIDAL, G.; TARRACH, R. Robustness of entanglement. **Phys. Rev. A**, v. 59, n. 1, p. 141-155, 1999. DOI: 10.1103/PhysRevA.59.141.

37 WILDE, M. M. **Quantum Information Theory**. 1. ed. Cambridge: Cambridge University Press, 2013. ISBN 978-1107034259.

38 WEBSTER, R. *Convexity*. Oxford: Oxford University Press, 2023. ISBN 978-0198531470. DOI: 10.1093/oso/9780198531470.001.0001.

39 BOYD, S.; VANDENBERGHE, L. **Convex Optimization**. Cambridge: Cambridge University Press, 2004.

40 MIRONOWICZ, P. Semi-definite programming and quantum information. *Journal of Physics A: Mathematical and Theoretical*, v. 57, n. 16, p. 163002, 2024. DOI: 10.1088/1751-8121/ad2b85.

41 SKRZYPCZYK, P.; CAVALCANTI, D. Semidefinite programming in quantum information science. Bristol: IOP Publishing, 2023. DOI: 10.1088/978-0-7503-3343-6.

42 BENAVOLI, Alessio; FACCHINI, Alessandro; ZAFFALON, Marco. Quantum mechanics: The Bayesian theory generalized to the space of hermitian matrices. **Physical Review A**, v. 94, n. 4, p. 042106, out. 2016. DOI: 10.1103/PhysRevA.94.042106.

43 LEIFER, M. S. Quantum dynamics as an analog of conditional probability. **Physical Review A**, v. 74, n. 4, p. 042310, out. 2006. DOI: 10.1103/PhysRevA.74.042310.

44 KITAEV, A. Y. Quantum computations: algorithms and error correction. **Russian Mathematical Surveys**, v. 52, n. 6, p. 1191, 1997.

45 BENENTI, G.; STRINI, G. Computing the distance between quantum channels: usefulness of the Fano representation. **Journal of Physics B: Atomic, Molecular and Optical Physics**, v. 43, n. 21, p. 215508, 2010. DOI: 10.1088/0953-4075/43/21/215508.

46 REGULA, B.; TAKAGI, R.; GU, M. Operational applications of the diamond norm and related measures in quantifying the non-physicality of quantum maps. **Quantum**, v. 5, p. 522, 2021.

47 NERY, R.; BERNARDES, N. K.; CAVALCANTI, D.; CHAVES, R.; DUARTE, C. Efficient and operational quantifier of nondivisibility in terms of channel discrimination. **Phys. Rev. A**, v. 111, n. 2, p. 022206, 2025.

48 THEURER, T.; EGLOFF, D.; ZHANG, L.; PLENIO, M. B. Quantifying operations with an application to coherence. **Phys. Rev. Lett.**, v. 122, n. 19, p. 190405, 2019.

49 WATROUS, John. **The Theory of Quantum Information**. 1. ed. Cambridge: Cambridge University Press, 2018. ISBN 1107180562.

50 FREMBS, M.; CAVALCANTI, E. G. *Variations on the Choi–Jamiołkowski isomorphism*. **Journal of Physics A: Mathematical and Theoretical**, v. 57, n. 26, p. 265301, June 2024. DOI: 10.1088/1751-8121/ad5394. Available at: https://doi.org/10.1088/1751-8121/ad5394.

51 XIE, W.; FANG, K.; WANG, X.; DUAN, R. Approximate broadcasting of quantum correlations. *Physical Review A*, v. 96, n. 2, p. 022302, 2017. DOI: 10.1103/PhysRevA.96.022302.

52 DIACONIS, P.; ZABELL, S. L. **Updating subjective probability**. Journal of the American Statistical Association, v. 77, n. 380, p. 822–830, 1982. DOI: 10.1080/01621459.1982.10477893.

53 VIRTANEN, P.; GOMMERS, R.; OLIPHANT, T. E.; HABERLAND, M.; REDDY, T.; COURNAUPEAU, D.; BUROVSKI, E.; PETERSON, P.; WECKESSER, W.; BRIGHT, J.; VAN DER WALT, S. J.; BRETT, M.; WILSON, J.; MILLMAN, K. J.; MAYOROV, N.; NELSON, A. R. J.; JONES, E.; KERN, R.; LARSON, E.; CAREY, C. J.; POLAT, İ.; FENG, Y.; MOORE, E. W.; VANDERPLAS, J.; LAXALDE, D.; PERKTOLD, J.; CIMRMAN, R.; HENRIKSEN, I.; QUINTERO, E. A.; HARRIS, C. R.; ARCHIBALD, A. M.; RIBEIRO, A. H.; PEDREGOSA, F.; VAN MULBREGT, P.; SCIPY 1.0 CONTRIBUTORS. **SciPy 1.0: Fundamental algorithms for scientific computing in Python**. Nature Methods, v. 17, p. 261–272, 2020. DOI: 10.1038/s41592-019-0686-2.

54 JUNIOR, A. B. P.; ZAMORA, S.; MACÊDO, R. A.; SARUBI, T. S.; VARELA, J. M.; ROCHA, G. W. C.; MOREIRA, D. A.; CHAVES, R. *Geometric analysis of the*

stabilizer polytope for few-qubit systems. arXiv preprint arXiv:2504.12518, 2025. Available at: https://arxiv.org/abs/2504.12518.

55 WANG, X.; DUAN, R. *Improved semidefinite programming upper bound on distillable entanglement*. Physical Review A, v. 94, n. 5, p. 050301, 2016. DOI: 10.1103/PhysRevA.94.050301.

56 WERNER, R. F. **Quantum states with Einstein–Podolsky–Rosen correlations admitting a hidden-variable model**. Physical Review A, v. 40, n. 8, p. 4277–4281, 1989. DOI: 10.1103/PhysRevA.40.4277.

57 TAVAKOLI, A.; POZAS-KERSTJENS, A.; BROWN, P.; ARAÚJO, M. *Semidefinite programming relaxations for quantum correlations*. Reviews of Modern Physics, v. 96, n. 4, p. 045006, 2024. DOI: 10.1103/RevModPhys.96.045006.

58 WATROUS, J. *Simpler semidefinite programs for completely bounded norms*. Chicago Journal of Theoretical Computer Science, v. 19, p. 008, 2013. DOI: 10.4086/cjtcs.2013.008.

59 LAUTENBACHER, L.; DE MELO, F.; BERNARDES, N. K. *Approximating invertible maps by recovery channels: Optimality and an application to non-Markovian dynamics*. **Physical Review A**, v. 105, n. 4, p. 042421, Apr. 2022. DOI: 10.1103/PhysRevA.105.042421. Available at: https://link.aps.org/doi/10.1103/PhysRevA.105.042421.

60 MOSEK ApS. *The MOSEK Python Fusion API Manual*. Version 11.0. Copenhagen, 2025. Available at: https://docs.mosek.com/latest/pythonfusion/index.html.

61 JIANG, J.; WANG, K.; WANG, X. Physical implementability of linear maps and its application in error mitigation. **Quantum**, v. 5, p. 600, 2021. DOI: 10.22331/q-2021-12-07-600.

62 FANG, K.; WANG, X.; TOMAMICHEL, M.; BERTA, M. Quantum channel simulation and the channel's smooth max-information. **IEEE Transactions on Information Theory**, v. 66, n. 4, p. 2129-2140, 2020. DOI: 10.1109/TIT.2019.2943858.

63 YE, M.; LUO, Y.; LI, Z.; LI, Y. Projective robustness for quantum channels and measurements and their operational significance. **Laser Physics Letters**, v. 19, n. 7, p. 075204, 2022. DOI: 10.1088/1612-202X/ac6c2e.

64 ALICKI, R.; FANNES, M.; POGORZELSKA, M. **Quantum generalized subsystems**. Physical Review A, v. 79, n. 5, p. 052111, 2009. DOI: 10.1103/PhysRevA.79.052111.

65 HARROW, A. W.; NIELSEN, M. A. Robustness of quantum gates in the presence of noise. **Phys. Rev. A**, v. 68, n. 1, p. 012308, 2003. DOI: 10.1103/PhysRevA.68.012308.

66 BARENCO, A.; BERTHIAUME, A.; DEUTSCH, D.; EKERT, A.; JOZSA, R.; MACCHIAVELLO, C. Stabilization of quantum computations by symmetrization. **SIAM Journal on Computing**, v. 26, n. 5, p. 1541-1557, 1997. DOI: 10.1137/S0097539796302452.

67 NISHIMURA, H. A survey: SWAP test and its applications to quantum complexity theory. In: MINATO, S.; UNO, T.; YASUDA, N.; HORIYAMA, T.; KAWARABAYASHI, K.; YAMASHITA, S.; ONO, H. (ed.). **Algorithmic foundations for social advancement: recent progress on theory and practice**. Singapore: Springer Nature Singapore, 2025. p. 243–261. DOI: 10.1007/978-981-96-0668-9_16.

68 SACHDEV, S. Quantum phase transitions. **Physics World**, v. 12, n. 4, p. 33, Apr. 1999. DOI: 10.1088/2058-7058/12/4/23.

69 HARRIS, C. R.; MILLMAN, K. J.; VAN DER WALT, S. J.; GOMMERS, R.; VIRTANEN, P.; COURNAUPEAU, D.; WIESER, E.; TAYLOR, J.; BERG, S.; SMITH, N. J.; KERN, R.; PICUS, M.; HOYER, S.; VAN KERKWIJK, M. H.; BRETT, M.; HALDANE, A.; FERNÁNDEZ DEL RÍO, J.; WIEBE, M.; PETERSON, P.; GÉRARD-MARCHANT, P.; SHEPPARD, K.; REDDY, T.; WECKESSER, W.; ABBASI, H.; GOHLKE, C.; OLIPHANT, T. E. Array programming with NumPy. **Nature**, v. 585, n. 7825, p. 357-362, 2020. DOI: 10.1038/s41586-020-2649-2.